NASA Contractor Report 166022

CONTROL CONCEPTS FOR THE ALLEVIATION OF WINDSHEARS AND GUSTS

E. G. Rynaski and K. S. Govindaraj

Contract NAS1-16691
July 1982

National Aeronautics and
Space Administration

Langley Research Center
Hampton, Virginia 23665

TABLE OF CONTENTS

LIST OF FIGURES

LIST OF SYMBOLS

Symbol	Description	Units
A	observer dynamics matrix	
E	matrix relating the outputs to the observer dynamics	
C_D	drag coefficient	
C_L	lift coefficient	
C_m	pitching moment coefficient	
$\bar{c}$	mean aerodynamic chord	ft
D	matrix relating the controls to the observer dynamics	
E	specific energy	ft
ΔE	change in the specific energy	ft
F	system dynamics matrix	
F_0	dynamic matrix of a third order system	
G	control input matrix	
G_0	control input matrix of a third order system	
g	gravity	ft/sec
h	actual aircraft altitude	ft
h_c	desired aircraft altitude	ft
Δh	difference between the actual and the desired altitude	ft
H	matrix relating the states to the outputs	
$\dot{h}_{AG}$	velocity of wind along the Z inertial axis	ft/sec
$\dot{h}_{PA}$	velocity of the airplane with respect to the airmass along the Z inertial axis	ft/sec
$\dot{h}_{PG}$	altitude rate	ft/sec
I_{yy}	moment of inertia about the Y axis	
J	gust input matrix	
K	control system gain matrix	
K_c	feedback gain on the altitude error	
K_E	feedback gain on the error in energy	
K_h	gain used to compute the command altitude from range	

LIST OF SYMBOLS (CONT'D)

Symbols	Description	Units
K_1	feedforward gain on the airspeed to the throttle	
K_{11}	feedback gain on the airspeed to the throttle	
L_u	scale for horizontal turbulence	ft
L_w	scale for vertical turbulence	ft
m	aircraft mass	slugs
M	transformation matrix	
M_u	change in pitching moment due to a variation in speed along the X-axis	1/ft-sec
M_w	change in pitching moment due to a variation in speed along the Z-axis	1/ft-sec
M_q	change in pitching moment due to a variation in pitch velocity	1/rad sec
M_{δ_e}	change in pitching moment due to a variation in elevator deflection	$1/deg\text{-}sec^2$
M_{δ_t}	change in pitching moment due to a variation in thrust	$1/sec^2\text{-}lb$
$M_{\delta_{sp}}$	change in pitching moment due to a variation in spoiler deflection	$1/deg\text{-}sec^2$
N	maximum number of transmission zeros	
P	solution of matrix Riccati equation	
P_s	static pressure	lb/ft^2
$\underline{q}$	weighting matrix on the outputs in the performance index	
q_i	weighting factor on the states in the performance index	
$\bar{q}$	dynamic pressure	lb/ft^2
q	pitch rate	deg/sec
R	range of the airplane to the touchdown point	ft
$\underline{r}$	weighting matrix on the controls in the performance index	
r_i	weighting factor on the controls in the performance index	
s	wing area	ft^2

LIST OF SYMBOLS (CONT'D)

Symbols	Description	Units
T	transformation matrix	
T_{x_i}	thrust component along the X-body axis due to the ith engine	lbs
T_{z_i}	thrust component along the Z-body axis due to the ith engine	lbs
u	control vector	
u_{AG}	velocity of wind along the X-inertial axis	ft/sec
u_g	wind disturbance vector	
U_0	trim air or ground speed along the X-body axis	ft/sec
u_{PA}	airspeed along the X-body axis	ft/sec
Δu_{PA}	perturbation in airspeed along the X-body axis	ft/sec
u_{PG}	inertial velocity along the X-body axis	ft/sec
Δu_{PG}	perturbation in inertial velocity along the X-body axis	ft/sec
u_w	velocity of wind along the X-body axis	ft/sec
V	performance index	ft/sec
V_{AG}	velocity of wind along the X-inertial axis	ft/sec
V_0	trim airspeed	ft/sec
V_{PA}	total velocity of the airplane with respect to the airmass	ft/sec
V_{PG}	total velocity of the airplane wiht respect to the ground	ft/sec
V_T	true airspeed	ft/sec
V_{X_E}	inertial velocity along the X-axis	ft/sec
V_{Z_E}	inertial velocity along the Z-axis	ft/sec
W_0	Trim airspeed along the Z-body axis	ft/sec
w_{PA}	airspeed along the Z-body axis	ft/sec
Δw_{PA}	perturbation in airspeed along the Z-body axis	ft/sec
w_{PG}	ground speed along the Z-body axis	ft/sec
Δw_{PG}	perturbation in ground speed along the Z-body axis	ft/sec
w_w	velocity of wind along the Z-body axis	ft/sec

LIST OF SYMBOLS (CONT'D)

Symbols	Description	Units
x	state vector representing the aircraft responses	
X_E	inertial X position of the aircraft	ft
X_u	change in X force due to a variation in X-body axis	1/sec
X_w	change in X force due to a variation in speed along the Z body axis	1/sec
X_q	change in the X force due to a variation in pitch rate	ft/rad-sec
X_{δ_e}	change in X force due to a varaition in elevator deflection	ft/deg-sec^2
X_{δ_t}	change in X force due to a variation in thrust	ft/lb-sec^2
$X_{\delta_{sp}}$	change in X force due to a variation in spoiler deflection	ft/deg-sec^2
y	output vector	
Z	observer states	
Z_E	inertial Z position of the aircraft	ft
Z_R	inertial Z position of the aircraft at a range R from the touchdown point	ft
Z_u	change in Z force due to a variation in speed along the X body axis	1/sec
Z_w	change in Z force due to a variation in speed along the Z body axis	1/sec
Z_q	change in Z force due to a variation in pitch rate	ft/rad-sec
Z_{δ_e}	change in Z force due to a variation in elevator deflection	ft/deg-sec^2
Z_{δ_t}	change in Z force due to a variation in thrust	ft/lb-sec^2
$Z_{\delta_{sp}}$	change in Z force due to a variation in spoiler deflection	ft/deg-sec^2
Z_ε	error in inertial Z position of the aircraft	ft
α_0	trim angle of attack	deg
α_{PA}	angle of attack with respect to the airmass	deg

LIST OF SYMBOLS (CONT'D)

Symbols	Description	Units
α_{PG}	inertial angle of attack	deg
γ_0	trim flight path angle	deg
γ_ϵ	flight path angle error	deg
γ_{PA}	flight path angle with respect to the airmass	deg
γ_{PG}	flight path angle with respect to the ground	deg
ρ	density of atmosphere	$slug/ft^3$
θ	pitch attitude	deg
θ_0	trim pitch attitude	deg
δ_e	elevator control input	deg
δ_{sp}	spoiler control input	deg
δ_t	throttle control input	lbs
Ω	scaled frequency	
ϕ_{u_w}	spectrum of the horizontal turbulence	
ϕ_{w_w}	spectrum of the vertical turbulence	
σ_u	root mean square intensity of u_w	
σ_w	root mean square intensity of w_w	

Section 1
INTRODUCTION

This report summarizes the results of a program performed for the NASA Langley Research Center by the Calspan Corporation to study windshear and gust alleviation methods with consideration of the application of the NASA total energy/energy rate probe to this particular task.

The study has several different objectives and related phases. One was to determine whether or not a successful control system design could be obtained for the TCV 737 aircraft using only elevator or only throttle, and then using both control effectors in concert. A second objective was to assess the usefulness of a direct measurement of the shear or turbulence as compared to a strict feedback regulation approach to gust alleviation. Still another objective was to test the concepts of alleviation with respect to *ground speed or with respect to airspeed, sometimes referred to as 4D or 3D* regulation. If the control system of the aircraft is designed to maintain a constant airspeed through a windshear, the alleviation system is said to be a 3D system. If ground speed is regulated through the windshear, the aircraft presumably will land at the touchdown point both in space and on time and is referred to as 4D regulation. The airspeed/ground speed regulation approach can be considered only with respect to horizontal velocity. However, regulation of vertical velocity only with respect to ground can be considered as a reasonable criteria in a wind gust/shear alleviation control system design study.

Infused in each of the windshear/gust alleviation designs and design philosophy is the application of the NASA total energy/energy rate probe described later in the body of the report. It was felt that the probe could be quite useful in this application for three reasons:

1. A constant rate of change of energy during a landing is consistent with the 3D philosophy of vehicle regulation in a windshear. Constant kinetic energy is approximately equivalent

to constant airspeed at constant air density while constant rate of change of altitude is equivalent to constant rate of change of potential energy. It was therefore found appropriate to consider energy to be an appropriate criteria in terms of direct inclusion in a quadratic performance index criteria for design purposes.

2. The probe as a major component in a control law would be an attractive instrumentation feature because of the simplicity and versatility of the device. Pneumatic methods of obtaining energy rate are straightforward and reliable. Therefore, effort was made to include the total energy/energy rate probe as a sensor to be incorporated into the control system design to simplify the overall system mechanization.

3. The total energy probe is basically an air data rather than an inertia measurement device. Because of this, it was felt that the sensor could be useful in the development of instrumentation that would directly detect and measure wind shear.

The study program was considered exploratory in the sense that sample and example methods of the approach to gust and shear alleviation were tried rather than trying to take into account all the possible nuances of the vehicle or the environment. For instance, secondary effects of a wind shear which often occur during a thunderstorm, such as changes in static pressure, were ignored as were higher order dynamics and nonlinearities of the airframe. The Dryden turbulence model was chosen, partly because of ease of programming, but also with the knowledge that other turbulence models, such as the Von Karman or Tomlinson models, would have relatively little effect on the results. It is clear, however, that a more complete simulation is advisable before flight test of any of the several systems described in this report.

The report is divided into four major sections and three appendices. The second section describes the dynamic and kinematic equations applicable to

the landing approach flight of an aircraft in wind shear and turbulence. The third section describes the control system design approaches used for wind shear/gust alleviation, while the fourth section includes the simulation results and an analysis of these results. Section five summarizes the results of the study and makes recommendations for further investigation of the use of the total energy probe in a wind shear/turbulence environment.

Because the particular computations apply only to the particular vehicle used in the study program, the vehicle specific results appear in several appendices. These appendices compile the results of the calculations performed during this program.

Section 2

DYNAMICS AND KINEMATICS

2.0 PROBLEM DEFINITION

In this section, the TCV airplane equations of motion, the shear and turbulence models, and the total energy probe measurement model are defined.

2.1 EQUATIONS OF MOTION

In defining the equations of motion of the TCV airplane, the following notation is used to identify velocities and angles relative to the ground or the atmosphere:

PA - plane relative to the air.
PG - plane relative to the ground.
AG - air relative to the ground.

It is assumed, in the definition of the equations of motion, that the earth is flat and the aircraft is rigid. The nonlinear longitudinal equations of motion are defined by the following equations:

Force Equations - Wind Tunnel Stability Axes

$$\dot{V}_{PG} = -\frac{\bar{q}S}{m} C_D - g \sin \gamma_{PG} + \sum_{i=1}^{n} [T_{x_i} \cos \alpha_{PG} + T_{z_i} \sin \alpha_{PG}] \frac{1}{m}$$

$$\dot{\alpha}_{PG} = \frac{57.3\bar{q}S}{mV_{PG}} C_L + \frac{57.3g}{V_{PG}} \cos \gamma_{PG} + q + \sum_{i=1}^{n} [T_{z_i} \cos \alpha_{PG} - T_{x_i} \sin \alpha_{PG}] \frac{57.3}{mV_{PG}}$$

$$\gamma_{PG} = \theta - \alpha_{PG}$$

$$T_{x_i} = T_i \cos \alpha_{T_i} \cos \beta_{T_i}$$

$$T_{z_i} = -T_i \sin \alpha_{T_i} \cos \beta_{T_i}$$

Thrust components in body axes.
i- each engine

Moment Equation - Body Axis

$$\dot{q} = \frac{57.3\bar{q}S\bar{c}}{I_{yy}} C_m + \sum_{i=1}^{n} \frac{57.3}{I_{yy}} [z_{T_i} T_{x_i} - x_{T_i} T_{z_i}]$$

$$\dot{\theta} = q$$

z_{T_i}, x_{T_i} distances from C.G. to a reference point for thrust vector in body axes - ft.

$$\dot{h}_{PG} = V_{PG} \sin \gamma_{PG} \tag{2-1}$$

$C_L = \frac{L}{\bar{q}S}$ Lift coefficient. Force perpendicular to velocity vector in the plane of symmetry.

$C_D = \frac{D}{\bar{q}S}$ Drag coefficient. Force parallel to velocity vector component in the plane of symmetry.

$\bar{q} = \frac{1}{2} \rho V_{PA}^2$ Dynamic pressure lb/ft^2

$\rho =$ Density of atmosphere slug/ft^3

$V_{PA} =$ True airspeed ft/sec

$\beta = p = r = 0$

The aerodynamic coefficients are functions of angle of attack, flap position, etc..

$$\begin{aligned} C_L &= f(\alpha_{PA}, \delta_e, \delta_f, etc.) \\ C_D &= f(\quad\quad " \quad\quad) \\ C_m &= f(\quad\quad " \quad\quad) \end{aligned} \tag{2-2}$$

The inertial positions and velocities are computed from the velocities with respect to the body fixed inertial frame as follows:

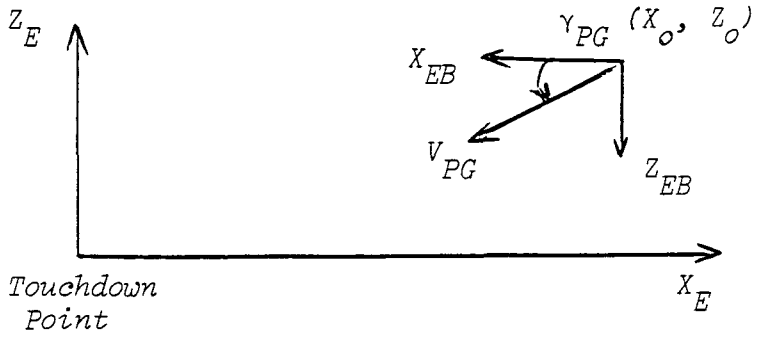

Position and Velocity

$$V_{XE} = - V_{PG} \cos \gamma_{PG}$$

$$\dot{h}_{PG} = V_{ZE} = + V_{PG} \sin \gamma_{PG}$$

$$X_E = X_o + \int_o^t V_{XE}\, dt = X_o - \int_o^t V_{PG} \cos \gamma_{PG}\, dt$$

$$Z_E = Z_o + \int_o^t V_{ZE}\, dt = Z_o + \int_o^t V_{PG} \sin \gamma_{PG}\, dt$$

Inertial Parameters

$$V_{PG} = V_o + \int_o^t \dot{V}_{PG}\, dt$$

$$\alpha_{PG} = \alpha_o + \int_o^t \dot{\alpha}_{PG}\, dt$$

$$\theta = \theta_o + \int_o^t q\, dt$$

$$\gamma_{PG} = \theta - \alpha_{PG} \qquad (2\text{-}3)$$

where V_o, α_o, and θ_o are trim values.

The guidance information is computed as follows:

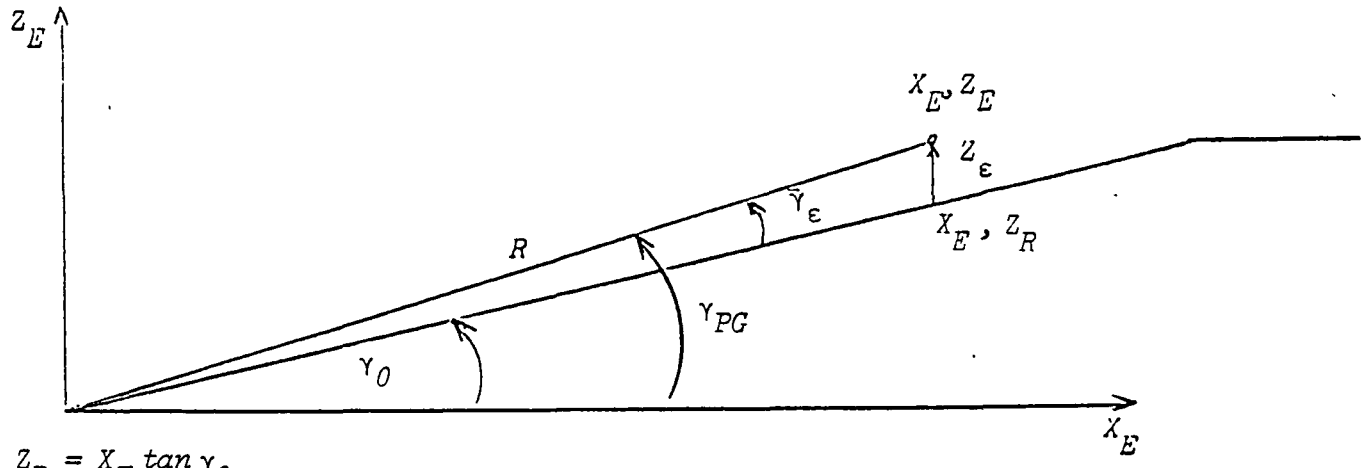

$$Z_R = X_E \tan \gamma_0$$

$$R = \sqrt{X_E^2 + Z_E^2}$$

$$Z_R = \sqrt{X_E^2 + Z_E^2} \sin \gamma_0$$

where: γ_0 is desired flight path angle

$$Z_\varepsilon = Z_E - Z_R$$

altitude error

$$= Z_E - X_E \tan \gamma_0$$

$$\gamma = \tan^{-1} \frac{Z_E}{X_E}$$

$$\gamma = \gamma - \gamma_0$$

ILS Glide Slope error

$$= \tan^{-1} \frac{Z_E}{X_E} - \gamma_0 \qquad (2\text{-}4)$$

The velocity and angular motions with respect to the air mass are defined as follows:

V_{PA}, α_{PA} and γ_{PA} equations expressed in terms of V_{PG} and γ_{PG}

$$\gamma_{PA} = \tan^{-1} \frac{V_{PG} \sin \gamma_{PG} - \dot{h}_{AG}}{V_{PG} \cos \gamma_{PG} + u_{AG}}$$

$$\alpha_{PA} = \theta - \gamma_{PA}$$

$$V_{PA}^2 = [V_{PG} \cos \gamma_{PG} + u_{AG}]^2 + [V_{PG} \sin \gamma_{PG} - \dot{h}_{AG}]^2$$

where: u_{AG} ~ + ve headwind

$\dot{h}_{AG}$ ~ + ve updraft

$$\dot{h}_{PA} = \dot{h}_{PG} - \dot{h}_{AG} \qquad (2\text{-}5)$$

where u_{AG} and $\dot{h}_{AG}$ are the horizontal and vertical wind velocities, respectively.

The nonlinear equations (2-1) are linearized about a nominal trajectory representing the steady state flight along a 3^0 glide slope. The linearized small perturbation equations of motion are expressed in the body axis system. The equations of motion are defined as follows:

$$\dot{\Delta u}_{PG} = X_u \Delta u_{PG} + X_w \Delta w_{PG} + (X_q - W_o) q - g \cos \theta_o \Delta\theta + X_{\delta_t} \delta_t + X_{\delta_e} \delta_e + X_{\delta_{sp}} \delta_{sp} + X_u u_w + X_w w_w$$

$$\dot{\Delta w}_{PG} = Z_u \Delta u_{PG} + Z_w \Delta w_{PG} + (Z_q + U_o) q + g \sin \theta_o \Delta\theta + Z_{\delta_t} \delta_t + Z_{\delta_e} \delta_e + Z_{\delta_{sp}} \delta_{sp} + Z_u u_w + Z_w w_w$$

$$\dot{q} = M_u \Delta u_{PG} + M_w \Delta w_{PG} + M_q q + M_\theta \Delta\theta + M_{\delta_t} \delta_t + M_{\delta_e} \delta_e + M_{\delta_{sp}} \delta_{sp} + M_u u_w + M_w w_w$$

$$\dot{\theta} = q \qquad (2\text{-}6)$$

where

$$\begin{aligned} \Delta u_{PG} &= u_{PG} - U_o \\ \Delta w_{PG} &= w_{PG} - W_o \\ \Delta\theta &= \theta - \theta_o \end{aligned} \tag{2-7}$$

U_o and W_o are trim velocities (air or inertial) along the X and Z body axis, u_{PG} and w_{PG} are the total velocities along X and Z body axis, θ_o is the trim pitch attitude, u_w and w_w are the wind velocities along the X and Z body axis, δ_t, δ_e, and δ_{sp} are the throttle, elevator and spoiler control inputs. The perturbation in velocities with respect to the airmass along the X and Z axes is defined by

$$\begin{aligned} \Delta u_{PA} &= \Delta u_{PG} + u_w \\ \Delta w_{PA} &= \Delta w_{PG} + w_w \end{aligned} \tag{2-8}$$

where u_w and w_w are the wind velocities along the X and Z body axes, respectively. The velocities along the X and Z body axes are defined in terms of the velocity in stability axis system by the following equations:

$$\begin{aligned} u_{PG} &= V_{PG} \cos \alpha_{PG} \\ w_{PG} &= V_{PG} \sin \alpha_{PG} \simeq V_{PG}\alpha_{PG} \end{aligned} \tag{2-9}$$

where α_{PG} is the angle of attack. The stability and control derivatives of Equation (2-6) are given in Appendix A. The equations of motion can be written compactly in state variable form as

$$\dot{x} = Fx + Gu + J u_g$$

$$x = \begin{bmatrix} \Delta u_{PG} \\ \Delta w_{PG} \\ q \\ \Delta\theta \end{bmatrix}, \quad u = \begin{bmatrix} \delta_t \\ \delta_e \\ \delta_{sp} \end{bmatrix}, \quad u_g = \begin{bmatrix} u_w \\ w_w \end{bmatrix} \tag{2-10}$$

$$J_{ij} = F_{ij} \qquad \begin{matrix} i = 1, 4 \\ j = 1, 2 \end{matrix}$$

2.2 SHEAR AND TURBULENCE MODELS

The wind shear models used in this study are the severe Kennedy incident (TOC), (Ref.1), Philadelphia (T-25A) and the moderate Tower (T-9A) profiles. These profiles define the horizontal and vertical wind velocities, u_{AG} and $\dot{h}_{AG}$, respectively, as a function of altitude. The sign convention is defined as:

$u_{AG} \equiv +ve$ for headwind (i.e. - X direction in aircraft axes)
Horizontal component of air motion relative to the ground.

$\dot{h}_{AG} \equiv +ve$ for updraft (i.e. - Z direction in aircraft axes)
Vertical component of air motion relative to the ground.

It is recommended in Ref.1 that the shear be defined both as a function of altitude and distance. However, in this study the shear profiles used are only a function of the altitude.

The horizontal and vertical velocities are defined by the Dryden spectra (Ref.2). The Dryden spectra are defined as:

$$\phi_{u_w}(\Omega) = \sigma_u^2 \frac{2L_u}{\pi} \frac{1}{1 + (L_u\Omega)^2} \qquad \text{where } \Omega = \frac{\omega}{V_o}$$

$$\phi_{w_w}(\Omega) = \sigma_w^2 \frac{L_w}{\pi} \frac{1 + 3(L_w\Omega)^2}{[1 + (L_w\Omega)]^2} \tag{2-11}$$

where V_o is the trim air or groundspeed. The turbulence velocities are obtained by filtering white noise using the following transfer functions obtained from the Dryden spectra.

$$T_{u_w}(s) = \sigma_u \sqrt{\frac{2 L_u}{\pi V_0}} \; \frac{1}{1 + \frac{L_u}{V_0} s}$$

$$T_{w_w}(s) = \sigma_w \sqrt{\frac{L_w}{\pi V_0}} \; \frac{1 + \frac{\sqrt{3} L_w}{V_0} s}{\left(1 + \frac{L_w}{V_0} s\right)^2} \qquad (2\text{-}12)$$

where the turbulence intensities, σ_u and σ_w and the other parameters, are defined as follows:

σ_w = 5.1 ft/sec Moderate
= 7.6 ft/sec Severe

$$\sigma_u = \frac{\sigma_w}{(0.177 + 0.000823\, h)^{0.4}} \qquad h < 1000 \text{ ft}$$

$$\sigma_u = \sigma_w \qquad h > 1000 \text{ ft}$$

$$L_w = 1000 \qquad h > 1000 \text{ ft}$$

$$L_w = h \text{ ft} \qquad 10 < h < 1000 \text{ ft}$$

$$L_w = 10 \qquad h < 10 \text{ ft}$$

(2-13)

$$L_u = 1000 \text{ ft} \qquad h > 1000 \text{ ft}$$

$$L_u = \frac{h}{(0.177 + 0.000823\, h)^{1.2}} \qquad 10 < h < 1000 \text{ ft}$$

$$L_u = 100 \text{ ft} \qquad h < 10 \text{ ft}$$

Experience at Calspan with the use of Dryden spectra for in-flight simulation has indicated the necessity of filtering the turbulence signal. This is done to remove the fairly significant low frequency content of the signal. In this study, the shear accounts for the low frequency wind disturbance. The shear profiles and the time domain equations to generate the turbulence are given in Appendix A.

2.3 ENERGY PROBE

A simple energy probe was developed recently (Ref. 3) by O. W. Nicks. The energy probe gives a measure of the total energy with respect to the air mass. It has been flight tested (Ref. 4) to verify its measurement and recent studies (Ref. 5) have considered the incorporation of energy rate feedback into the control law for control of aircraft in a wind shear environment.

The energy sensor measures static minus dynamic pressure. If this is differentiated, it gives a rate of change of pressure which is related to the rate of change in total energy relative to the air mass. The following equations model what the probe actually measures:

$$P_{probe} = P_{static} - \bar{q}$$

$$= P_s(h) - \frac{1}{2}\rho V_T^2 = P_s(h) - \frac{1}{2}\rho_o V_{IAS}^2$$

$$\frac{dP_{probe}}{dt} = \frac{dP_s}{dh}\frac{dh}{dt} - \frac{2}{2}\rho V_T \frac{dV_T}{dt} - \frac{1}{2}V_T\frac{d\rho}{dh}\frac{dh}{dt}$$

$$\text{or} = \frac{dP_s}{dh}\frac{dh}{dt} - \rho_o V_{IAS}\frac{dV_{IAS}}{dt} \qquad (2\text{-}14)$$

where V_T is the true airspeed (ft/sec), V_{IAS} is the indicated airspeed (ft/sec), ρ is the density of atmosphere (slug/ft^3), ρ_o is the density of atmosphere at sea level and h is the altitude. The pressure measurement is differentiated pneumatically using a one second time constant and a transducer converts the rate of change of pressure to an electrical signal proportional to energy rate.

The airspeed can be calculated from the inertial speed and the assumed wind speed. The variation of the static pressure with altitude (below 4,000 ft) is approximated by the equation

$$P_s = 2115 - .07196h \qquad (2\text{-}15)$$

The air density and the temperature vary in a thunderstorm as a function of position. These variations are given by the following equations:

$$V_{IAS} = \left[\frac{2}{\rho_o}\left(P_s\left\{\left[.0001383\ \frac{V_T^2}{T} + 1\right]^{3.5} - 1\right\}\right)\right]^{1/2} \quad \text{ft/sec}$$

$$\rho = -6.519x10^{-8}\ h + .0023769 - 8.0x10^{-6}\ \Delta T \quad \text{slugs/ft}^3$$

where $\Delta T = T_c - 15^o$

$T_c \sim$ Temp. in ^{o}Centigrade

$h \leq 4000$ ft

$$T_K = -.001975\ h + 288.15 + \Delta T \quad \text{Deg. Kelvin}$$

$h \leq 4000$ ft (2-16)

In Section 3, a control system based on total energy considerations will be described. The energy sensor which has been verified for measurement of energy rate can be used in the control system by deriving the energy information from the rate measurement.

2.4 ESTIMATION OF WIND VELOCITIES

A technique for estimating the horizontal and vertical components of the wind velocity is suggested in this subsection. These velocity components can be estimated from the airspeed and the inertial speed. The earth and body axis system and the various angles are shown in Figure 1. The notation *PG* represents plane to ground, *PA* represents plane to air, and *AG* represents air to ground; X_b, Z_b refer to the body axis system and X_e, Z_e refer to the earth fixed axis system.

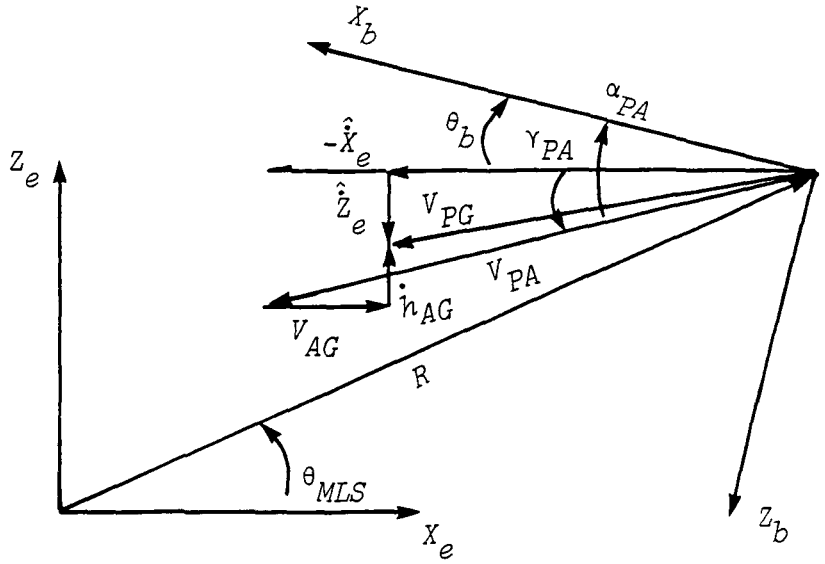

Figure 1. EARTH AND BODY AXES SYSTEMS

The horizontal and vertical wind velocities are given by the equations

$$V_{AG} = \left[V_{PA} \cos \gamma_{PA} + \hat{\dot{X}}_e\right] \qquad \text{Headwind + ve}$$

$$\hat{\dot{X}}_e = -V_{PG} \cos \gamma_{PG}$$

$$\dot{h}_{AG} = -\left[V_{PA} \sin \gamma_{PA} - \hat{\dot{Z}}_e\right] \qquad \text{Updraft + ve}$$

$$\hat{\dot{Z}}_e = -V_{PG} \sin \gamma_{PG}$$

$$\gamma_{PA} \quad \theta_b - \alpha_{PA}$$

$$\alpha_{PA} = \alpha_{vane_{cg}} \tag{2-17}$$

where $\dot{X}_e$ and $\dot{Z}_e$ are horizontal and vertical components of the inertial velocity

The true airspeed is obtained from the airdata system, the angle of attack from the vane corrected for position and flow distortion. The inertial velocities are estimated from the DME, MLS, attitude and accelerometer measurements.

The accelerations along the X and Z body axes are given by

$$\ddot{x}_b = n_{X_b} - g \sin \theta$$

$$\ddot{z}_b = n_{Z_b} + g \cos \theta \tag{2-18}$$

where n_{X_b} and n_{Z_b} are the accelerometer readings in ft/sec. The accelerations along the earth X and Z axes are computed using the Euler angle transformation

$$\begin{bmatrix} \ddot{x}_e \\ \ddot{z}_e \end{bmatrix} = -\begin{bmatrix} \cos \theta & \sin \theta \\ -\sin \theta & \cos \theta \end{bmatrix} \begin{bmatrix} n_{X_b} - g \sin \theta \\ n_{Z_b} + g \cos \theta \end{bmatrix} \tag{2-19}$$

The inertial position and velocity are estimated by complementary filtering of MLS position and aircraft accelerometer signals. The equations relating x and z to radar range and elevation are

$$x = R \cos \theta_{MLS}$$
$$z = R \sin \theta_{MLS} \qquad (2\text{-}20)$$

Smooth estimates of earth-referenced position and velocity are obtained through blending of the MLS derived data with inertial data using complementary filters. The inertial data is obtained from body axis accelerometer signals transformed into earth-referenced accelerations as given by Equation (2-19). The block diagram of the MLS complementary filters is shown in Figure 2.

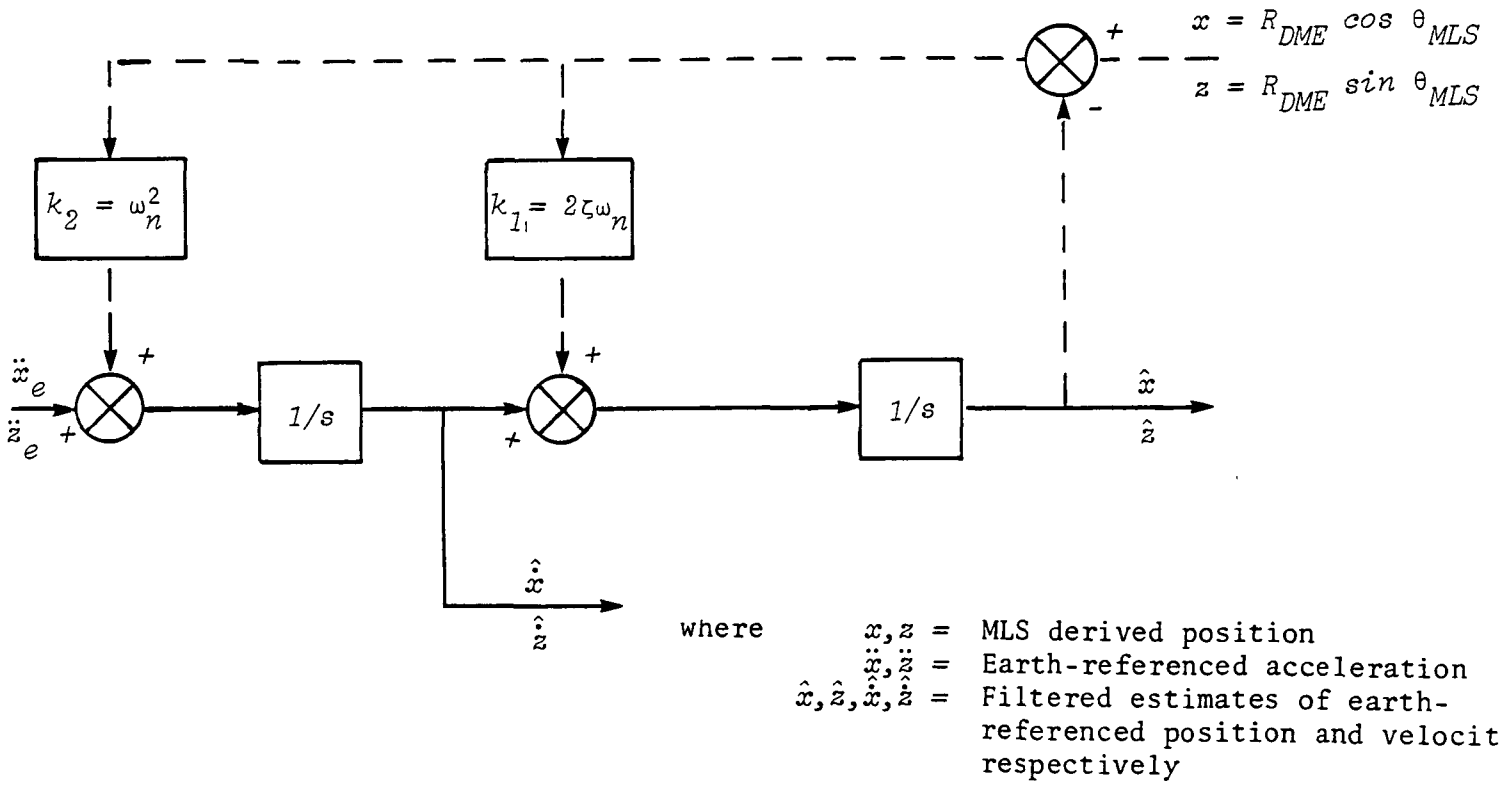

Figure 2. MLS COMPLEMENTARY FILTER BLOCK DIAGRAM

The equations for the complementary filters are given as follows:

$$\dot{\hat{x}} = \frac{(s+k_1)\ddot{x} + k_2 s x}{s^2+k_1 s+k_2}$$

$$\hat{x} = \frac{\ddot{x} + (sk_1+k_2)x}{s^2+k_1 s+k_2} \qquad (2\text{-}21)$$

where $k_1 = 2\zeta\omega_n$

$k_2 = \omega_n^2$

ζ = damping ratio

ω_n = undamped natural frequency

x = MLS derived position information

$\ddot{x}$ = earth-referenced acceleration

$\hat{x}$ = filtered estimate of position

$\dot{\hat{x}}$ = filtered estimate of velocity

The same filters are used for the estimation of Z position and velocity. These complementary filters were used successfully by Calspan (Reference 6) in the X-22A flight program. The damping ratio was selected as 0.7 and the natural frequency selected as the ratio of accelerometer noise to position noise. It is emphasized that the discussion of this subsection represents a suggested approach for estimating the wind velocity components and that the complementary filters were not used in the control system simulation.

Section 3
CONTROL SYSTEM DESIGN

3.1 GENERAL DESIGN APPROACH

The objective of the control system design is to obtain the most effective shear/gust alleviation system based upon the three tradeoffs listed below.

1. Number of controllers - i.e., throttle or elevator alone, throttle and elevator, and finally throttle, elevator and spoiler.

2. Shear and gust alleviation based upon assumptions associated with the ability to sense the shear and turbulence directly or not.

3. Regulation or alleviation with respect to the airspeed or groundspeed.

Other considerations are associated with the axis system in which the aircraft is described. For instance, regulation could be with respect to γ and V_{PA} (V_{PG}) or to h and u. Either is acceptable for one represents the flight requirements in a polar axis system while the other is rectilinear axis system oriented.

There are at least three different fundamental approaches that can be taken in the design of a gust/shear alleviation system. The most basic approach and the one that is most often taken is the one of fundamental regulation of the plant; i.e.,if the feedback is "large enough," the airplane closed-loop dynamics will be of high frequency and statically rigid. It will be difficult to perturb the aircraft from its initial flight condition. This approach involves feedback in the classical negative sense: any feedback signal is used to attenuate the perturbation motion that caused the signal.

The second approach is to design a system that is less insensitive to turbulence or external disturbances. This is done by effectively destabilizing the airplane to a gust or disturbance input. However, if feedback is used to effectively reduce C_{ℓ_α}, the maneuverability of the aircraft will be adversely affected as well. This approach can, therefore, be useful only when the aircraft is in an autopilot mode of operation because this design approach cannot differentiate between a commanded input and a gust input.

The two general methods of gust and shear alleviation described above involve feedback around the aircraft and, in fact, the airplane must respond to the gusts before the motions are sensed and fed back to the vehicle controllers. Therefore, the response of the vehicle to turbulence can be reduced, but never totally eliminated.

The third and most direct way to accomplish the gust alleviation task is to directly sense the turbulence component of the air mass relative to the aircraft and use this signal to directly drive the control surfaces of the airplane in such a way that the controllers produce forces and moments that directly counter the forces and moments generated on the vehicle by the gusts.

Design methods used in this study include the first and third methods described above.

3.2 SINGLE CONTROLLER DESIGN

The single controller system makes use only of the elevator for flight path control. The regulator control law is obtained by minimizing the performance index

$$V = \frac{1}{2}\int_0^\infty (q_1 \Delta u_{PG}^2 + q_2 \Delta h^2 + r\delta_e^2)\,dt \qquad (3\text{-}1)$$

where Δu_{PG} is the deviation in the inertial speed and Δh is the deviation in altitude.

subject to the aircraft dynamics

$$\begin{bmatrix} \Delta\dot{u}_{PG} \\ \Delta\dot{w}_{PG} \\ \dot{q} \\ \Delta\dot{\theta} \end{bmatrix} = F \begin{bmatrix} \Delta u_{PG} \\ \Delta w_{PG} \\ q \\ \Delta\theta \end{bmatrix} + G\,\delta_e + J \begin{bmatrix} u_w \\ w_w \end{bmatrix} \tag{3-2}$$

$$\Delta\dot{h} = \sin\theta_o \Delta u_{PG} - \cos\theta_o\, w_{PG} + (U_o \cos\theta_o + W_o \sin\theta_o)\Delta\theta$$

$$\begin{aligned} \Delta u_{PG} &= u_{PG} - U_o \\ \Delta w_{PG} &= w_{PG} - W_o \\ \Delta\theta &= \theta - \theta_o \end{aligned}$$

and U_o, W_o and θ_o are trim values. The derivation of $\Delta\dot{h}$ equation is given in Appendix A.

The minimization of the performance index through the use of the Euler-Lagrange equation results in the control law

$$\delta_e = -r^{-1} G^T P \begin{bmatrix} \Delta u_{PG} \\ \Delta w_{PG} \\ q \\ \Delta\theta \\ \Delta h \end{bmatrix} \tag{3-3}$$

where P is the solution of the Riccati equation and Δh is the error in altitude given by

$$\Delta h = h_c - h \tag{3-4}$$

and h_c is computed from the range as

$$h_c = k_h R = |\sin\gamma_o| R \tag{3-5}$$

and γ_o is the glide path angle. The performance index is minimized for several sets of values of q_1, q_2 and r and one set is chosen that produces good regulation in the sense that the perturbation motions are minimized relative to the required control activity.

As noted earlier, feedback regulation alone has limited ability to produce gust and shear alleviation because the motions of the vehicle due to the gusts and shears must be sensed before the force and moment producing devices on the vehicle can be activated to reduce the effects of gusts and wind shear on the airplane.

Feedforward control using direct gust and shear sensing is sequentially added to the control system by calculating the control deflections required to totally counter the forces and moments produced on the vehicle by the gusts. The linearized equations of motion are defined as

$$\dot{x} = Fx + Gu + Ju_g \tag{3-6}$$

where $u_g = [u_w \; w_w]^T$

The total excitation to the aircraft is zero if the controls are activated according to the control law

$$Gu + Ju_g = 0 \quad , \quad u = -G^{-1}J\,u_g \tag{3-7}$$

For the application described in this report, the control effectiveness matrix G is singular, so a generalized solution to the control law of Equation (3-7) is required. This can be obtained by considering the minimum of the mathematical norm

$$\left|\left|Gu + Ju_g\right|\right|_q = (u^T G^T + u_g^T J^T)\,\underline{q}\,(Gu + Ju_g) \tag{3-8}$$

which yields a control law

$$u = -(G^T \underline{q} G)^{-1} G^T J\,u_g \tag{3-9}$$

A more detailed discussion of gust and shear alleviation using the method of direct measurements of the gusts and wind shears is given in References 7, 8 and 9. For several of the applications described in this report, only the throttle was driven by the sensed wind shear.

3.3 MULTICONTROLLER REGULATOR DESIGN

The quadratic performance index of linear optimal control serves as a criteria for the regulator design investigated in this program. In all cases, it was assumed that the inertial states could be measured directly without the use of Kalman filtering or other forms of state estimation. For many states, such as pitch angle and pitch rate, this approach appears justified because the measurements are made directly with respect to an inertial axis system. Air data measurements (such as an angle of attack measurement device) sense a combination of inertial (steady air mass) quantities and gusts, or environmental quantities. They are then used in combination with the inertial measurements to obtain direct estimates of the environmental quantities.

During this study it was assumed that the aircraft and disturbance states are measured with sensors that are noise free. In practice, the assumption of noise free inertial quantity measurements is a good assumption. States derived from air data measurements usually require filtering. The required filtering is a function of the individual application and can be done really successfully only by experimentation. In practice, it is found that accurate knowledge of the vehicle stability and control derivatives is of utmost importance. The plant noise is usually attributable to unknown derivatives or higher order modes excluded from the original vehicle model equations of motion. Filtering should be designed to attenuate the higher frequency noise or "observation spillover" excluded from the plant model description. As shown in Section 3.5, robust deterministic observers, based upon noise free measurements, can be designed as low pass filters that would have the desired result of attenuating the higher frequency plant noise associated with reduced order modeling.

The quadratic performance index of linear optimal control represents an input-output approach to control system design. In general, the closed-loop eigenvalues are a direct function of the transmission zeros of the system and the weighting matrices in the performance index. The closed-loop eigenvalues asymptotically tend toward these transmission zeros as the output weighting becomes large with respect to the input (Reference 10). The response to a command input would then tend to resemble the response of a Butterworth filter.

In the gust alleviation application, the input is the turbulence or wind shear vector, not the actual controllers. Therefore, the optimal response of the system should be Butterworth in behavior with respect to a turbulence input rather than a command. The problem then reduces to one of defining a performance index or optimal closed-loop system that reflects the proper inputs.

The system is defined by the linearized equations of motion

$$\begin{aligned} \dot{x}(t) &= Fx(t) + Gu(t) + Ju_g(t) \\ y(t) &= Hx(t) \end{aligned} \tag{3-10}$$

where $x^T(t) = [\Delta u_{PG}(t),\ \Delta w_{PG}(t),\ q(t),\ \Delta\theta(t)]$, $u^T = [\delta_t(t),\ \delta_e(t)]$ and $u_g(t)$ represents the shear/gust vector. The matrices F, G and J represent, respectively, the system matrix of dimensional stability derivatives, the control effectiveness matrix of dimensionalized control derivatives and the gust effectiveness matrix. It is assumed that the airspeed is closely approximated by

$$\begin{aligned} \Delta u_{PA} &= \Delta u_{PG} + u_w \\ \Delta w_{PA} &= \Delta w_{PG} + w_w \end{aligned} \tag{3-11}$$

The state Δu_{PG} then represents the inertial velocity or airspeed before the vehicle encounters the gust or shear. The gust or shear represents a perturbation input to the system.

A performance index is defined as

$$V = \min_{u_g} \int_0^\infty [y^T \underline{Q} y + u_g^T \underline{R} u_g]\, dt \tag{3-12}$$

that yields a closed-loop system matrix

$$\dot{x} = (F - JK)x + Gu_c + J u_g \tag{3-13}$$

This closed-loop matrix would define a system whose response is optimal, i.e. Butterworth with respect to a gust or shear input.

The system realization problem is to define a feedback control law $u = -K_1 x$ such that the closed-loop system matrix is the same as the system matrix defined by Equation (3-13), i.e. find K_1 such that

$$F - JK = F - GK_1$$

$$K_1 = G^{-1}JK \doteq (G^T G)^{-1} G^T JK \tag{3-14}$$

An alternate method is to define an output matrix H_1 such that

$$H_1 (Is - F)^{-1} G = H(Is - F)^{-1} J \tag{3-15}$$

thereby guaranteeing that the transfer function matrix of the outputs y_1 with respect to the control inputs would be the same as the matrix of transfer function y with respect to the gust or shear inputs. The performance index

$$V = \min_{u} \int_0^\infty (x^T H_1^T \underline{q} H x + u^T \underline{r} u)\, dt \tag{3-16}$$

then yields a control law $u = -K_1 x$ that would produce an optimal response with respect to the gust and shear inputs rather than the control inputs, although the system would be mechanized in terms of the control inputs.

3.4 MULTICONTROLLER DESIGN

It is possible, theoretically, to counter exactly the forces and moments produced by the wind disturbance with the three controllers, throttle, elevator, and spoilers used in a feedforward control law without feedback. The aircraft dynamics are given by the equation

$$\begin{bmatrix} \Delta\dot{u}_{PG} \\ \Delta\dot{w}_{PG} \\ \dot{q} \\ \Delta\dot{\theta} \end{bmatrix} = F \begin{bmatrix} \Delta u_{PG} \\ \Delta w_{PG} \\ q \\ \Delta\theta \end{bmatrix} + G \begin{bmatrix} \delta_t \\ \delta_e \\ \delta_{sp} \end{bmatrix} + J \begin{bmatrix} u_w \\ w_w \end{bmatrix} \tag{3-17}$$

$$
\begin{aligned}
\Delta u_{PG} &= u_{PG} - U_o \\
\Delta w_{PG} &= w_{PG} - W_o \\
\Delta\theta &= \theta - \theta_o \\
J_{i1} &= F_{i1} \\
J_{i2} &= F_{i2} \qquad\qquad i = 1, \ldots 4
\end{aligned}
$$

where U_o, W_o, and θ_o are trim values. The feedforward control law is given by the equation:

$$
\begin{bmatrix} \delta_t \\ \delta_e \\ \delta_{sp} \end{bmatrix} = - G^{-1} J \begin{bmatrix} u_w \\ w_w \end{bmatrix} \tag{3-18}
$$

Since with three controllers, independent control over the three degrees of freedom of longitudinal motion is possible; the control law of Equation (3-18) counters the effects of the wind disturbance exactly. It is assumed that the exact measurement of wind velocities is possible. As will be shown in Section 4, the spoiler control activity is excessive with the use of this control law indicating insufficient spoiler control effectiveness for this application.

The objective of this study is to use the two controllers, the throttle and elevator, to alleviate the effects of wind disturbance.

The two-controller control system is based on the performance index that would yield a control law that would produce an optimal response with respect to the elevator and throttle control inputs. Four types of control systems are designed. These are:

- Control system 1 consists of a feedback part that regulates the inertial speed and altitude and a feedforward part that drives the throttle using the sensed gust signals to minimize the deviation in the inertial speed.

- Control system 2 consists of a feedback part that regulates the inertial speed, altitude, and altitude rate and a feedforward part that drives the throttle using the sensed gust signals to minimize the deviation in inertial speed.

- Control system 3 regulates airspeed and altitude or airspeed altitude and altitude rate.

- Control system 4 is obtained by minimizing the deviation in the desired energy profile to fly constant airspeed using the throttle and minimizing the deviation in the glide path using the elevator.

Control systems can be designed either to fly constant inertial speed or constant airspeed on the glide slope. The control system structure is shown in Figure 3. Figure 3a shows the feedback regulation of either the inertial speed or airspeed through the feedback of the appropriate measured quantity. Figure 3b shows the regulation of the inertial speed through the feedback of the measured inertial speed and a feedforward part that uses the measured wind disturbance to drive the control surfaces. The feedback gain $\bar{K}$ is determined using, for example, optimal control method and the gain K_1 using a generlized inverse method. Figure 3c shows the regulation of the airspeed using the measured inertial speed and wind disturbance. The feedback and feedforward gains are equal and same as the gain K in Figures 3a and 3b. The inertial/airspeed is regulated by the control laws in the presence of both steady and accelerating winds.

Control System 1

The aircraft dynamics used for the design of the feedback regulator are given by:

$$\begin{bmatrix} \Delta\dot{u}_{PG} \\ \Delta\dot{w}_{PG} \\ \dot{q} \\ \Delta\dot{\theta} \end{bmatrix} = F \begin{bmatrix} \Delta u_{PG} \\ \Delta w_{PG} \\ q \\ \Delta\theta \end{bmatrix} + G \begin{bmatrix} \delta_t \\ \delta_e \end{bmatrix} + J \begin{bmatrix} u_w \\ w_w \end{bmatrix} \tag{3-19}$$

$$\Delta\dot{h} = \sin\theta_o\, u_{PG} - \cos\theta_o\, w_{PG} + (U_o \cos\theta_o + W_o \sin\theta_o)\Delta\theta$$

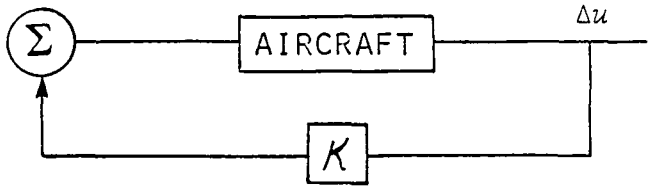

Δu - INERTIAL OR AIRSPEED

Figure 3a. INERTIAL OR AIRSPEED REGULATION

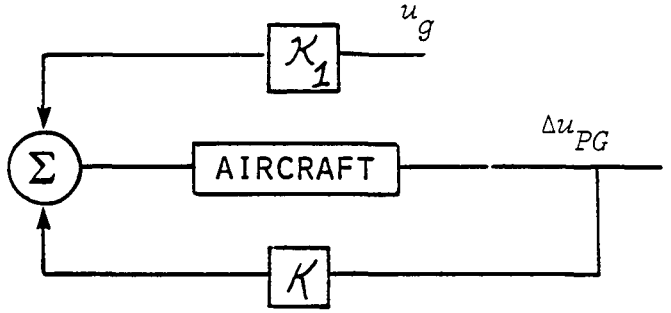

Figure 3b. INERTIAL SPEED REGULATION AND DIRECT GUST ALLEVIATION

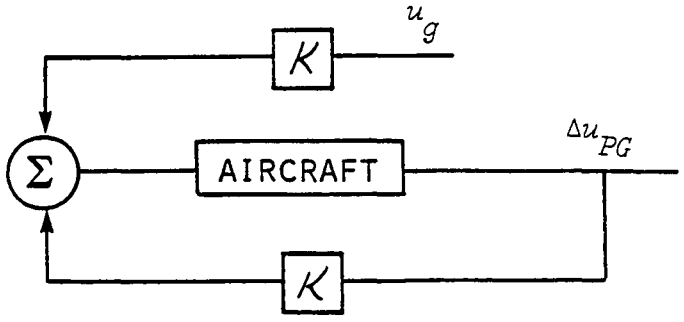

Figure 3c. IF INERTIAL SPEED IS MEASURED, BUT AIRSPEED IS REGULATED

Figure 3. INERTIAL AND AIRSPEED REGULATION

$$\Delta u_{PG} = u_{PG} - U_o$$
$$\Delta w_{PG} = w_{PG} - W_o$$

where U_o, W_o and θ_o are trim values and Δh is the error in altitude.

The feedback regulator is formulated using the control law by minimizing the performance index:

$$V = \frac{1}{2}\int_0^\infty (q_1 \Delta u_{PG}^2 + q_2 \Delta h^2 + r_1 \dot{\delta}_t^2 + r_2 \delta_e^2) dt \tag{3-20}$$

The objectives specified in the performance index are to minimize deviations in the inertial velocity and altitude to keep the aircraft on the glide path.

The performance index does not include any wind disturbance terms. The control law obtained by the performance index minimization regulates against the wind disturbance and minimizes the deviation from the glide path.

The minimization of the performance index is accomplished through the use of the Euler-Lagrange equation. The performance index is minimized for several sets of q_i, r_i, $i=1,2$ and the set that produces good regulation for the worst case shear is chosen. The feedback control law is given by

$$\begin{bmatrix} \delta_t \\ \\ \delta_e \end{bmatrix} = -\underline{r}^{-1} G^T P \begin{bmatrix} \Delta u_{PG} \\ \Delta w_{PG} \\ q \\ \Delta\theta \\ \Delta h \end{bmatrix} = K \begin{bmatrix} \Delta u_{PG} \\ \Delta w_{PG} \\ q \\ \Delta\theta \end{bmatrix} + K_c \Delta h \tag{3-21}$$

$$\underline{r} = \begin{bmatrix} r_1 & 0 \\ 0 & r_2 \end{bmatrix}$$

where P is the solution of the Riccati equation. The performance index weighting factors, the gain matrix and the closed-loop transfer functions are given in Appendix B.

The altitude error, Δh, is given by

$$\Delta h = h_c - h \tag{3-22}$$

where h_c is the desired altitude and h is the actual altitude. The desired altitude is computed as

$$h_c = K_h R \tag{3-23}$$

where R is the range to touchdown and the gain K_h is determined from the glide slope angle as

$$K_h = |\sin \gamma_0| \tag{3-24}$$

The feedforward control is based on measuring the gust (shear and turbulance) signals and using them directly to drive the control surfaces to counter the forces and moments produced by the gusts. It is possible, as discussed previously, to completely counter the forces and moments produced by the gusts using the three controllers, the elevator, throttle and the spoilers.

The feedforward control is formulated using two controllers, the elevator and the throttle. There are several ways to formulate the feedforward control system. One way is to minimize the cost function

$$J = (Gu+Ju_g)^T(Gu+Ju_g) \tag{3-25}$$

where u_g is the gust vector, u is the control vector, and J is the gust effectiveness matrix. The resulting controller is given by

$$u = -(G^TG)^{-1}G^TJu_g \tag{3-26}$$

A second possible feedforward control law is to use the sensed gust signals to drive the throttle and elevator to minimize the deviation in velocities along the X and Z axes. A third possible control law is to drive the

throttle using the sensed horizontal gusts and the elevator using the sensed vertical gust to minimize the deviations in velocities along X and Z axes. For the severity of wind disturbance considered in this study, these feedforward control laws would introduce undesirable excursions in angular motions of the aircraft. Therefore, the feedforward control system formulated uses the sensed gust signals to drive only the throttle. The inertial velocity equation with gust term is given as

$$\Delta\dot{u}_{PG} = X_u \Delta u_{PG} + X_w \Delta w_{PG} + (X_q - W_o)q - g \cos\theta_o + X_{\delta_t}\delta_t + X_{\delta_e}\delta_e + X_u u_w + X_w w_w \qquad (3\text{-}27)$$

The feedforward control law is given by

$$\delta_{t_f} = -\frac{X_u}{X_{\delta_t}} u_w - \frac{X_w}{X_{\delta_t}} \overline{w_w} = K_1 \begin{bmatrix} u_w \\ w_w \end{bmatrix} \qquad (3\text{-}28)$$

where the sensed gust signals drive the throttle directly to alleviate the effects due to wind gusts on the inertial velocity along the X axis. The coupling effects due to other responses are alleviated through feedback regulation. The complete control law is given by

$$\begin{bmatrix} \delta_t \\ \delta_e \end{bmatrix} = K \begin{bmatrix} \Delta u_{PG} \\ \Delta w_{PG} \\ q \\ \Delta\theta \end{bmatrix} + K_c \Delta h + \begin{bmatrix} k_{11} & k_{12} \\ 0 & 0 \end{bmatrix} \begin{bmatrix} u_w \\ w_w \end{bmatrix} \qquad (3\text{-}29)$$

The complete control system is shown in Block diagram form in Figure 4. The outer loop determines the proper controls for minimizing the glide slope error.

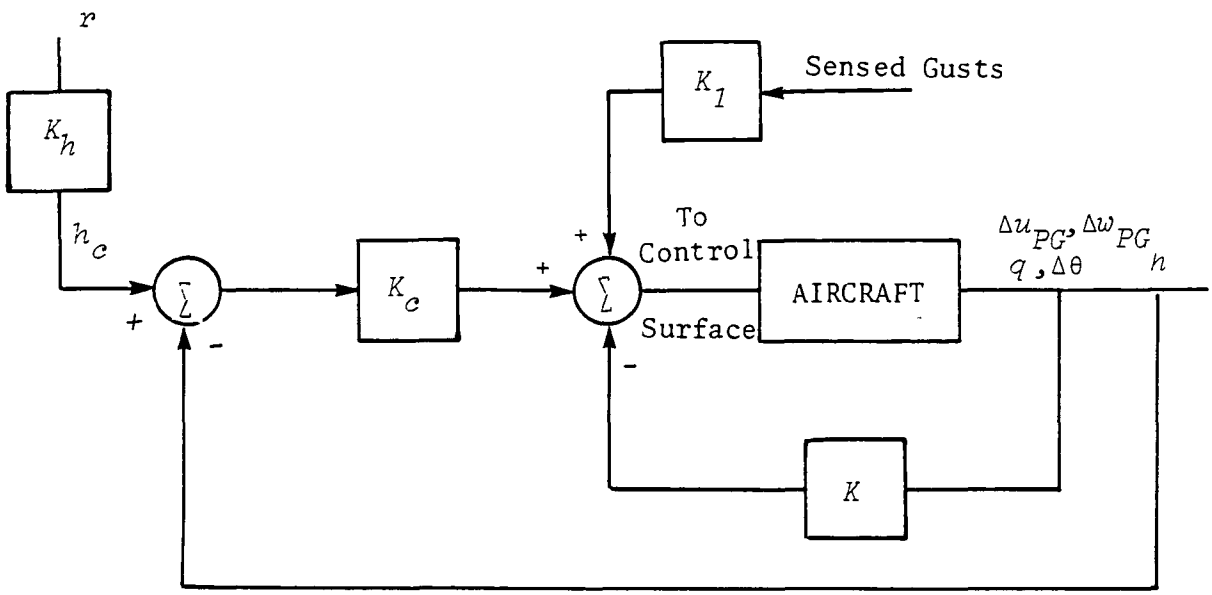

Figure 4. BLOCK DIAGRAM OF CONTROL SYSTEM 1

Control System 2

The aircraft dynamics used for the design of control system 2 is given by

$$\begin{bmatrix} \Delta\dot{u}_{PG} \\ \Delta\dot{w}_{PG} \\ \dot{q} \\ \Delta\dot{\theta} \end{bmatrix} = F \begin{bmatrix} \Delta u_{PG} \\ \Delta w_{PG} \\ q \\ \Delta\theta \end{bmatrix} + G \begin{bmatrix} \delta_t \\ \delta_e \end{bmatrix} + J \begin{bmatrix} u_w \\ w_w \end{bmatrix}$$

$$\Delta\dot{h} = \sin\theta_o \Delta u_{PG} - \cos\theta_o \Delta w_{PG} + (U_o \cos\theta_o + W_o \sin\theta_o)\Delta\theta$$

$$\Delta\ddot{h} = (X_u \sin\theta_o - Z_u \cos\theta_o)\Delta u_{PG} + (X_w \sin\theta_o - Z_w \cos\theta_o)\Delta w_{PG}$$

$$+ (X_q \sin\theta_o - Z_q \cos\theta_o)q + (X_{\delta_t} \sin\theta_o - Z_{\delta_t} \cos\theta_o)\delta_t$$

$$+ (X_{\delta_e} \sin\theta_o - Z_{\delta_e} \cos\theta_o)\delta_e \qquad (3\text{-}30)$$

$$\Delta u_{PG} = u_{PG} - U_o$$
$$\Delta w_{PG} = w_{PG} - W_o$$
$$\Delta\theta = \theta - \theta_o$$

where U_o, W_o and θ_o are trim values. Derivation of $\Delta\ddot{h}$ equation is given in Appendix A.

The feedback control law is formulated by minimizing the performance index:

$$V = \frac{1}{2}\int_0^\infty (q_1\,\Delta u_{PG}^2 + q_2\,\Delta h^2 + q_3\,\Delta\dot{h}^2 + r_1\,\delta_t^2 + r_2\,\delta_e^2)dt \qquad (3\text{-}31)$$

The objectives specified in the performance index are to minimize the deviations in the inertial velocity, altitude, and altitude rate. Since the altitude rate is proportional to the potential energy rate, inclusion of this term in the performance index can be considered as minimizing the deviation in the potential energy rate. The inclusion of the rate term in the performance index will provide lead information about the deviation from the glide path due to wind disturbance. The feedback control law is given by

$$\begin{bmatrix}\delta_t\\ \delta_e\end{bmatrix} = -R^{-1}G^TP\begin{bmatrix}\Delta u_{PG}\\ \Delta w_{PG}\\ q\\ \Delta\theta\\ \Delta h\\ \Delta\dot{h}\end{bmatrix} = K\begin{bmatrix}\Delta u_{PG}\\ \Delta w_{PG}\\ q\\ \Delta\theta\end{bmatrix} + K_{c_1}\Delta h + K_{c_2}\Delta\dot{h} \qquad (3\text{-}32)$$

where P is the solution of the Riccati equation. The performance index weighting factors, the gain matrix and the closed-loop transfer functions are given in Appendix B.

The altitude error and the altitude rate are given by

$$\Delta h = |\sin \gamma_o| R, \quad \Delta \dot{h} = |\sin \gamma_o| \dot{R} \tag{3-33}$$

where R and $\dot{R}$ are the range and the rate of change of range. The feedforward control is the same as the feedforward control of control system 1:

$$\delta_{t_f} = -\frac{X_u}{X_{\delta_t}} u_w - \frac{X_w}{X_{\delta_t}} w_w = K_1 \begin{bmatrix} u_w \\ w_w \end{bmatrix} \tag{3-34}$$

The complete control system is shown in block diagram form in Figure 5.

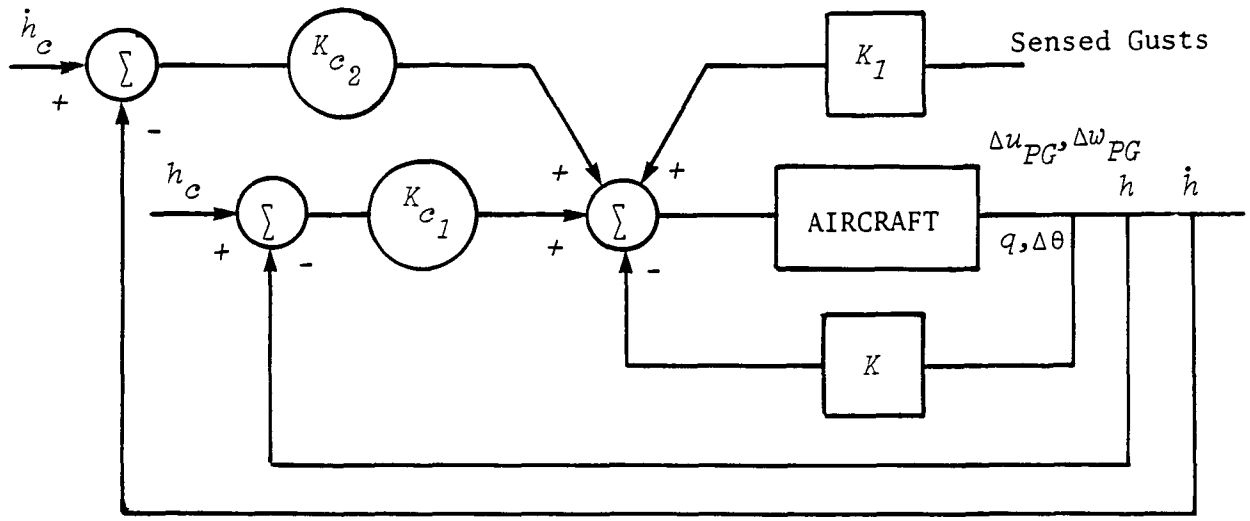

Figure 5. BLOCK DIAGRAM OF CONTROL SYSTEM 2

Control System 3

The objectives in the design of control systems 1 and 2 were to minimize the deviation in the inertial speed and the glide path. The performance indices used in the design of these control systems can also be used to design a control that minimizes the deviation in the airspeed and glide path. The two performance indices, the first minimizing the deviations in the airspeed and altitude, and the second minimizing the deviations in airspeed, altitude, and altitude rate, are given as:

$$V_1 = \frac{1}{2}\int_0^\infty (q_1\Delta u_{PA}^2 + q_2\Delta h^2 + r_1\delta_t^2 + r_2\delta_e^2)\,dt$$

$$V_2 = \frac{1}{2}\int_0^\infty (q_1\Delta u_{PA}^2 + q_2\Delta h^2 + q_3\Delta \dot{h}^2 + r_1\delta_t^2 + r_2\delta_e^2)\,dt$$

$$\Delta u_{PA} = \Delta u_{PG} + u_w \tag{3-35}$$

where Δu_{PA} is the perturbation in the airspeed. The dynamic equations are as defined by Equation (3-19) and Equation (3-30). The same weighting factors used in control systems 1 and 2 are used resulting in the same gain matrices.

The feedback control law obtained from the first performance index is given by

$$\begin{bmatrix} \delta_t \\ \delta_e \end{bmatrix} = -\underline{r}^{-1} G^T P \begin{bmatrix} \Delta u_{PA} \\ \Delta w_{PG} \\ q \\ \Delta\theta \\ \Delta h \end{bmatrix} = K \begin{bmatrix} \Delta u_{PA} \\ \Delta w_{PG} \\ q \\ \Delta\theta \end{bmatrix} + K_c \Delta h \tag{3-36}$$

where Δh is as defined by Equation (3-22).

It was necessary to change the gain on airspeed to the throttle, the first element K_{11} of K, as defined by:

$$K_{11} = \frac{aX_u}{X_{\delta_t}} \Delta u_{PA} = \frac{aX_u}{X_{\delta_t}} (\Delta u_{PG} + u_w) \tag{3-37}$$

This gain is determined based on the feedforward control law as defined by Equation (3-28) with the sign on the gain on u_w changed. The factor a was determined to obtain good airspeed regulation for the severe shear. The feedback control law with the feedback of inertial velocities is given by:

$$\begin{bmatrix} \delta_t \\ \delta_e \end{bmatrix} = K \begin{bmatrix} \Delta u_{PG} \\ \Delta w_{PG} \\ q \\ \Delta\theta \end{bmatrix} + K_c \Delta h \tag{3-38}$$

where the gain on Δu_{PG} to δ_t is as defined by Equation (3-37). The feedforward control law is given by

$$\delta_{t_f} = \frac{aX_u}{X_{\delta_t}} u_w - \frac{X_w}{X_{\delta_t}} w_w = K_1 \begin{bmatrix} u_w \\ w_w \end{bmatrix} \tag{3-39}$$

The gains on Δu_{PG} and u_w to throttle are the same. The feedforward control changes the inertial speed along the X-axis proportionately to the horizontal wind speed and compensates directly for the vertical wind. If the airspeed is measured and fed back to the throttle with a sufficiently high gain, feedback regulation will be sufficient to alleviate the effects of wind disturbance. The full control law is given by

$$\begin{bmatrix} \delta_t \\ \delta_e \end{bmatrix} = K \begin{bmatrix} \Delta u_{PG} \\ \Delta w_{PG} \\ q \\ \Delta\theta \end{bmatrix} + K_c \Delta h + K_1 \begin{bmatrix} u_w \\ w_w \end{bmatrix} \tag{3-40}$$

The final gain matrices and the closed-loop transfer functions are given in Appendix B. The control system is shown in block diagram form in Figure 6.

The second performance index in Equation (3-35) includes the altitude rate in the performance index. The complete control law including the feedback and feedforward parts is given by

$$\begin{bmatrix} \delta_t \\ \delta_e \end{bmatrix} = K \begin{bmatrix} \Delta u_{PG} \\ \Delta w_{PG} \\ q \\ \Delta\theta \end{bmatrix} + K_{c_1} \Delta h + K_{c_2} \dot{\Delta h} + K_1 \begin{bmatrix} u_w \\ w_w \end{bmatrix} \tag{3-41}$$

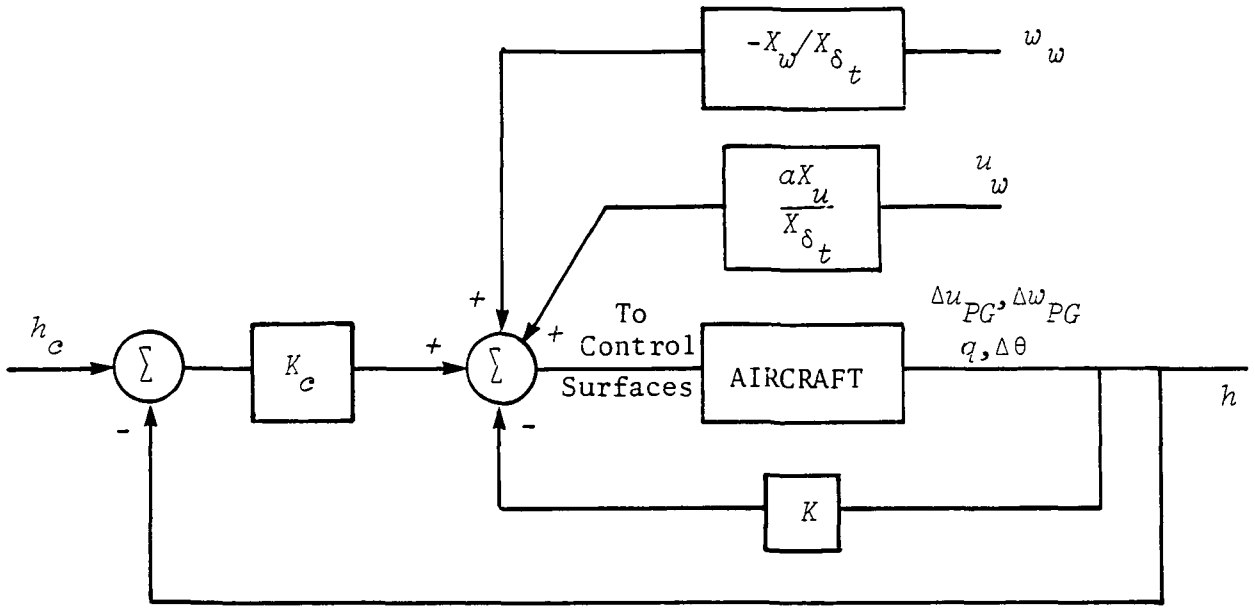

Figure 6. BLOCK DIAGRAM FOR CONTROL SYSTEM 3

The gains on Δu_{PG} and u_w to the throttle are the same and as defined by Equation (3-37). The performance index weighting factors, the gain matrix and the closed-loop transfer functions are given in Appendix B. The error in altitude and altitude rate are as defined by Equation (3-33). The energy probe can be used as a measure of $\dot{h}$ in the feedback loop.

Control System 4

Control system 4 is designed in two stages. In the first stage a performance is defined with the objective of minimizing the deviation in the energy expended by the aircraft with respect to the airmass. The total specific energy expended by the aircraft with respect to the airmass is given by the expression

$$E = h + \frac{u_{PA}^2}{2g} \tag{3-42}$$

where u_{PA} is the actual airspeed.

The desired energy to be expended by the aircraft with respect to the airmass to stay on the glide path is given by

$$E_c = h_c + \frac{U_o^2}{2g} \tag{3-43}$$

where h_c is the proper altitude to stay on the glide path and U_o is the reference airspeed.

A performance index that minimizes the deviation in the energy using the throttle control is defined as

$$V = \frac{1}{2}\int_0^\infty (q\Delta E^2 + r\delta_t^2)dt \tag{3-44}$$

subject to the dynamics

$$\begin{bmatrix} \Delta\dot{u}_{PA} \\ \Delta\dot{w}_{PG} \\ \dot{q} \\ \Delta\dot{\theta} \end{bmatrix} = F \begin{bmatrix} \Delta u_{PA} \\ \Delta w_{PG} \\ q \\ \Delta\theta \end{bmatrix} + G\delta_t$$

$$\Delta\dot{E} = \dot{E} - \dot{E}_c = \dot{h} - \dot{h}_c + \frac{u_{PA}\dot{u}_{PA}}{g} \tag{3-45}$$

The $\Delta\dot{E}$ equation is expressed in terms of the stability and control derivatives. The derivation of the $\Delta\dot{E}$ equation is given in Appendix A. The energy term in the performance index could have been expressed as a function of altitude and airspeed. However, this would have resulted in the velocity term raised to the fourth power. Including the energy term directly in the performance index and defining the dynamic equation for ΔE will result in a straightforward synthesis of the control law with a direct feedback from energy. Minimization of the performance index results in the control law

$$\delta_t = K_1 \begin{bmatrix} \Delta u_{PA} \\ \Delta w_{PG} \\ q \\ \Delta\theta \\ \Delta E \end{bmatrix}$$

$$\Delta E = h - h_c + \frac{u_{PA}^2}{2g} - \frac{U_o^2}{2g} \tag{3-46}$$

The energy sensor probe measures the total energy rate with respect to the airmass as defined by

$$\dot{E} = \dot{h} + \frac{u_{PA}\dot{u}_{PA}}{g} \tag{3-47}$$

The energy can be obtained from energy rate by integrating Equation (3-47) with the proper initial condition for use in the feedback loop. In the second stage, another performance index is defined that minimizes the deviation in airspeed and altitude using the elevator subject to the dynamics as defined by Equation (3-20).

$$V = \frac{1}{2}\int_0^\infty (q_1 \Delta u_{PA}^2 + q_2 \Delta h^2 + r\delta_e^2)\,dt \tag{3-48}$$

Minimization of the performance index yields the control law

$$\delta_e = K_2 \begin{bmatrix} \Delta u_{PA} \\ \Delta w_{PG} \\ q \\ \Delta\theta \\ \Delta h \end{bmatrix} \tag{3-49}$$

The complete control system is obtained by combining the control laws of Equations (3-46) and (3-49) and is given by

$$\begin{bmatrix} \delta_t \\ \delta_e \end{bmatrix} = K \begin{bmatrix} \Delta u_{PA} \\ \Delta w_{PG} \\ q \\ \Delta\theta \end{bmatrix} + K_E \Delta E + K_c \Delta h \tag{3-50}$$

where the gain matrices K, K_E and K_c are formed from K_1 and K_2. The feedforward control that uses the sensed wind shear and turbulence signals to drive the control surfaces is not required. The control system block diagram is given in Figure 7. The final gain matrix and the closed-loop transfer functions are given in Appendix B. A performance index could have been defined including the energy term, the throttle and the elevator to perform an integrated design.

However, this would have resulted in undesirable feedback from the energy term to the elevator. The throttle can change the energy of the aircraft with respect to the airmass appropriately by proper change in thrust level. Consequently, the control system design was carried out separately.

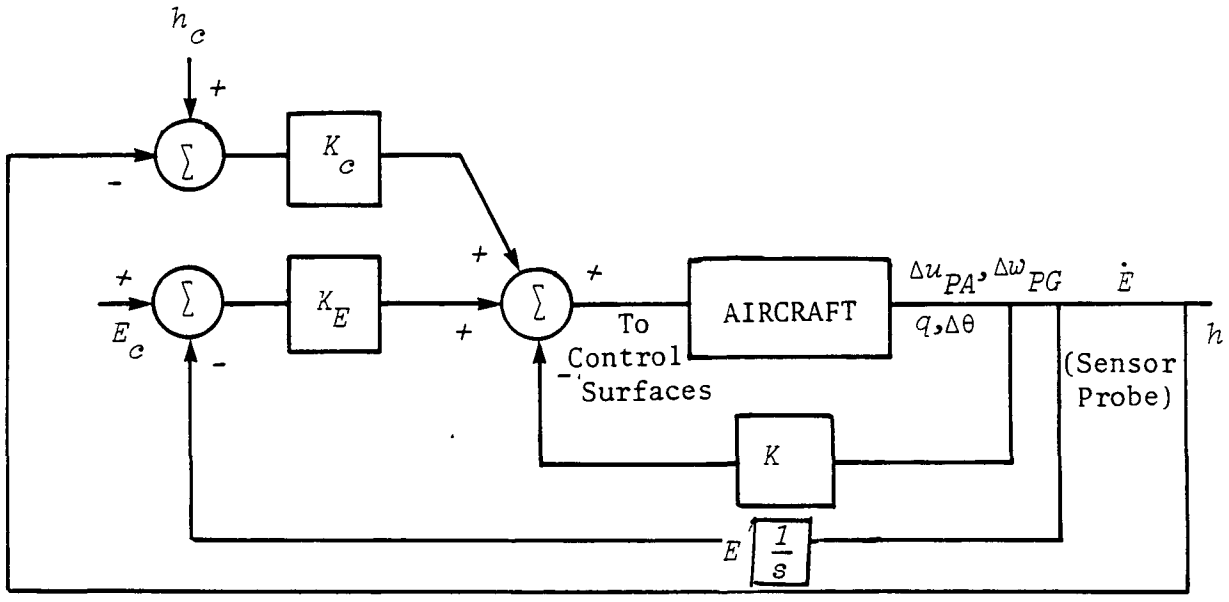

Figure 7. BLOCK DIAGRAM FOR CONTROL SYSTEM 4

3.5 OBSERVER METHODS OF SYNTHESIS

Although much progress has been made, the systems that result from the application of modern control theory are generally too complex to be implemented practically. Feedback from all the states to each of the controllers is generally required. In an attempt to avoid or sidestep the requirement that all the states be measured, state estimator or observer systems have been devised in an attempt to reduce the number of required sensors or to improve the accuracy of the state measurements. This has led to a new crop of problems, including reduced robustness through reduction of gain and phase margins as compared to state feedback systems, and an increase in the order of the dynamic response of the system which always degrades the flying qualities of the airplane.

The observer designs are based upon the assumption that the sensors are in themselves noisy and accurate measurements of the corresponding motions of the aircraft cannot be made. Fictitious plant noise, either white or colored, is often added to the system description to improve the system sensitivity. In practice, the addition of fictitious plant noise is equivalent in many ways to an assumed reduction of sensor noise. But sensor noise in itself is an unjustified quantity; sensors used in aircraft have very low noise levels. To demonstrate, all one has to do is activate a pitch rate gyro or accelerometer and observe the very low noise level. The noise one usually observes on the output of an installed instrument is usually due to higher order modeling effects such as structural dynamics and vibration, and this should be represented as plant noise.

Because sensors in themselves are noise free, the observer design used in this study is deterministic. These observers depend upon accurate knowledge of the stability and control derivatives of the aircraft model, and, in fact, the robustness of the observer system depends upon this knowledge. In practice, this dependency is not too strong, because the poles of the observers are directly related to the zeros of the system transfer function matrix. Knowledge of stability derivatives such as Z_w, accurately obtained in a wind tunnel, are often dominant.

The original observer theory by Luenberger (Reference 11)was developed as a state reconstruction technique in which the output of the observer system approached, as time increased, the state that is to be reconstructed. The theory developed by Luenberger described deterministic observers which are in themselves unobservable and do not contribute to an increase in the order of the response of the system. In general, the poles of the observer can be chosen arbitrarily but this choice usually results in a requirement that the control input to the aircraft also is a control input to the observer system. In fact, by properly selecting the observer poles the observer system itself can be considerably simplified, as is shown in this section.

Consider the linearized, small perturbation equations of vehicle motion

$$\dot{x}(t) = Fx(t) + Gu(t) \qquad (3\text{-}51)$$
$$y(t) = Hx(t)$$

where x is the state vector, u the control input vector and y the measurement set such as a pitch rate gyro and accelerometer. The observer is of the form

$$\dot{z}(t) = Az(t) + By(t) + Du(t) \qquad (3\text{-}52)$$

subject to the conditions:

1. The matrix A is chosen such that the observer is stable.

2. A transformation T can be found such that
$$TF-AT = BH \qquad (3\text{-}53)$$

3. $TG = D$ where F G and H are defined above. (3-54)

In order for the observer to be as simple as possible, not requiring measurements of the input to the aircraft but operating entirely on the system outputs, the following conditions must also be satisfied:

4. The observer poles, defined from $|Is-A| = 0$ are chosen from the transmission zeros of the system, defined by $|H(Is-F)^{-1}G| = 0$ (3-55)

5. $TG = D = 0$ (3-56)

6. The matrices H and T constitute a transformation M

$$\begin{bmatrix} y \\ z \end{bmatrix} = Mx \tag{3-57}$$

such that the equivalent output and observer control law is defined by

$$u = -Kx = -KM^{-1}\begin{bmatrix} y \\ z \end{bmatrix} \tag{3-58}$$

The condition that $TG = D = 0$ is automatically satisfied if the observer poles are chosen from among the system transmission zeros. Not only does this simplify the observer network but also reduces the number of required measurements of the vehicle dynamics. Condition 6 implies that the output measurements must be such that the aircraft dynamics are completely observable through the output. This condition is usually easily satisfied with an accelerometer or angle of attack sensor.

Example:

Observers can often be used to enhance the observability of the system in the sense that much lower feedback gains are often required to obtain the same closed-loop dynamic behavior as compared to state feedback. This comes about because the feedback through the observers is shaped as a function of frequency and this can often be used to the advantage of the designer. Consider the system

$$\begin{bmatrix} \dot{x}_1 \\ \dot{x}_2 \\ \dot{x}_3 \end{bmatrix} = \begin{bmatrix} 0 & 2 & -1 \\ 1 & 6 & -12 \\ 1 & 6 & -11 \end{bmatrix}\begin{bmatrix} x_1 \\ x_2 \\ x_3 \end{bmatrix} + \begin{bmatrix} 1 \\ 0 \\ 0 \end{bmatrix}u$$

with a single measurement $y = x_1 - 2x_2 + 3x_3$. (3-59)

If it is assumed that it is for some reason desirable to alter the open-loop characteristic polynomial $D(s) = |Is-F| = s^3 + 5s^2 + 5s + 2$ to a closed-loop characteristic polynomial $\Delta(s) = |Is-F+GK| = s^3 + 5s^2 + 6s + 7$, then the state feedback control law is given by

$$u = 5x_2 - 6x_3 \tag{3-60}$$

According to condition (4), the poles of the observers can be chosen from among the system transmission zeros which, for this example, are the zeros of the transfer function

$$y/u(s) = \frac{s^2+6s+8}{s^3+5s^2+5s+2} = \frac{(s+2)(s+4)}{s^3+5s^2+5s+2} \tag{3-61}$$

This output transfer function represents a minimum phase, completely observable measurement so two output observers can be constructed with observer poles equal to the zeros of the output transfer function; i.e. $s_1 = -2$, $s_2 = -4$. The observers can then be chosen automatically as

$$\begin{aligned} \dot{z}_1 &= -4z_1 + y \\ \dot{z}_2 &= -2z_1 + y \end{aligned} \tag{3-62}$$

The matrix T of condition 6 listed above and the control law is most easily obtained by first transforming into the phase variable form

$$\begin{aligned} \dot{w} &= F_o w + G_o u \\ x &= Nw \end{aligned} \tag{3-63}$$

where

$$F_o = \begin{bmatrix} 0 & 1 & 0 \\ 0 & 0 & 1 \\ -2 & -5 & -5 \end{bmatrix} \quad G_o = \begin{bmatrix} 0 \\ 0 \\ 1 \end{bmatrix} \quad N = \begin{bmatrix} 6 & 5 & 1 \\ -1 & 1 & 0 \\ 0 & 1 & 0 \end{bmatrix} \tag{3-64}$$

The transformation $\begin{bmatrix} y \\ z \end{bmatrix} = Mx$ can then be determined as follows (Reference 12):

a) The elements of the first row of the matrix M are made up of the coefficients of the numerator polynomial of the output transfer function, i.e.

$$m_1 = [8 \quad 6 \quad 1] \tag{3-65}$$

b) The second row of the matrix is made up from the coefficients that result when $s+4$ has been factored out of the numerator polynomial of the output transfer function, i.e.

$$m_2(s) = \frac{s^2+6s+8}{s+4} = s+2 \tag{3-66}$$

so $$m_2 = [2 \quad 1 \quad 0]$$

c) Similarly, the third row is formed from the coefficients that result when the factor $s+2$ has been factored out of the numerator polynomial

$$m_3(s) = \frac{s^2+6s+8}{s+2} = s+4$$

so $$m_3 = [4 \quad 1 \quad 0] \tag{3-67}$$

This process is exactly the same as defining the matrix T in the equation

$$TF - AT = BH$$

when F and H are defined in the phase variable form.

The observer control law is then given by

$$u = -KM^{-1}\begin{bmatrix} y \\ z \end{bmatrix} = \frac{1}{2} z_1 - \frac{3}{2} z_2 \tag{3-68}$$

The closed loop system defined by the control law of Equation (3-68) has the same robustness or gain and phase margins as the state feedback system, but the system employing observers uses only one output or sensor, the feedback gains are much lower and the observers constitute low pass filters, useful for structural mode stabilization or noise suppression.

It is shown above that if the observer poles are chosen from among the zeros of the transfer functions, no plant input measurements are required in the observer synthesis for systems that are completely observable. For multicontroller systems, exactly the same principle holds except that the observer poles are chosen from the transmission zeros of the system, defined as the roots of the polynomial

$$|H(Is-F)^{-1}G| = 0 \tag{3-69}$$

when the system is defined by the standard equations of motion

$$\dot{x}(t) = Fx(t) + Gu(t)$$
$$y(t) = Hx(t)$$

As indicated by Equation (3-69), the transmission zeros are a function of the sensors or outputs as well as the controller inputs. In general, a robust output observer can be obtained if the system is completely controllable and observable with the chosen sensors and if the number of non-minimum phase transmission zeros is equal to $n-m$, where m is the number of sensors used. For an nth order system with m independent output measurements and p independent inputs, the maximum number of transmission zeros is given by

$$N = (n-p)\,\frac{m!}{(m-p)!\;p!} \tag{3-70}$$

Ordinarily, the number of transmission zeros exceeds the number of observers to be constructed so there is design freedom, as shown by the following example.

Consider the 4th order system given by

$$\begin{bmatrix} \dot{x}_1 \\ \dot{x}_2 \\ \dot{x}_3 \\ \dot{x}_4 \end{bmatrix} = \begin{bmatrix} -1 & 0 & 1 & 0 \\ 0 & -2 & 0 & 1 \\ 1 & 0 & -3 & 0 \\ 0 & 2 & 0 & -4 \end{bmatrix} \begin{bmatrix} x_1 \\ x_2 \\ x_3 \\ x_4 \end{bmatrix} + \begin{bmatrix} 1 & 1 \\ 0 & -1 \\ -1 & 0 \\ 0 & 1 \end{bmatrix} \begin{matrix} u_1 \\ u_2 \end{matrix}$$

$$\begin{bmatrix} y_1 \\ y_2 \\ y_3 \end{bmatrix} = \begin{bmatrix} 1 & 0 & -1 & 0 \\ 1 & 2 & 0 & 0 \\ 0 & 0 & 0 & 1 \end{bmatrix} \begin{bmatrix} x_1 \\ x_2 \\ x_3 \\ x_4 \end{bmatrix} \qquad (3\text{-}71)$$

According to Equation (3-70), the maximum number of transmission zeros of this system is

$$N = (n-p)\left[\frac{m!}{(m-p)!\ p!}\right] = (4-2)\left[\frac{3!}{1!\ 2!}\right] = 6 \qquad (3\text{-}72)$$

A maximum of two of a possible six transmission zeros must be minimum phase in order to be able to construct a stable output observer system. There are three sets of transmission zeros that can be used in the selection of the output observer poles. These three sets involve the outputs $(y_1 y_2)$, $(y_1 y_3)$ and $y_2, y_3)$ and produce the transmission zeros

$$\begin{aligned} (y_1\ y_2) \quad & -3s^2-20s-31 = -3(s+2.45)(s+4.215) \\ (y_1\ y_3) \quad & 3s^2-8s+6 = 3\left(s-\frac{4}{3} \pm \frac{1}{3}\, j\sqrt{2}\right) \\ (y_2\ y_3) \quad & 2s+6 = 2(s+3) \end{aligned} \qquad (3\text{-}73)$$

The system possesses five of a possible six transmission zeros and three are non-minimum phase. Any two can be chosen for the system design. The obvious choice is to design an output observer using the two measurements y_1 and y_2. The third measurement y_3 is not required. In fact, an observer set for the measurement pair $y_1 y_2$ is given by

$$\begin{bmatrix} \dot{z}_1 \\ \dot{z}_2 \end{bmatrix} = \begin{bmatrix} -2.45 & 0 \\ 0 & -4.215 \end{bmatrix} \begin{bmatrix} z_1 \\ z_2 \end{bmatrix} + \begin{bmatrix} -.45 & 2.90 \\ 2.215 & -6.43 \end{bmatrix} \begin{bmatrix} y_1 \\ y_2 \end{bmatrix} \qquad (3\text{-}74)$$

Appendix C defines a multicontroller observer configuration for the multivariable control system 1 defined previously in this section. It is included to show how the control system would actually be mechanized for flight test purposes.

Section 4
SIMULATION RESULTS

This section presents the simulation results of the TCV aircraft flying in a wind shear and turbulence environment on a 3^{o} glide slope for touchdown. The linearized model of the TCV aircraft, linearized for the landing flight condition, is used in the simulation. The flight conditions (trim conditions) are summarized as follows:

U_o (airspeed along X-axis) = 213.92 ft/sec
W_o (airspeed along Z-axis) = 8.63 ft/sec)
α_o (angle of attack) = 2.31^{o}
θ_o (pitch attitude) = $-.69^{o}$
γ_o (flight path angle) = -3^{o}
δ_t (throttle) = 9000 lb
δ_e (elevator) = 2.7^{o}
δ_{sp} (spoilers) = 0^{o}
Flaps = 40^{o}

Two severe shear profiles (Kennedy and Philadelphia incidents) and one moderate shear profile (Tower) are used in the simulation. These profiles define the wind velocities as a function of altitude. The turbulence is generated from the Dryden spectra. This turbulence is filtered to remove the low frequency content. The shear represents the low frequency part of the wind disturbance. A σ of 7.6 ft/sec is used for the Dryden spectra. The shear profiles and the generation of turbulence is given in Appendix A. Nonlinearities and engine dynamics were not included in this simulation.

The simulation results presented in this section are summarized as follows:

- Controls fixed simulation in a windshear and windshear and turbulence environment.
- Simulation with the elevator, throttle and spoilers driven by the sensed shear and turbulence signals.
- Single control (elevator) system simulation with Kennedy incident shear.

- Simulation of control system 1 (feedback only) with the Kennedy incident horizontal shear only.

- Simulation of control system 1 with both the horizontal and vertical Kennedy incident shear, the shear and turbulence, and the other two shear profiles (Philadelphia and Tower).

- Simulation of control system 2 with all the shear profiles.

- Simulation of control systems 3 and 4 with the Kennedy incident shear.

For the control-fixed simulation the following responses are shown: the shear and turbulence profiles, desired and actual altitude vs. range, perturbation in inertial velocity along the X-axis, altitude rate, the flight path angle, inertial angle of attack, pitch rate, pitch attitude, angle of attack with respect to the airmass, γ with respect to airmass, airspeed and time histories of shear and turbulence. For the feedforward control simulation, in addition to the above time histories, the control activities are shown. For the remainder of the simulations, the following responses are shown: the wind profile, the desired and actual altitude vs. range, perturbation in inertial velocity along the X-axis, the altitude rate, the flight path angle, angle of attack with respect to the airmass, pitch rate, pitch attitude, the airspeed, elevator and throttle control activities. All the responses shown are total.

The first set of simulation results shown are the airplane flying in a wind shear environment with the controls fixed. The Kennedy incident severe shear profile is used in the simulation. The time histories of the controls-fixed simulation are shown in Figure 8.

For almost the first 50 seconds, the vertical shear is practically zero. During this period, the horizontal shear has an initial increasing headwind component, then steadies out, and at about 35 seconds has a further

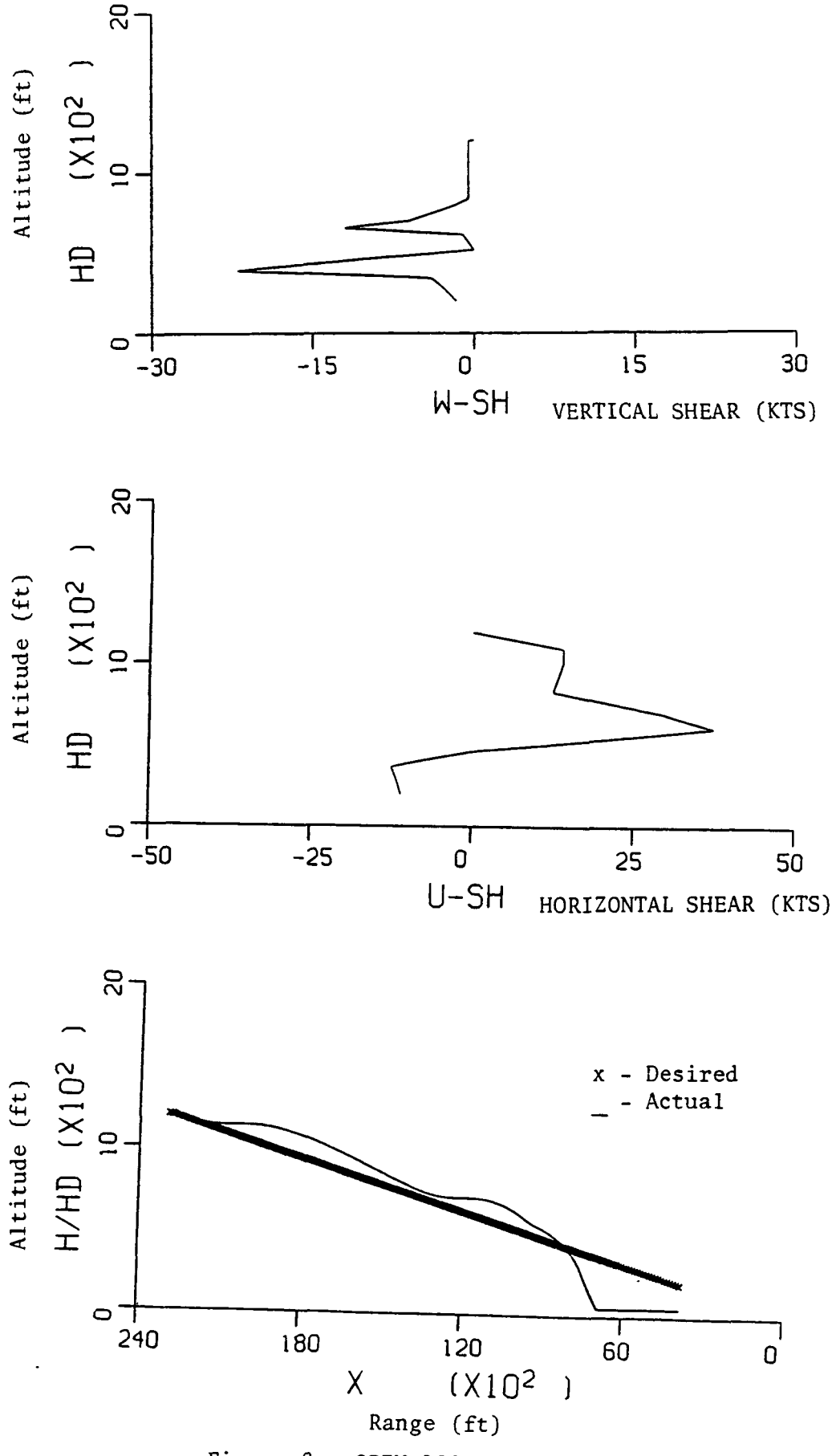

Figure 8. OPEN LOOP SIMULATION WITH KENNEDY SEVERE SHEAR

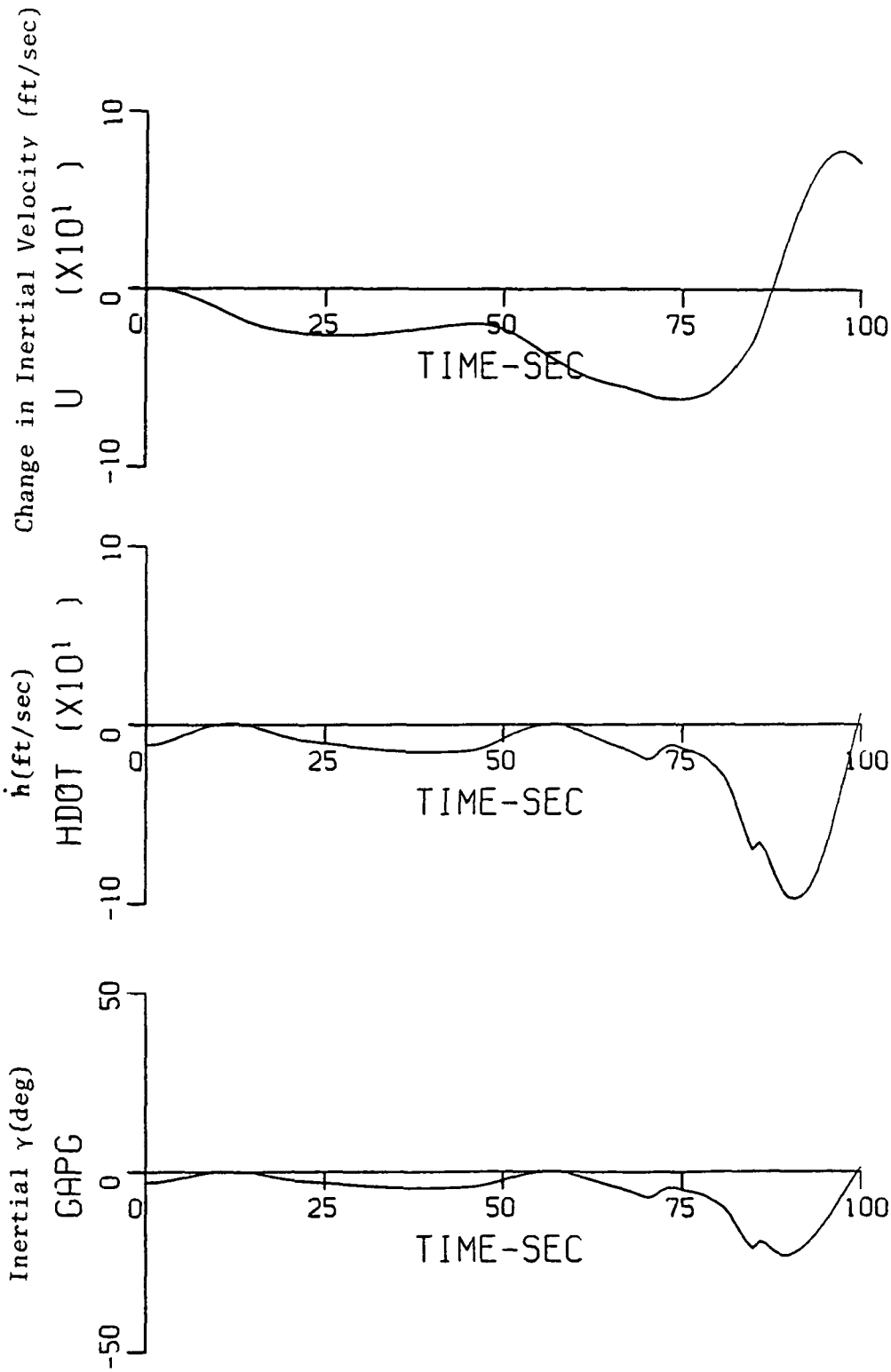

Figure 8. OPEN LOOP SIMULATION WITH
(Cont'd) KENNEDY SEVERE SHEAR

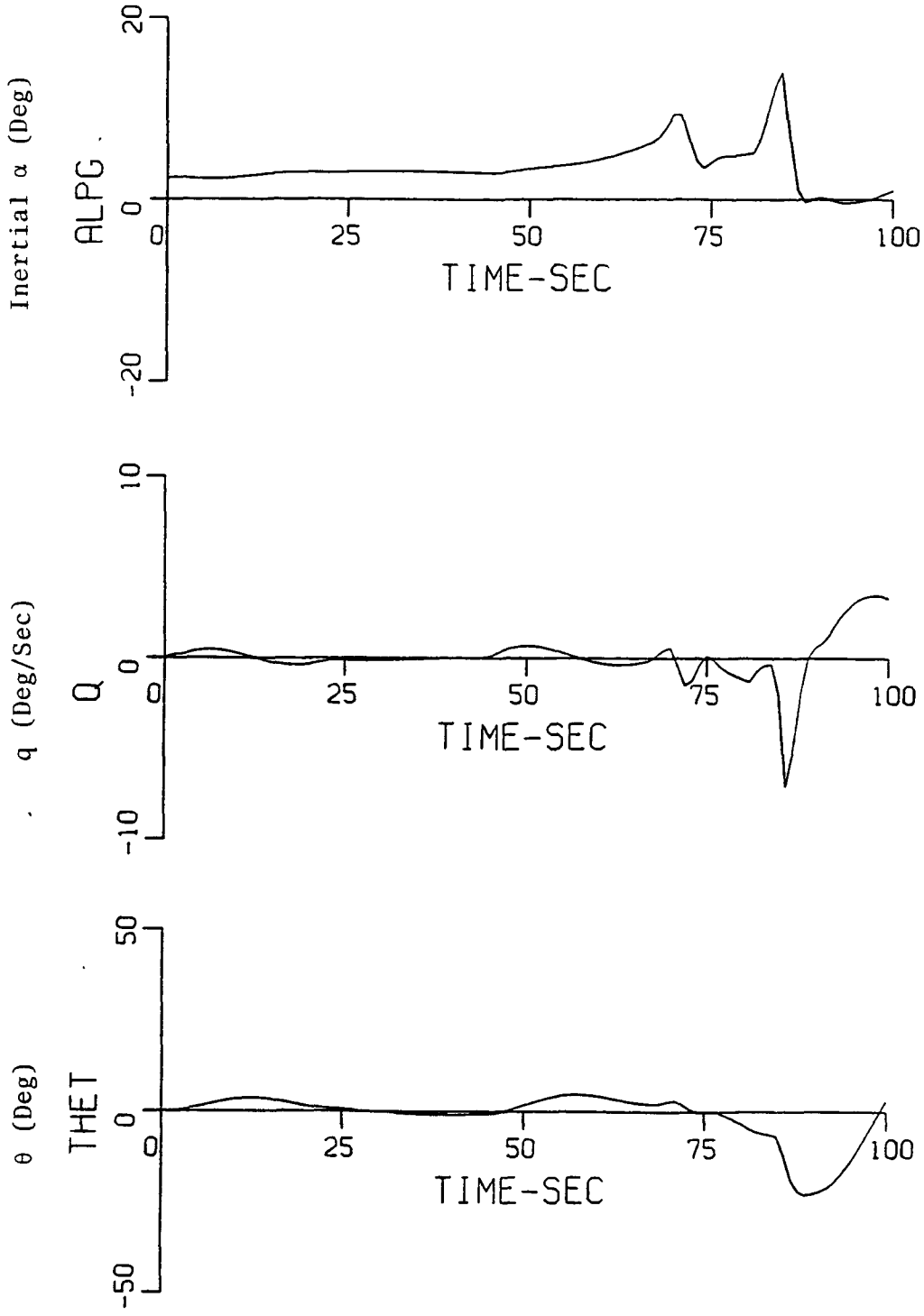

Figure 8. OPEN LOOP SIMULATION WITH
(Cont'd) KENNEDY SEVERE SHEAR

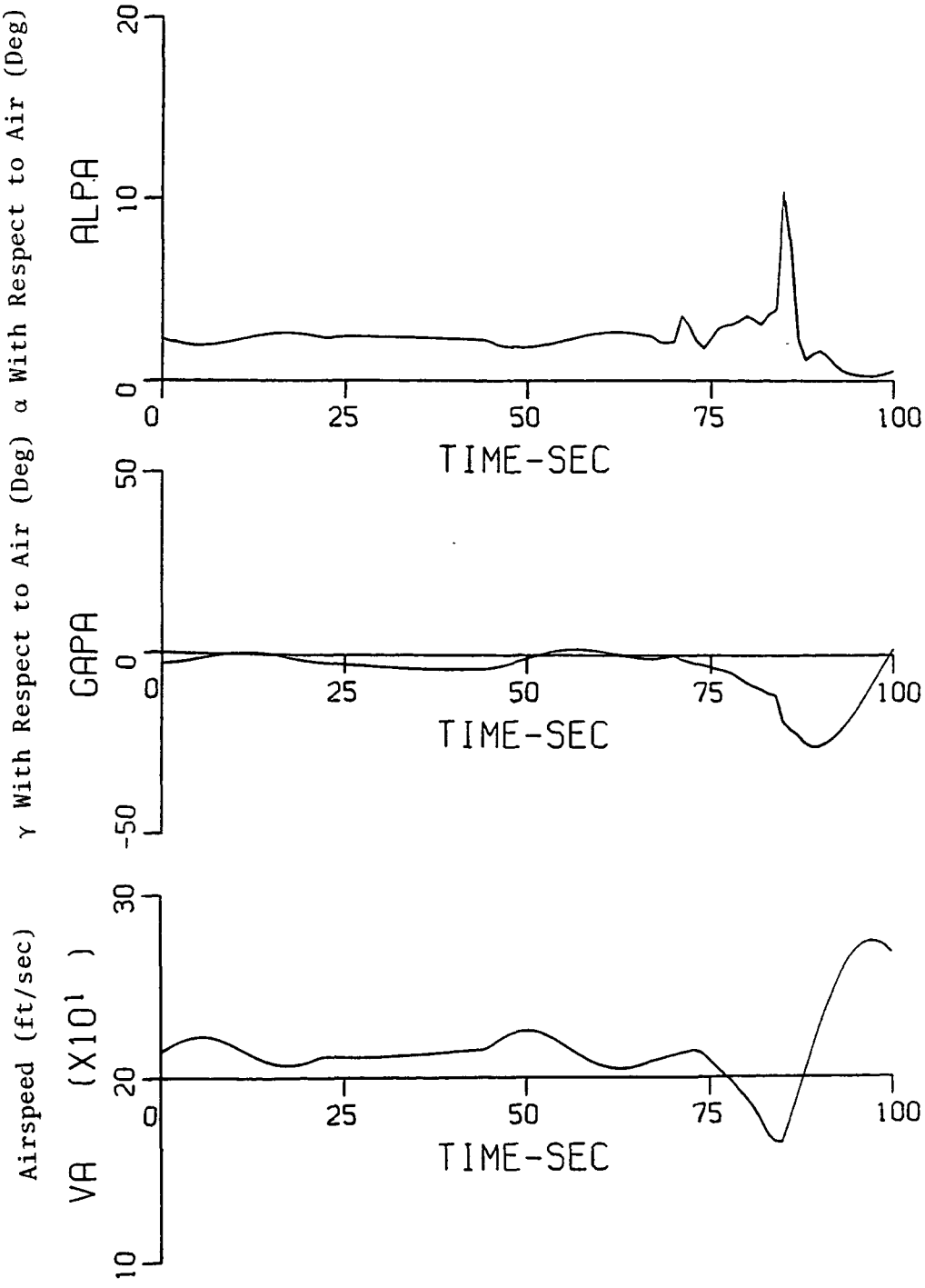

Figure 8. (Cont'd) OPEN LOOP SIMULATION WITH KENNEDY SEVERE SHEAR

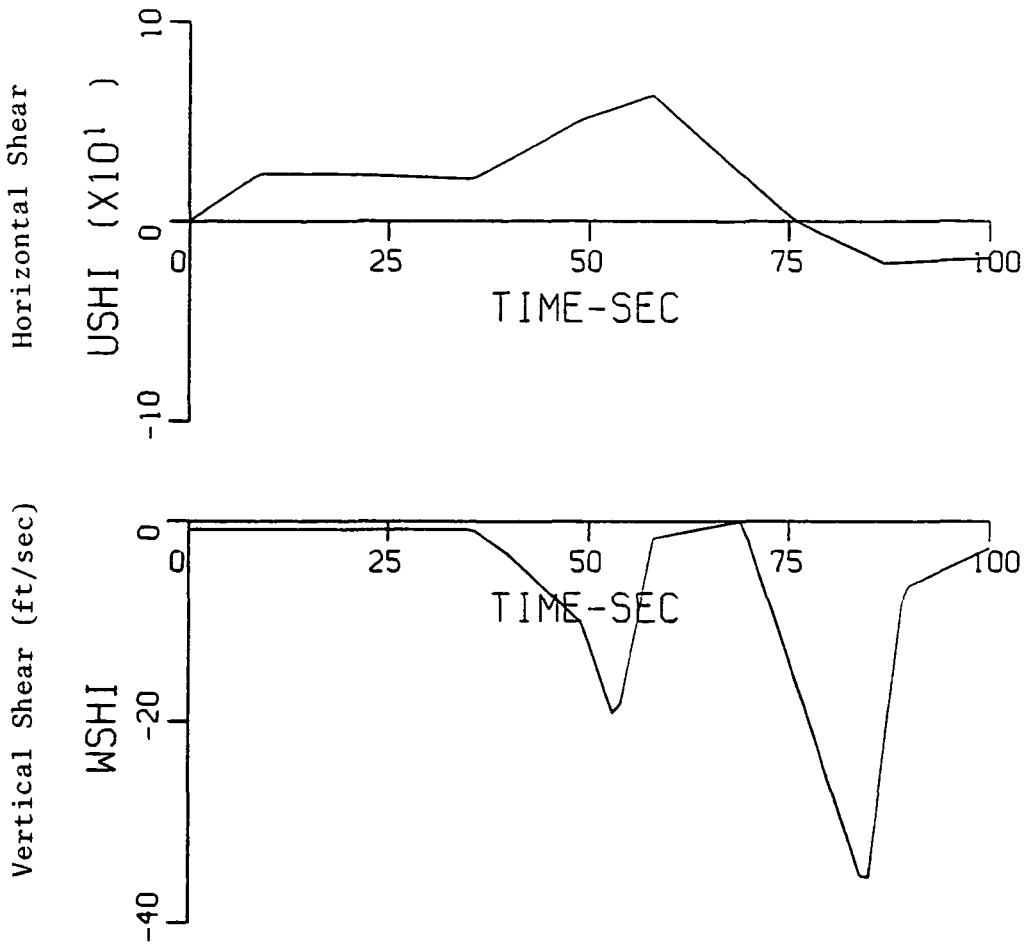

Figure 8. OPEN LOOP SIMULATION WITH
(Cont'd) KENNEDY SEVERE SHEAR

increase in headwind component increasing to about 37 kts. at its peak. During this period, the angle of attack increases, the flight path becomes shallower, and consequently the aircraft is above the glide path. Beyond this point, the headwind reverses to an increasing tailwind and there is also a down draft. The altitude starts decreasing. At about 75 seconds, the combination of the increasing tailwind and down draft forces the flight path angle to steepen, decreases airspeed and increases the angle of attack, causing a dramatic drop in altitude. In the simulation, the altitude was not allowed to go below 50 ft. which is reflected in the altitude vs. range plot. The controls fixed simulation demonstrates the severe effects of wind shear on aircraft flight during landing. Simulation time histories with both shear and turbulence are shown in Figure 9. The results are similar to the shears only case, except the responses have more high frequency content.

Simulation time histories of the feedforward control system using elevator, throttle and spoilers are shown in Figure 10. The sensed turbulence and shear signals are used directly to drive the control surfaces. The elevator, throttle and spoilers are used to exactly counter the pitching moment, X and Z forces produced by the wind disturbance. The control activities are such as to counter the perturbations in inertial responses due to shear and turbulence. However, control activities are excessive, especially the spoilers, but these can be reduced by simply scaling down the gains to the controllers.

Simulation time histories of the single control system with the Kennedy incident shear are shown in Figure 11. The elevator is used to minimize the deviation in the glide path. Initially when the headwind is encountered, the airplane is pitched down to keep the aircraft on the glide path. When the headwind turns to tailwind and the severe downdraft is encountered, the elevator alone cannot prevent the deviation from the glide path. The airplane loses airspeed and altitude. In the simulation, the altitude was not allowed to get below 50 feet. The time histories clearly show the instability of the aircraft flight in this windshear environment. The elevator can counter the forces and moments of headwind but not the tailwind and the severe downdraft.

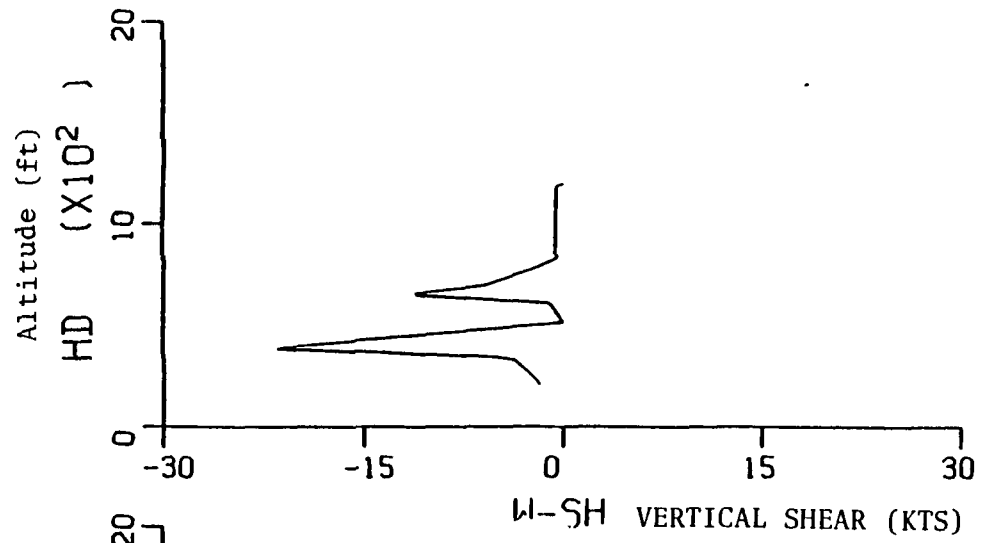

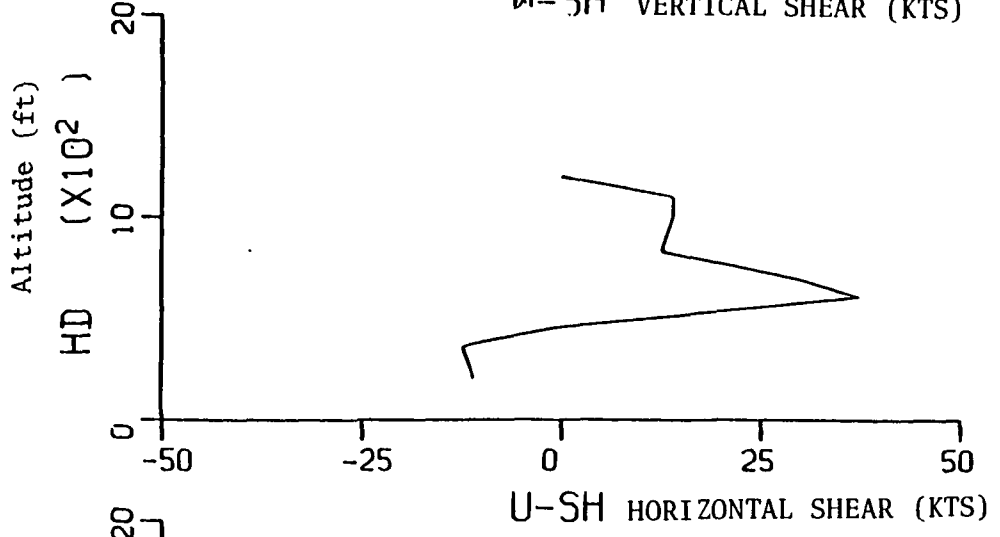

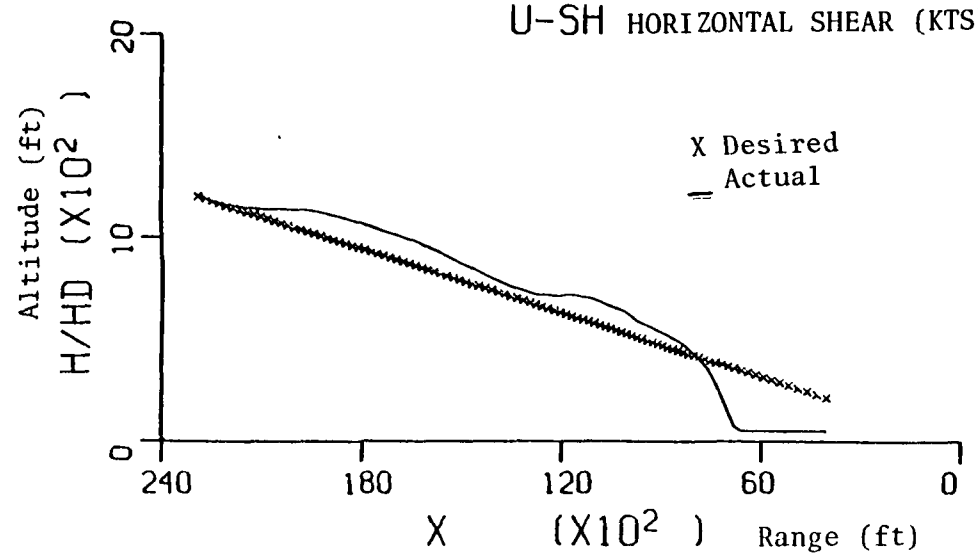

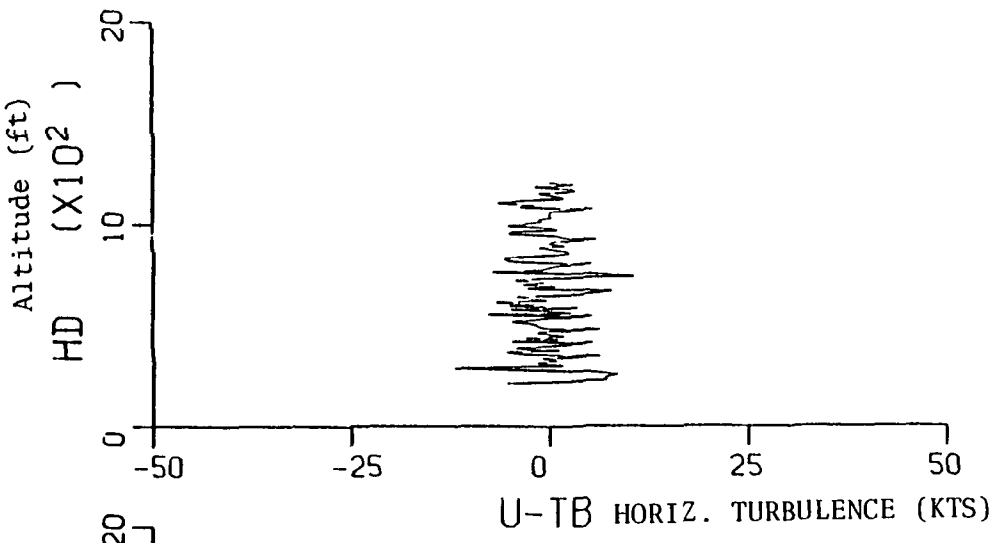

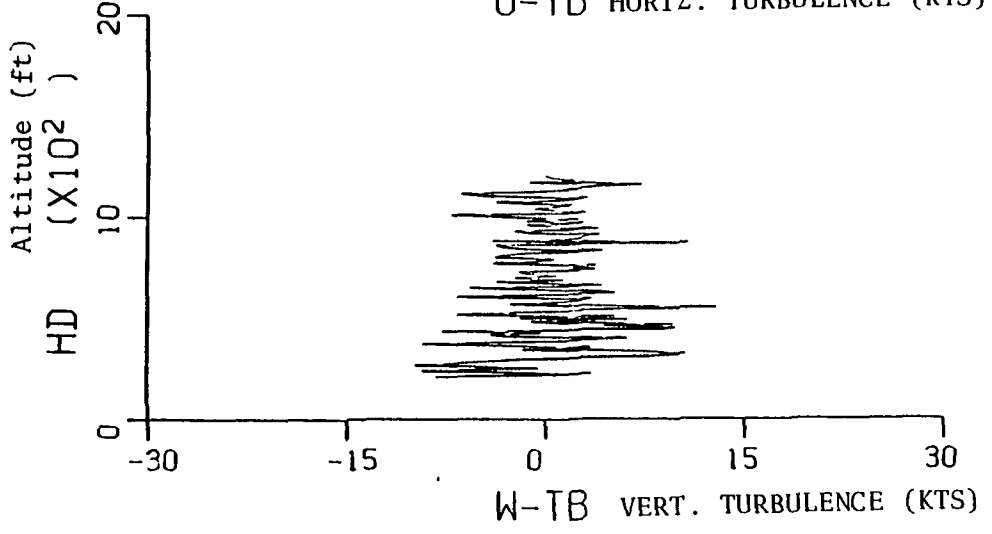

Figure 9. OPEN LOOP SIMULATION WITH KENNEDY SEVERE SHEAR AND TURBULENCE

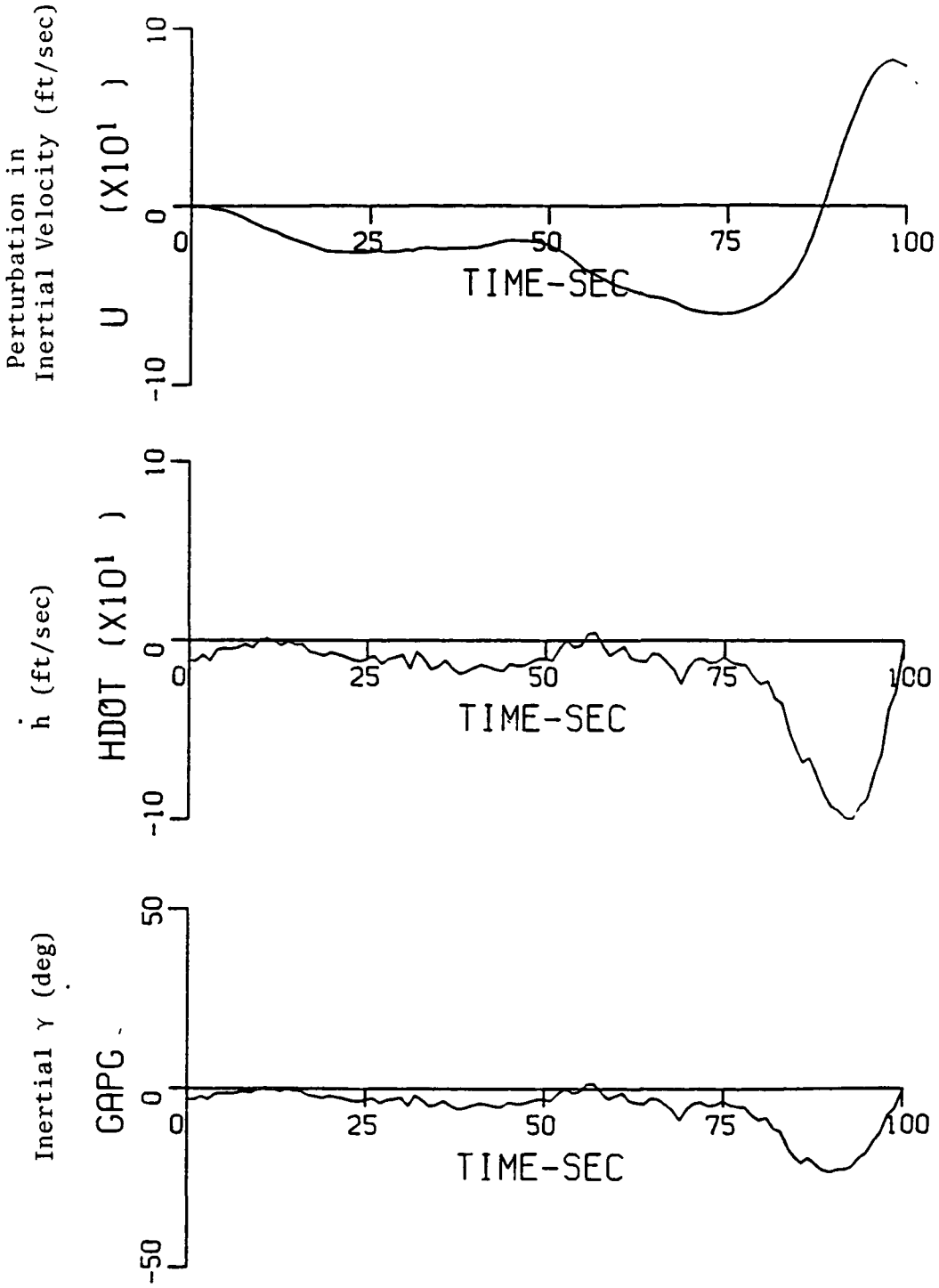

Figure 9. (Cont'd) OPEN LOOP SIMULATION WITH KENNEDY SEVERE SHEAR AND TURBULENCE

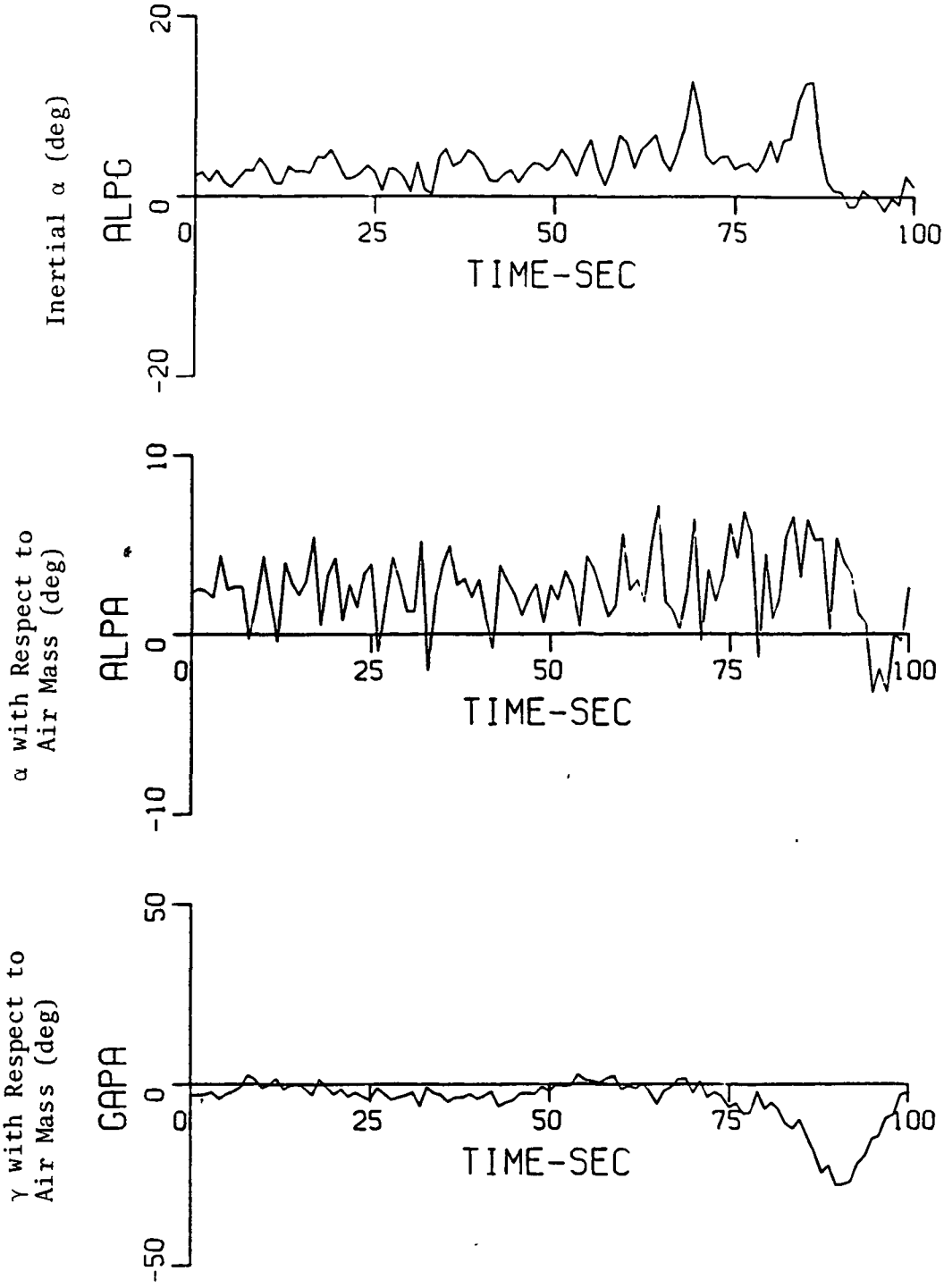

Figure 9. (Cont'd) OPEN LOOP SIMULATION WITH KENNEDY SEVERE SHEAR AND TURBULENCE

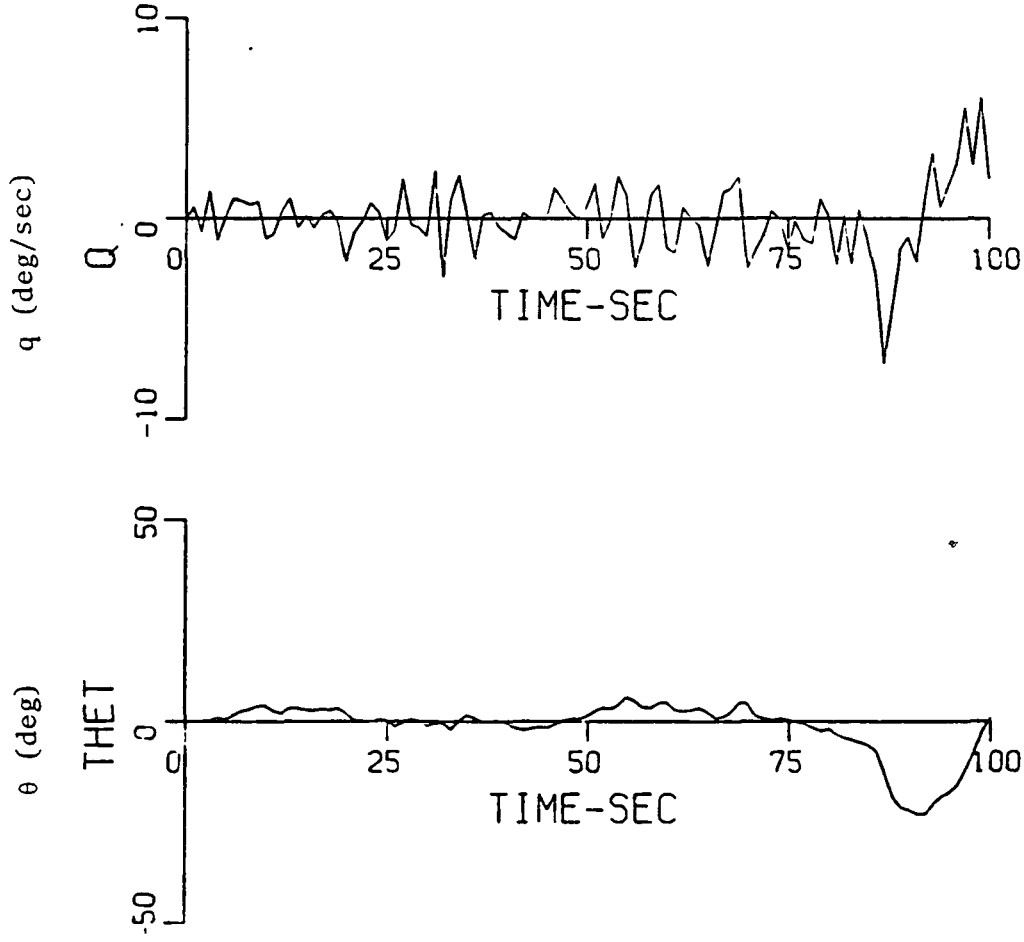

Figure 9. (Cont'd) OPEN LOOP SIMULATION WITH KENNEDY SEVERE SHEAR AND TURBULENCE

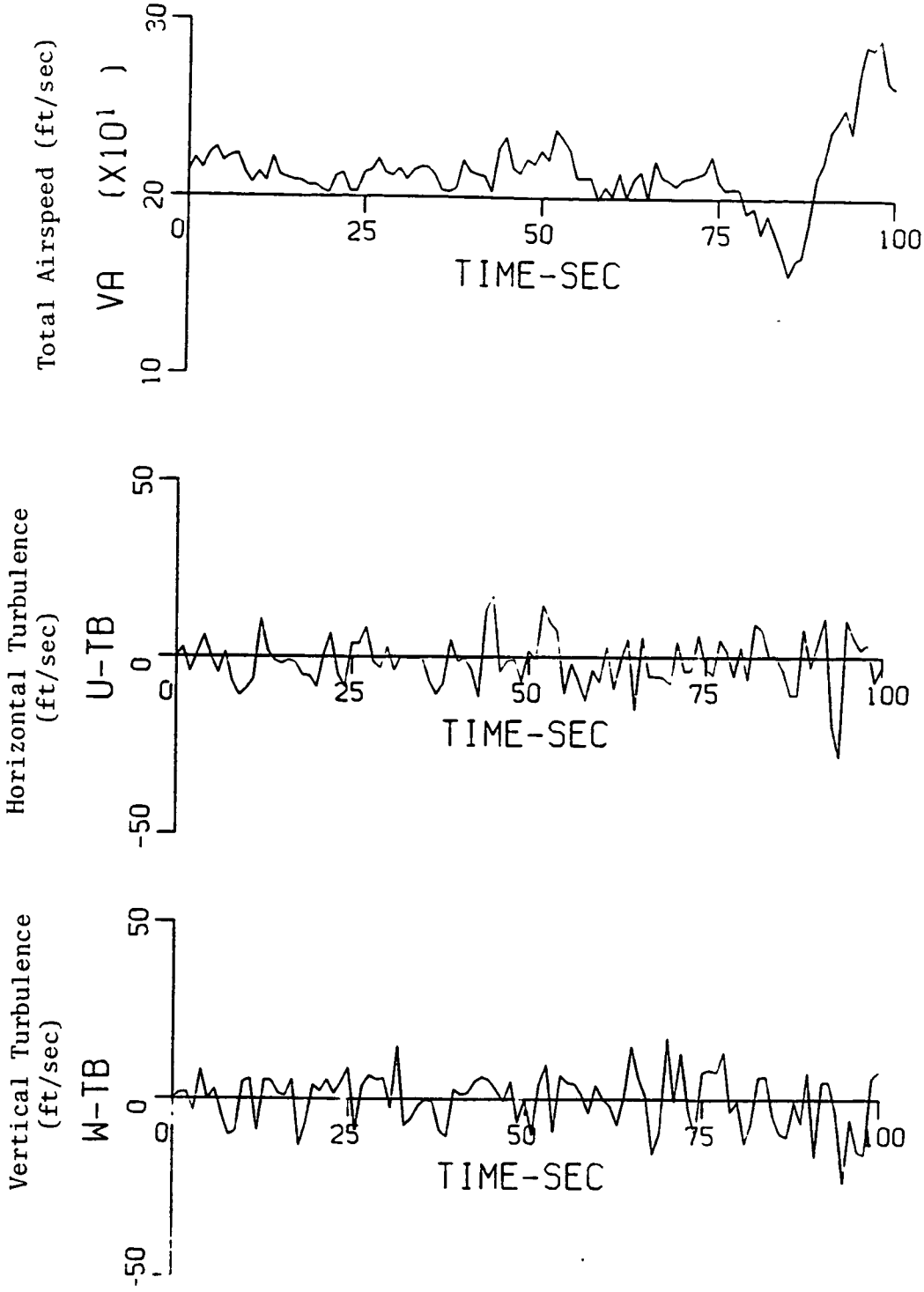

Figure 9. OPEN LOOP SIMULATION WITH KENNEDY
(Cont'd) SEVERE SHEAR AND TURBULENCE

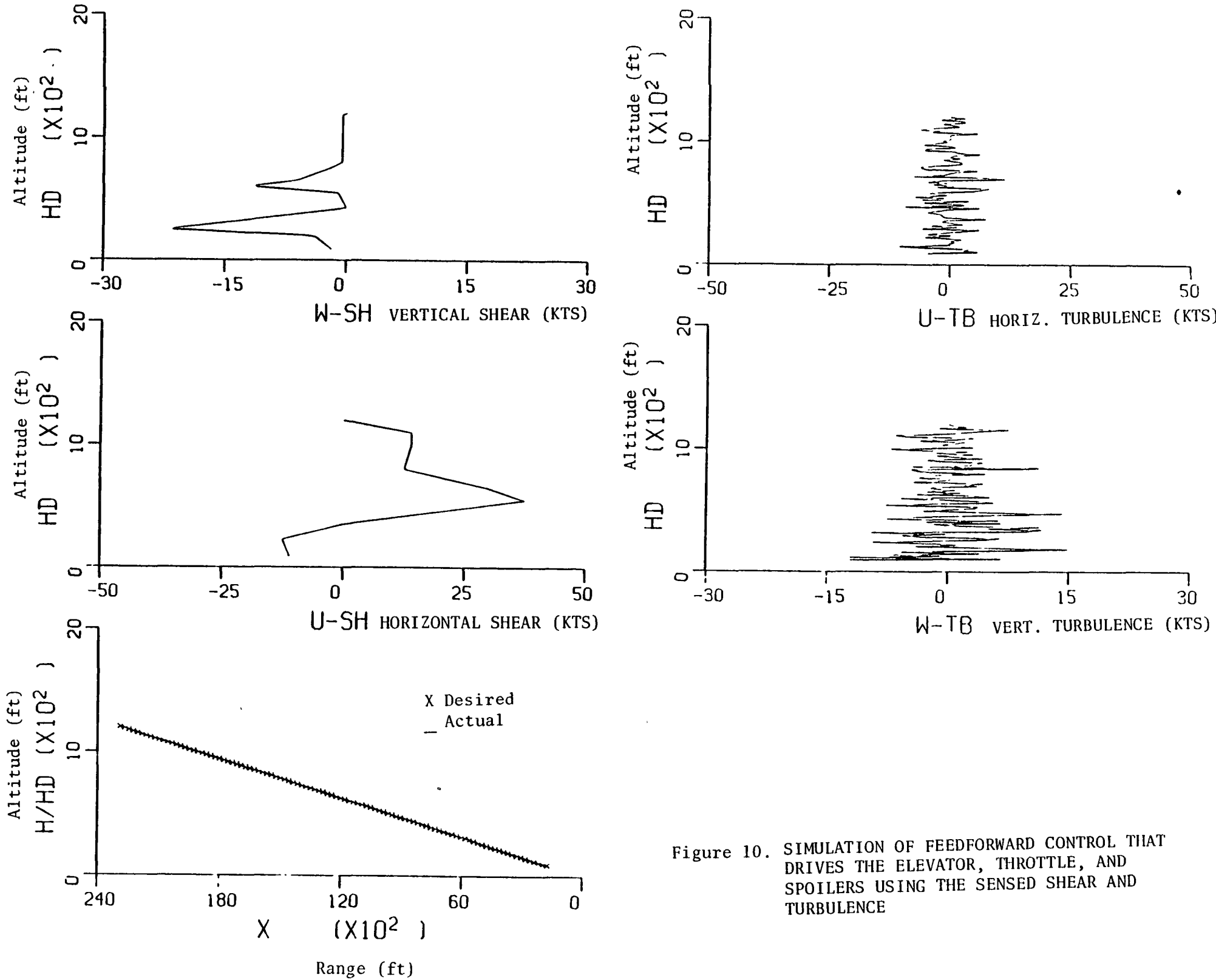

Figure 10. SIMULATION OF FEEDFORWARD CONTROL THAT DRIVES THE ELEVATOR, THROTTLE, AND SPOILERS USING THE SENSED SHEAR AND TURBULENCE

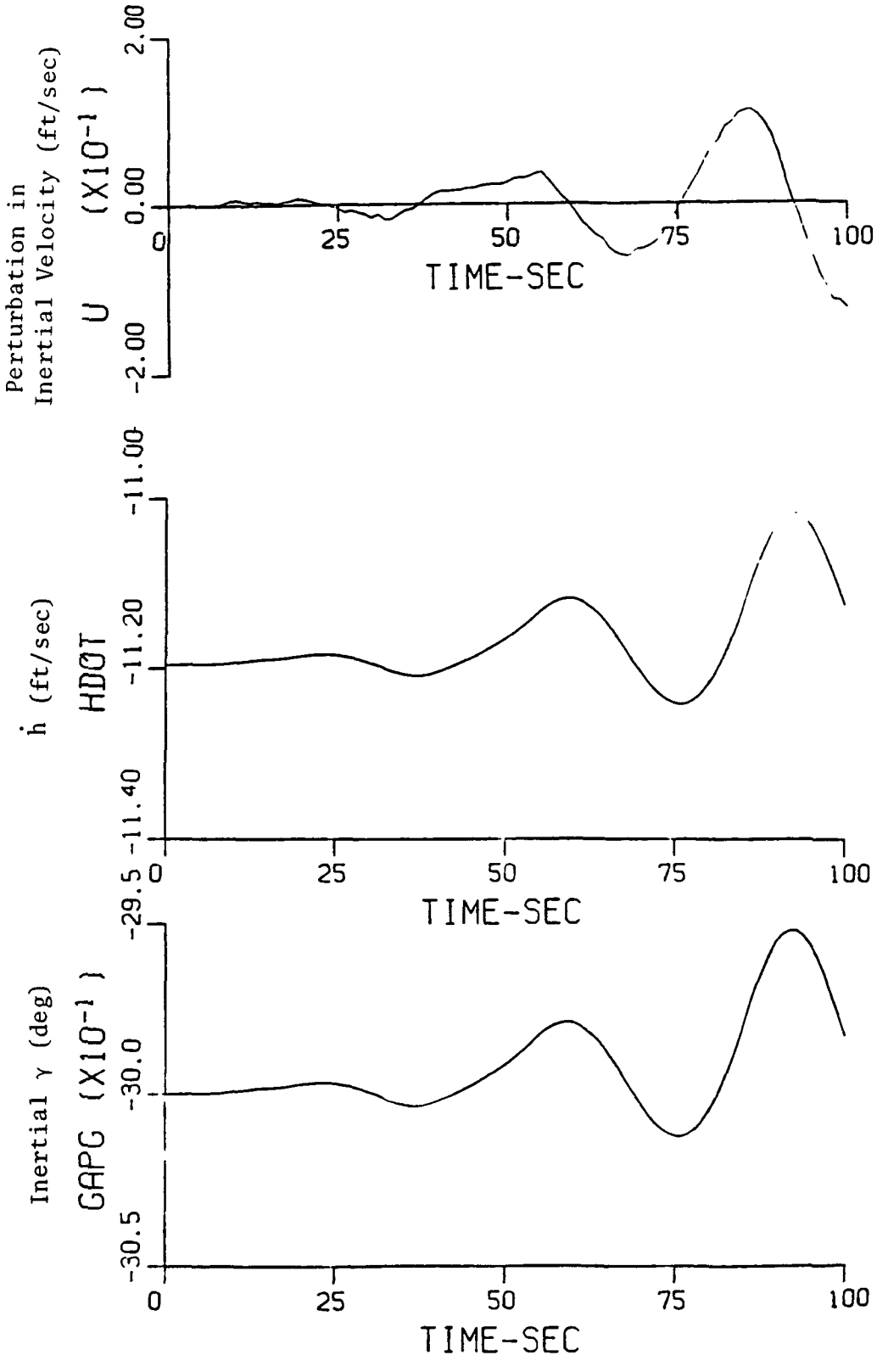

Figure 10. (Cont'd) SIMULATION OF FEEDFORWARD CONTROL THAT DRIVES THE ELEVATOR, THROTTLE, AND SPOILERS USING THE SENSED SHEAR AND TURBULENCE

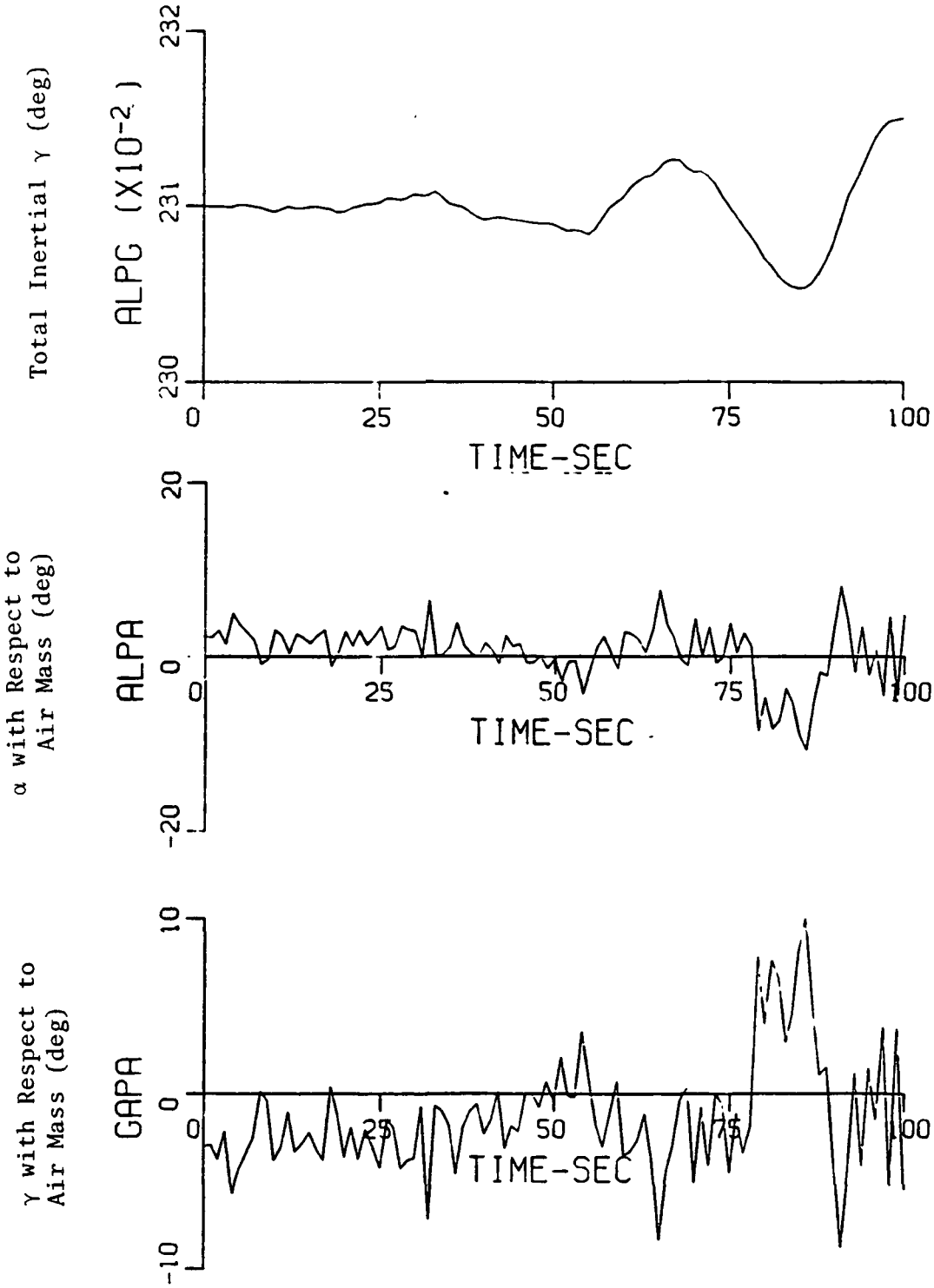

Figure 10. (Cont'd) SIMULATION OF FEEDFORWARD CONTROL THAT DRIVES THE ELEVATOR, THROTTLE, AND SPOILERS USING THE SENSED SHEAR AND TURBULENCE

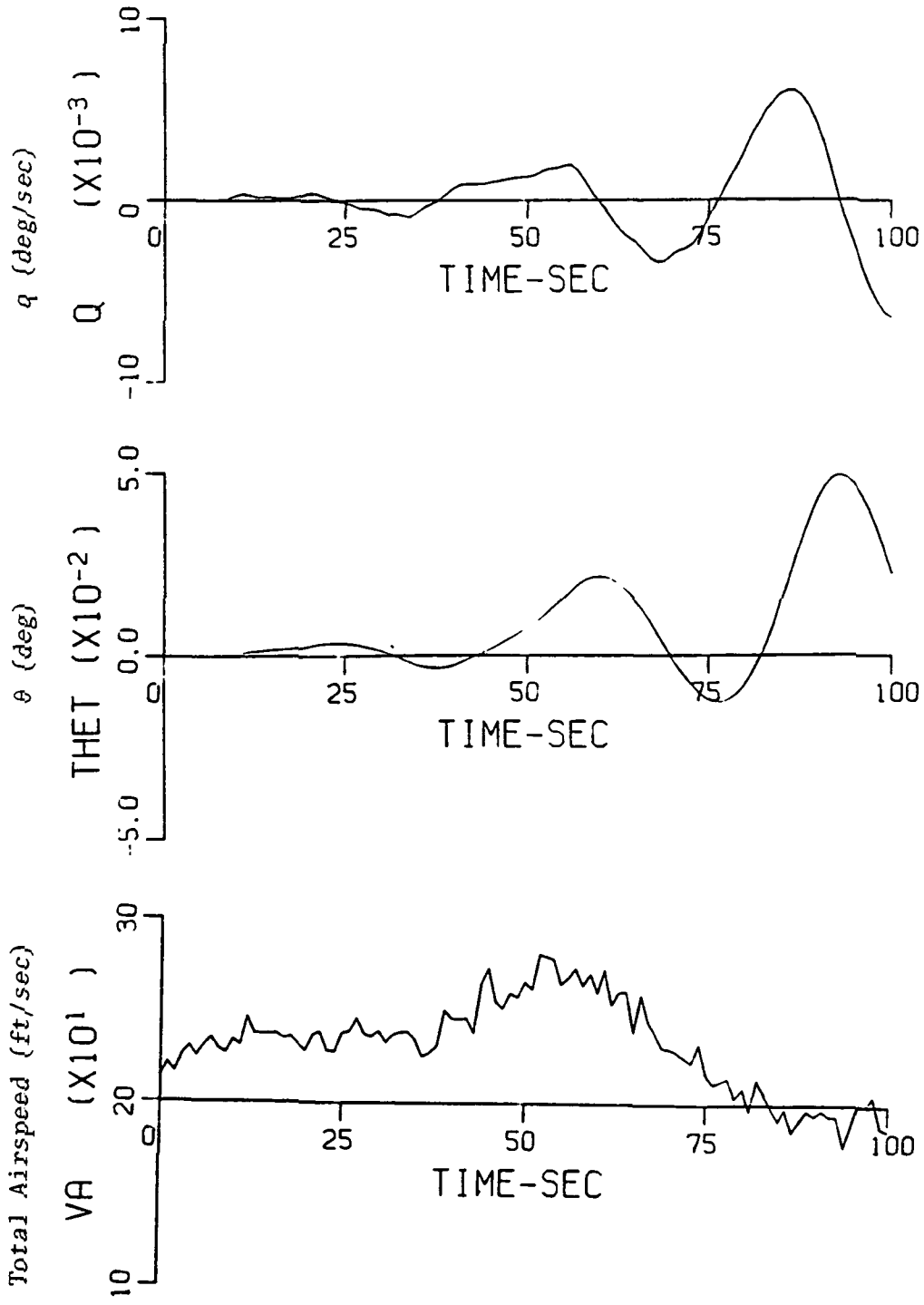

Figure 10. (Cont'd) SIMULATION OF FEEDFORWARD CONTROL THAT DRIVES THE ELEVATOR, THROTTLE, AND SPOILERS USING THE SENSED SHEAR AND TURBULENCE

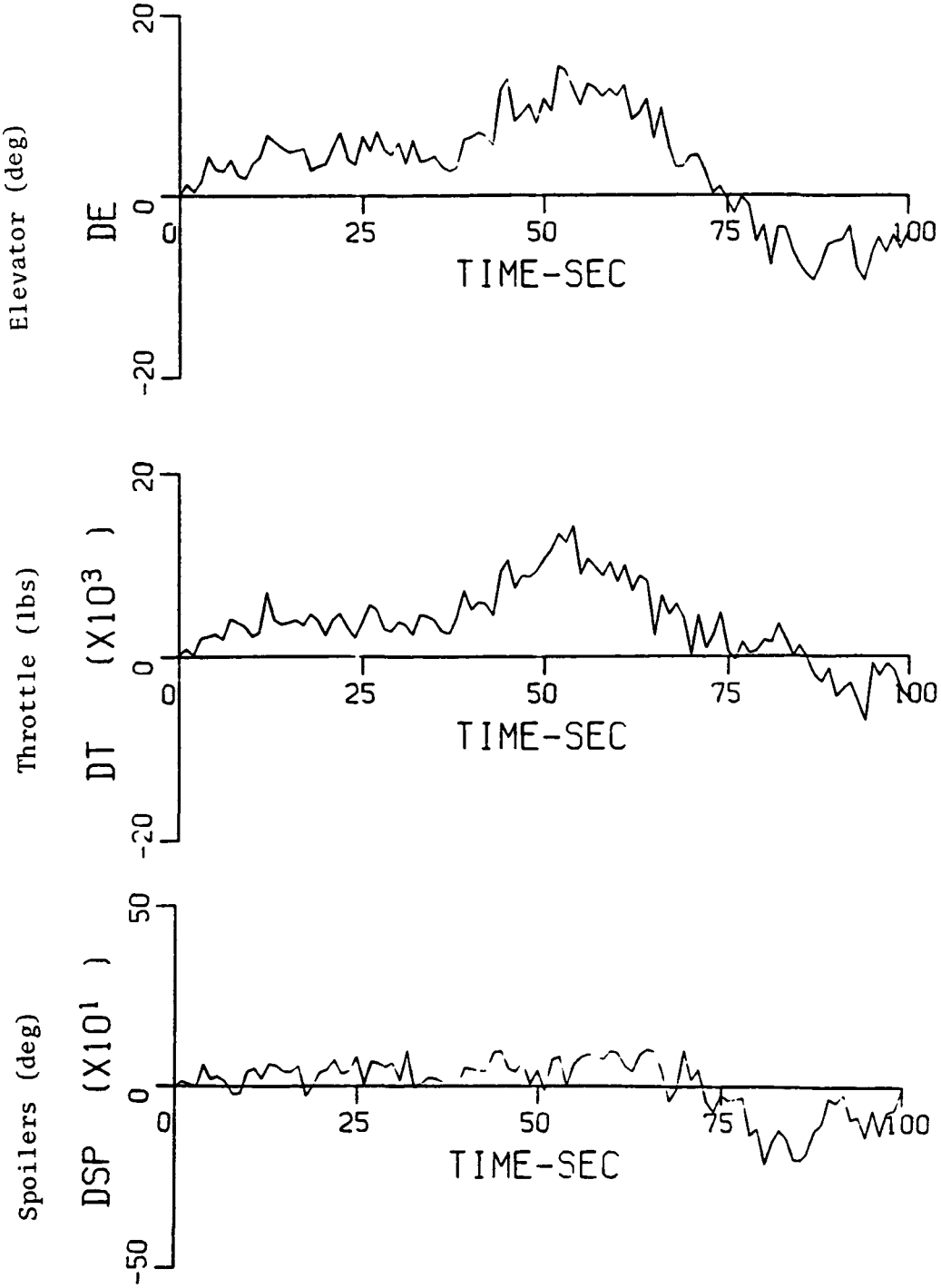

Figure 10. (Cont'd) SIMULATION OF FEEDFORWARD CONTROL THAT DRIVES THE ELEVATOR, THROTTLE, AND SPOILERS USING THE SENSED SHEAR AND TURBULENCE

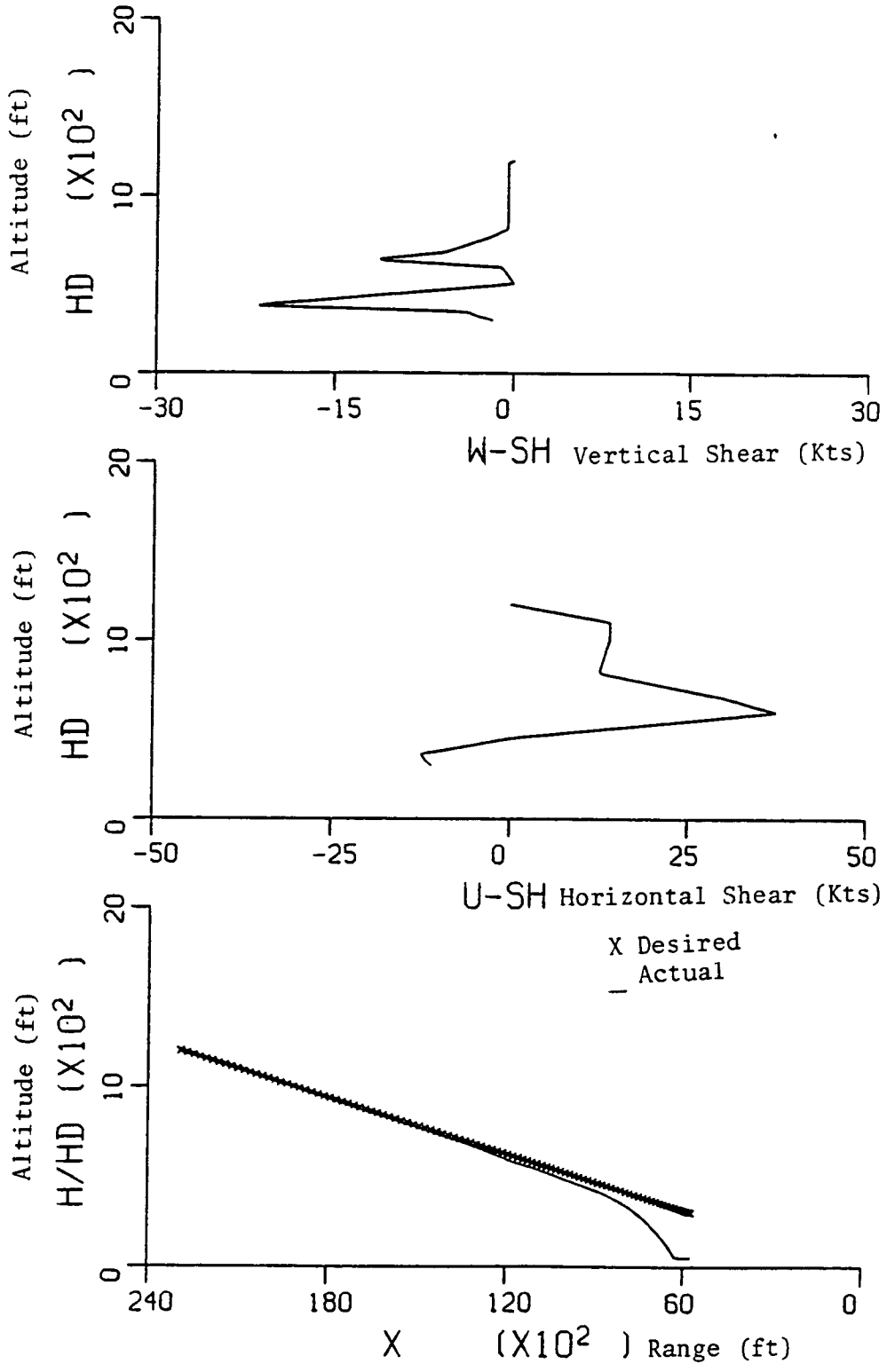

Figure 11. SIMULATION OF THE SINGLE CONTROL SYSTEM WITH THE KENNEDY SHEAR

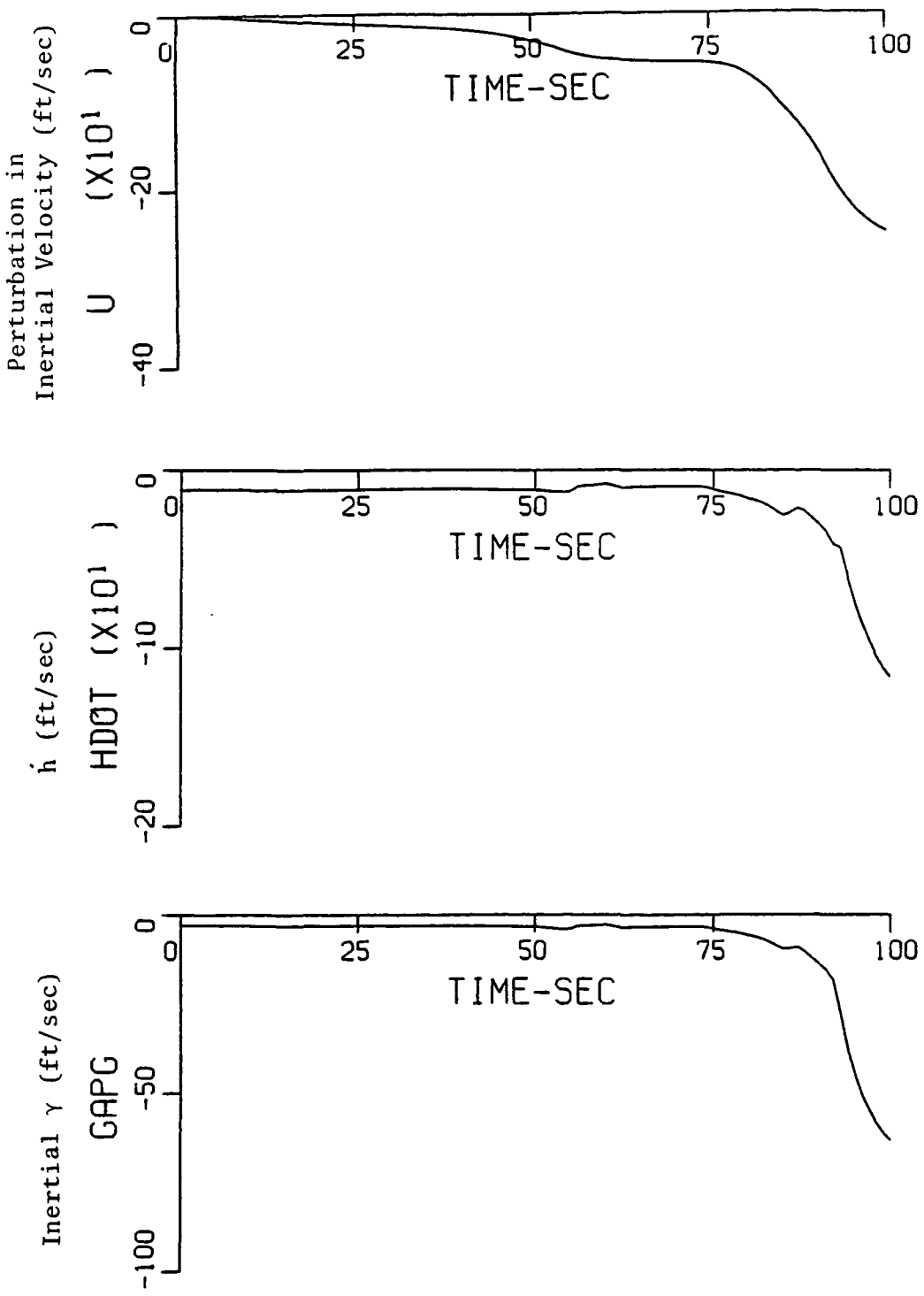

Figure 11. SIMULATION OF THE SINGLE CONTROL SYSTEM WITH THE KENNEDY SHEAR (Cont'd)

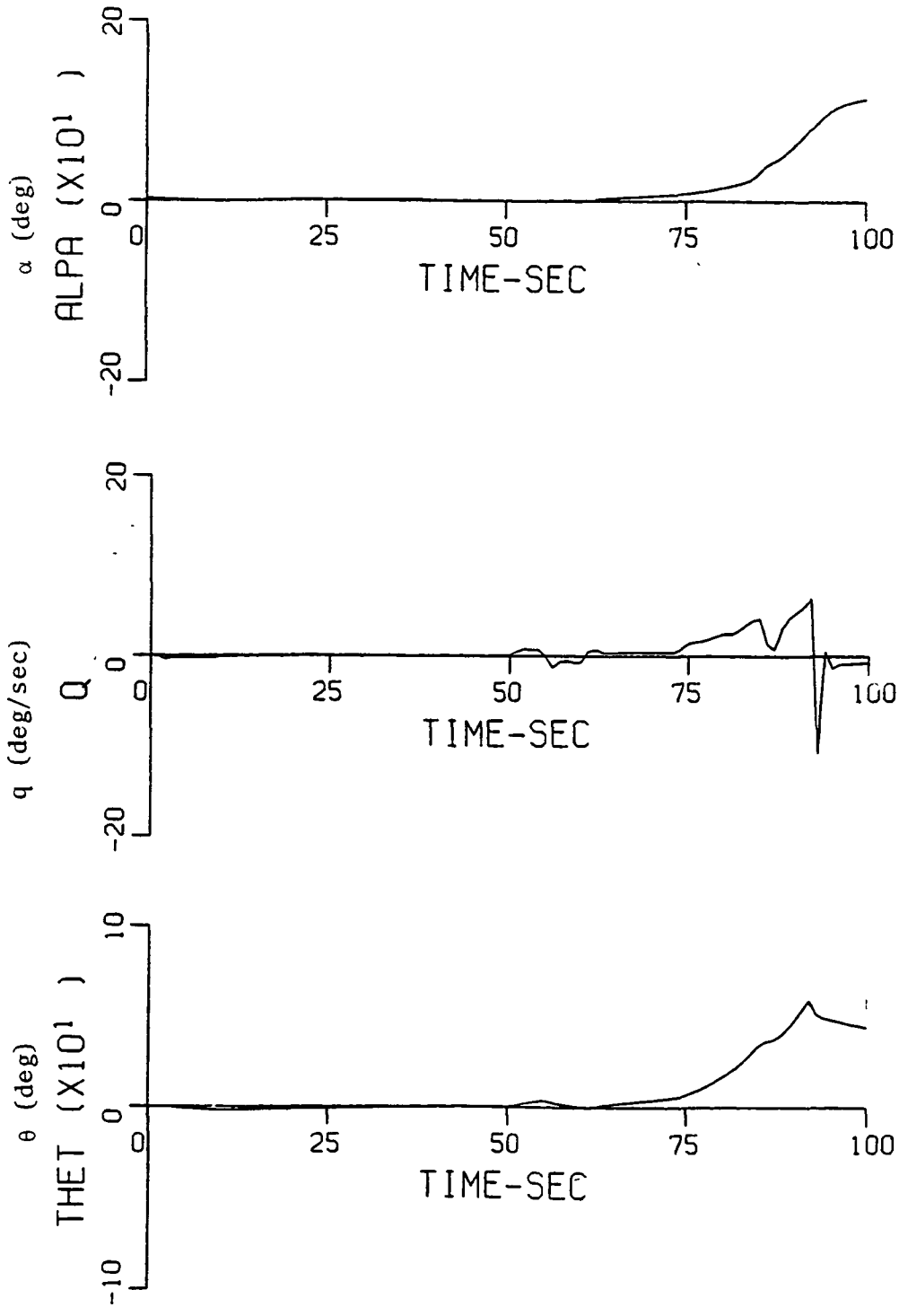

Figure 11. SIMULATION OF THE SINGLE CONTROL SYSTEM WITH THE KENNEDY SHEAR (Cont'd)

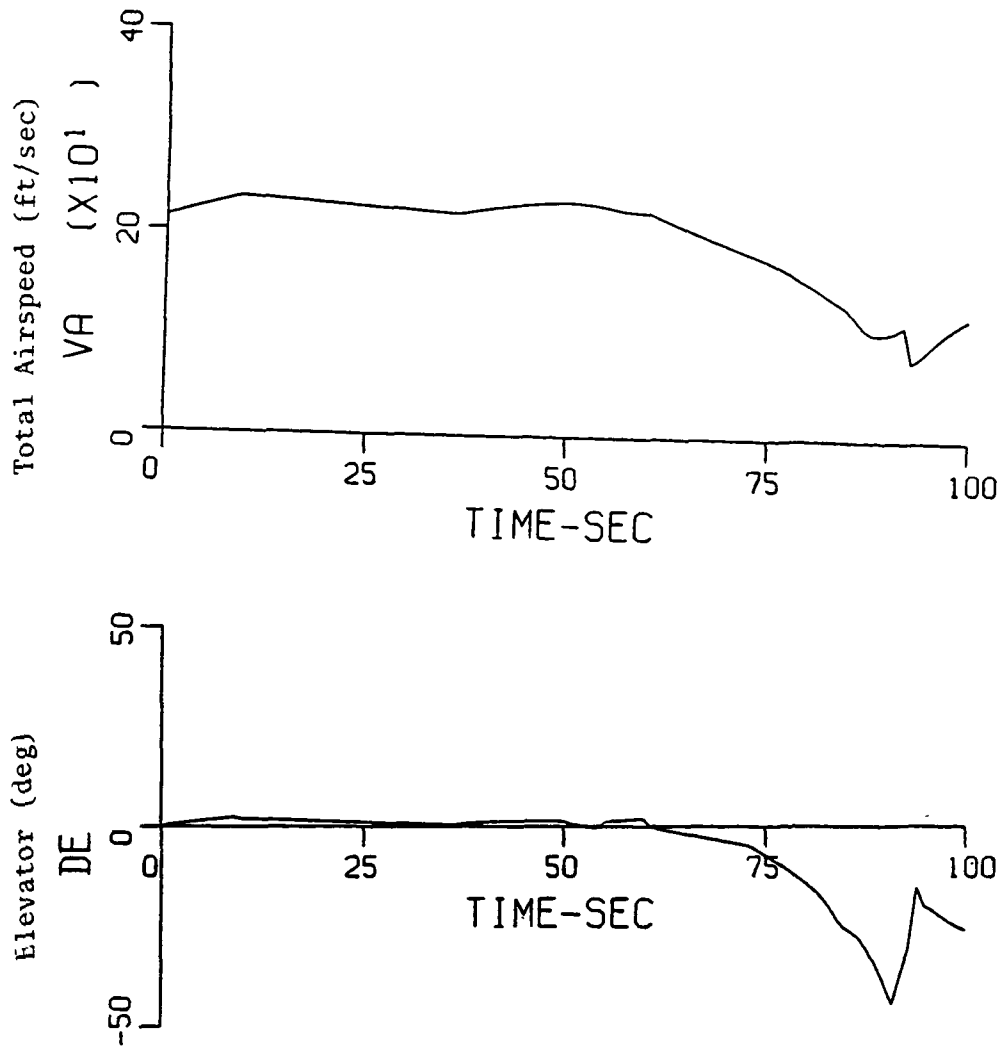

Figure 11. SIMULATION OF THE SINGLE CONTROL SYSTEM WITH THE KENNEDY SHEAR (Cont'd)

The time histories of the control system 1 (feedback regulation only) simulation with the Kennedy incident horizontal shear only is shown in Figure 12. Initially when the airplane encounters the headwind, the elevator and throttle are activated to reduce the angle of attack with respect to the airmass and the attitude and to regulate the inertial speed and altitude rate to stay on the glide path. The airspeed increases as the headwind increases. The simulation was not carried far enough for the headwind to tailwind.

Simulation of the control system 1 including the feedforward control with the Kennedy incident horizontal and vertical shears is shown in Figure 13. Initially, when the headwind is encountered, the throttle and elevator are activated to minimize the deviation in the inertial speed by increasing the airspeed and reducing the angle of attack and attitude. The glide path is well regulated as shown by the altitude and flight path angle time history. As the headwind turns to tailwind, the throttle activity is decreased and the elevator is activated to increase the angle of attack. When the severe down draft is encountered, the throttle activity is increased to minimize the deviation in the glide path. The angle of attack decreases to a minimum of -4.5^{o} and increases to a maximum of about 6.3^{o}. The elevator is deflected about 12^{o} maximum from its trim position. The thrust is increased to a maximum of about 11,700 lbs from its trim setting. The variation in the inertial speed is minimized and the airspeed variation is proportional to windspeed.

Simulation of this control system with the shears and turbulence is shown in Figure 14. The flight path angle is again very well regulated. Examination of the control motions indicates that the throttle activity is high. This is because the sensed turbulence is fed to the throttle. In practice, this level of throttle activity is undesirable and the throttle dynamics are not fast enough to respond to the turbulence. A more desirable means of control would be to use sensed shear signals, which are low frequency in content, to drive the throttle. Turbulence alleviation can be accomplished through the elevator or spoilers either by feedback regulation and/or direct gust sensing.

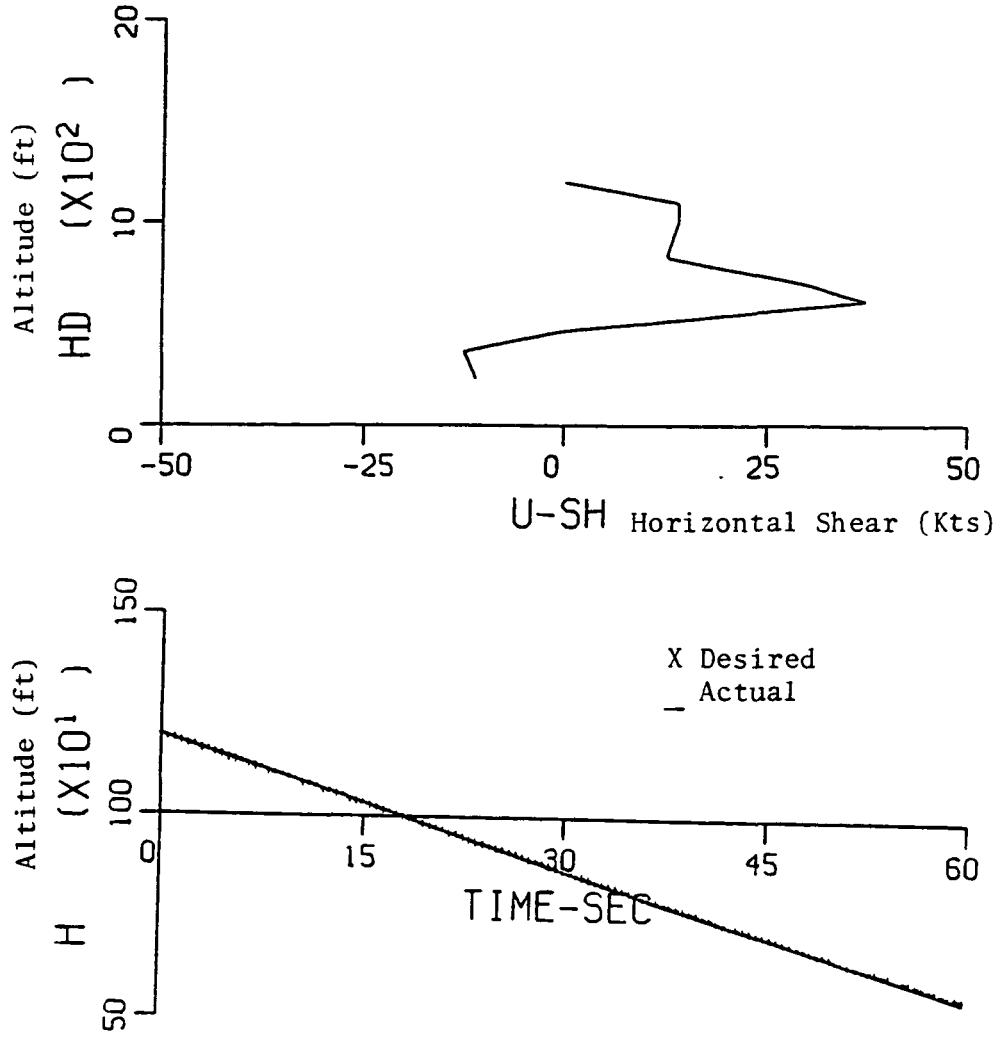

Figure 12. SIMULATION OF CONTROL SYSTEM 1 (FEEDBACK ONLY) WITH KENNEDY HORIZONTAL SHEAR ONLY

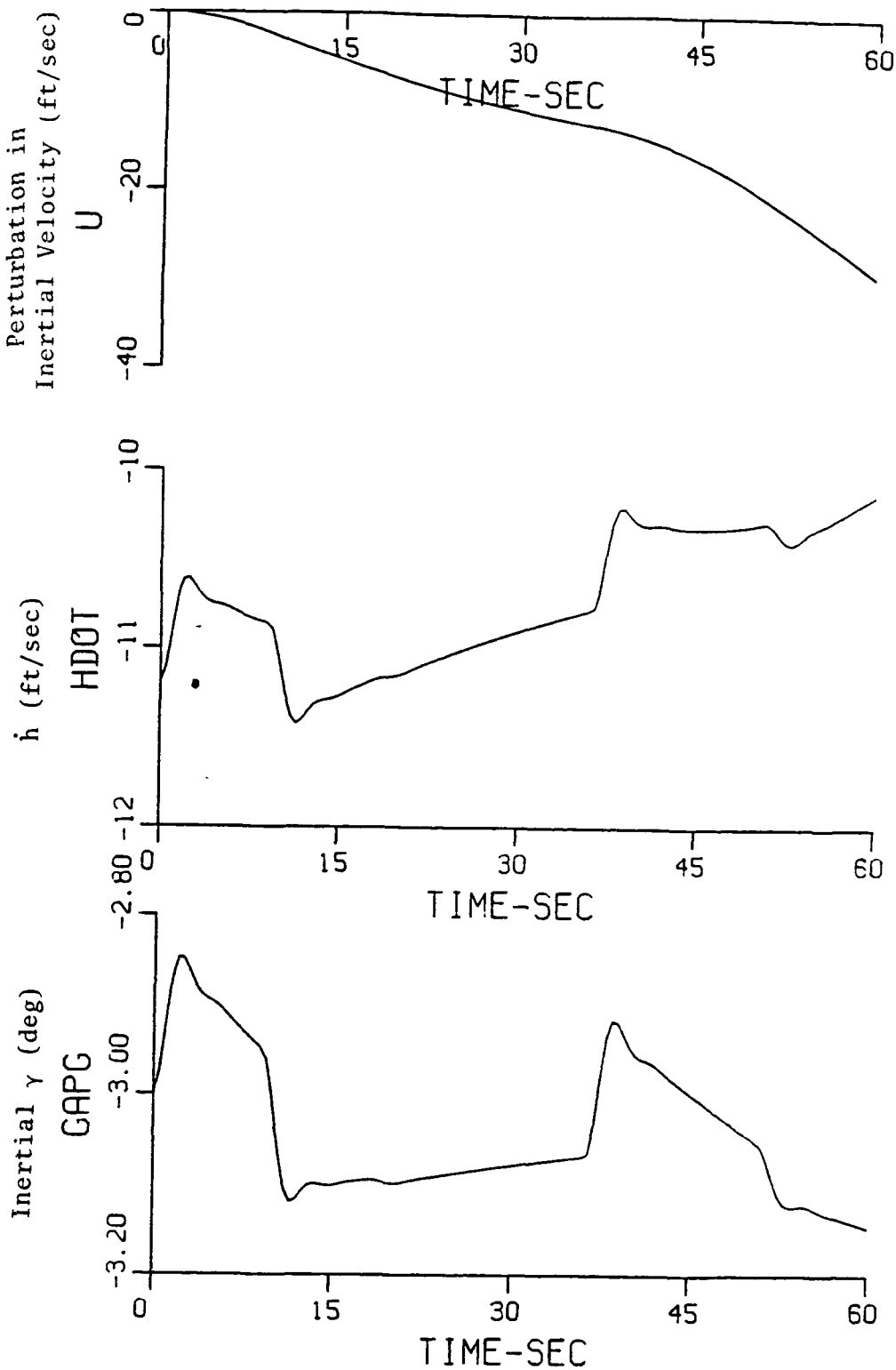

Figure 12. SIMULATION OF CONTROL SYSTEM 1 (Cont'd) (FEEDBACK ONLY) WITH KENNEDY HORIZONTAL SHEAR ONLY

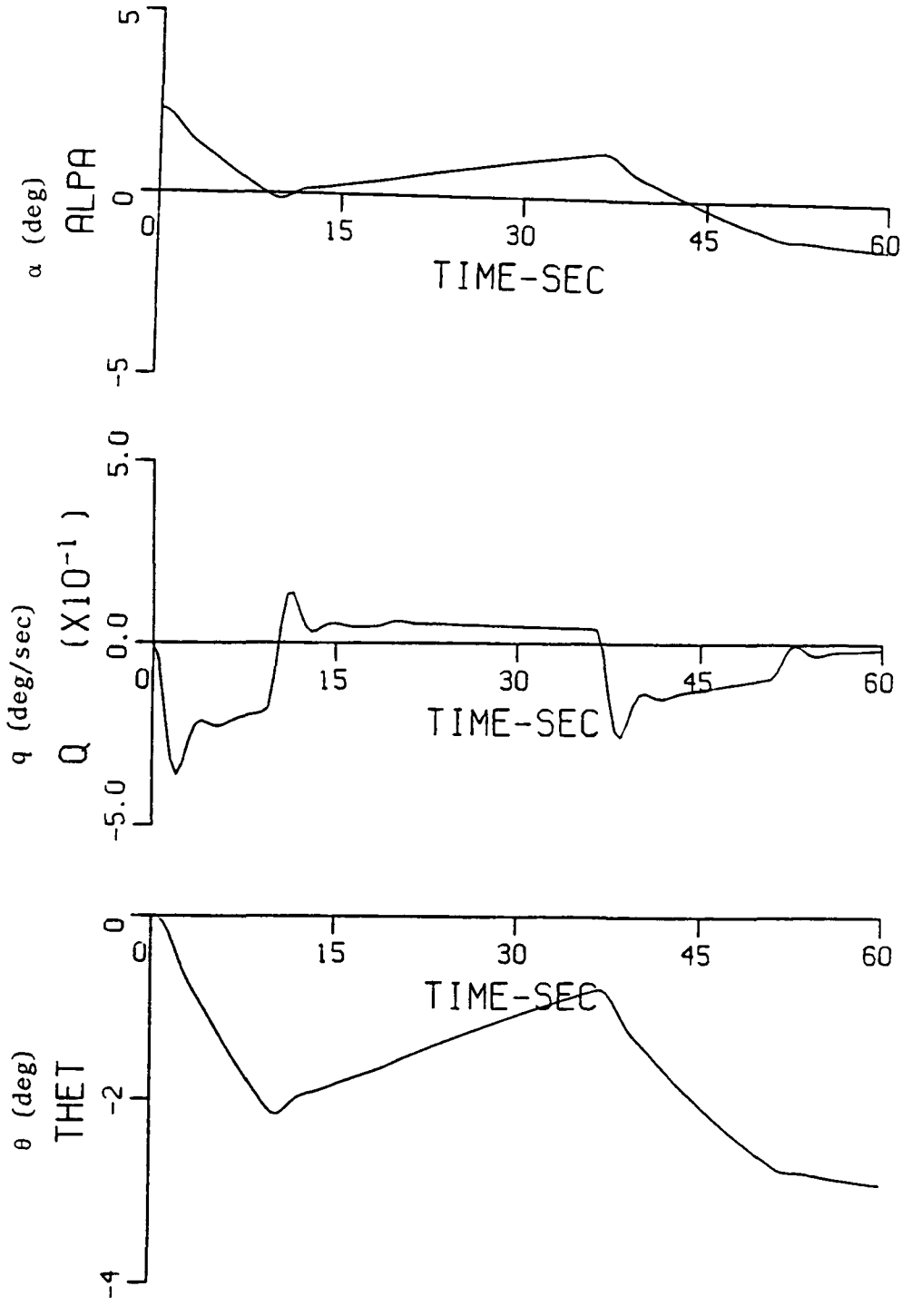

Figure 12. (Cont'd) SIMULATION OF CONTROL SYSTEM 1 (FEEDBACK ONLY) WITH KENNEDY HORIZONTAL SHEAR ONLY

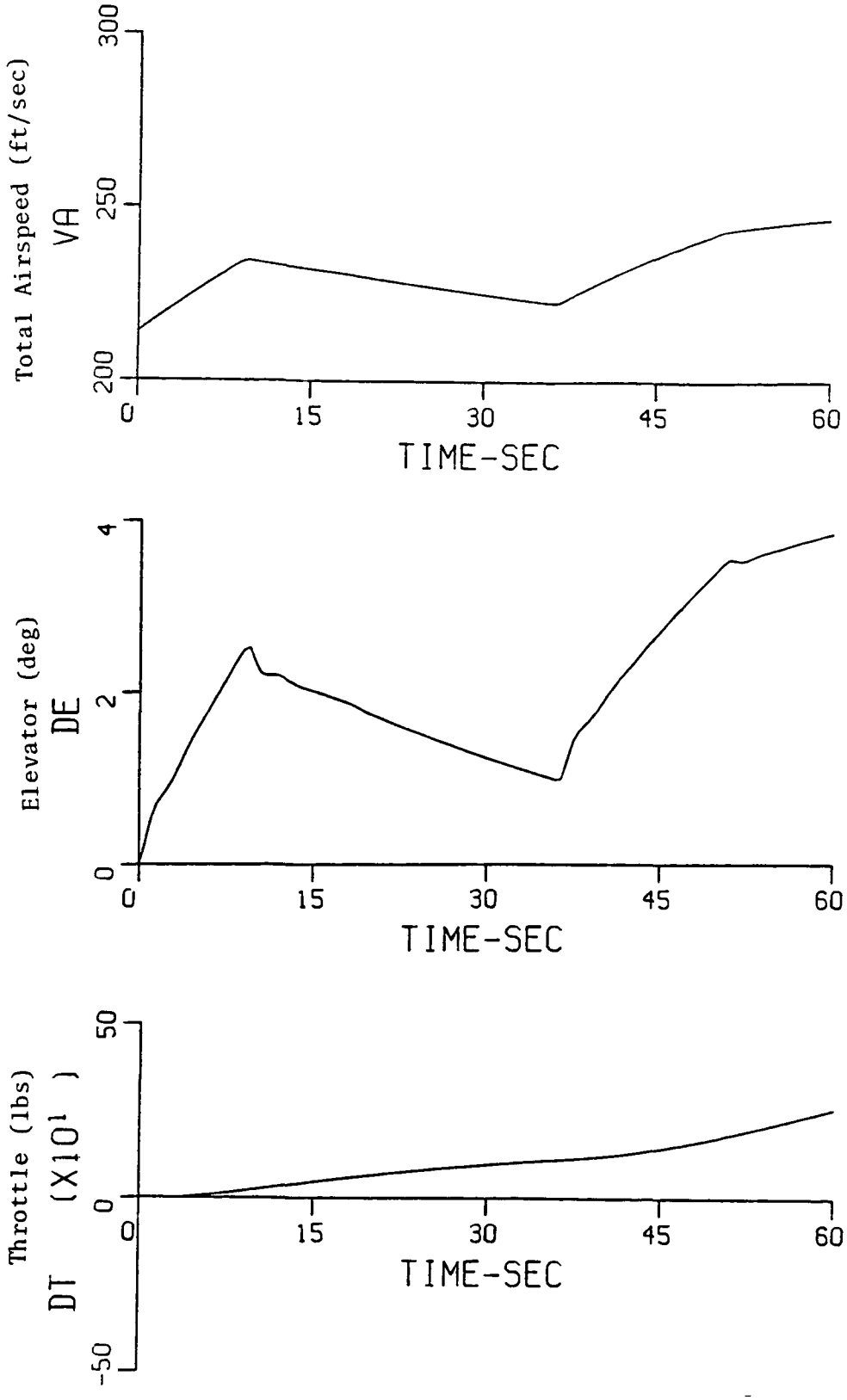

Figure 12. (Cont'd) SIMULATION OF CONTROL SYSTEM 1 (FEEDBACK ONLY) WITH KENNEDY HORIZONTAL SHEAR ONLY

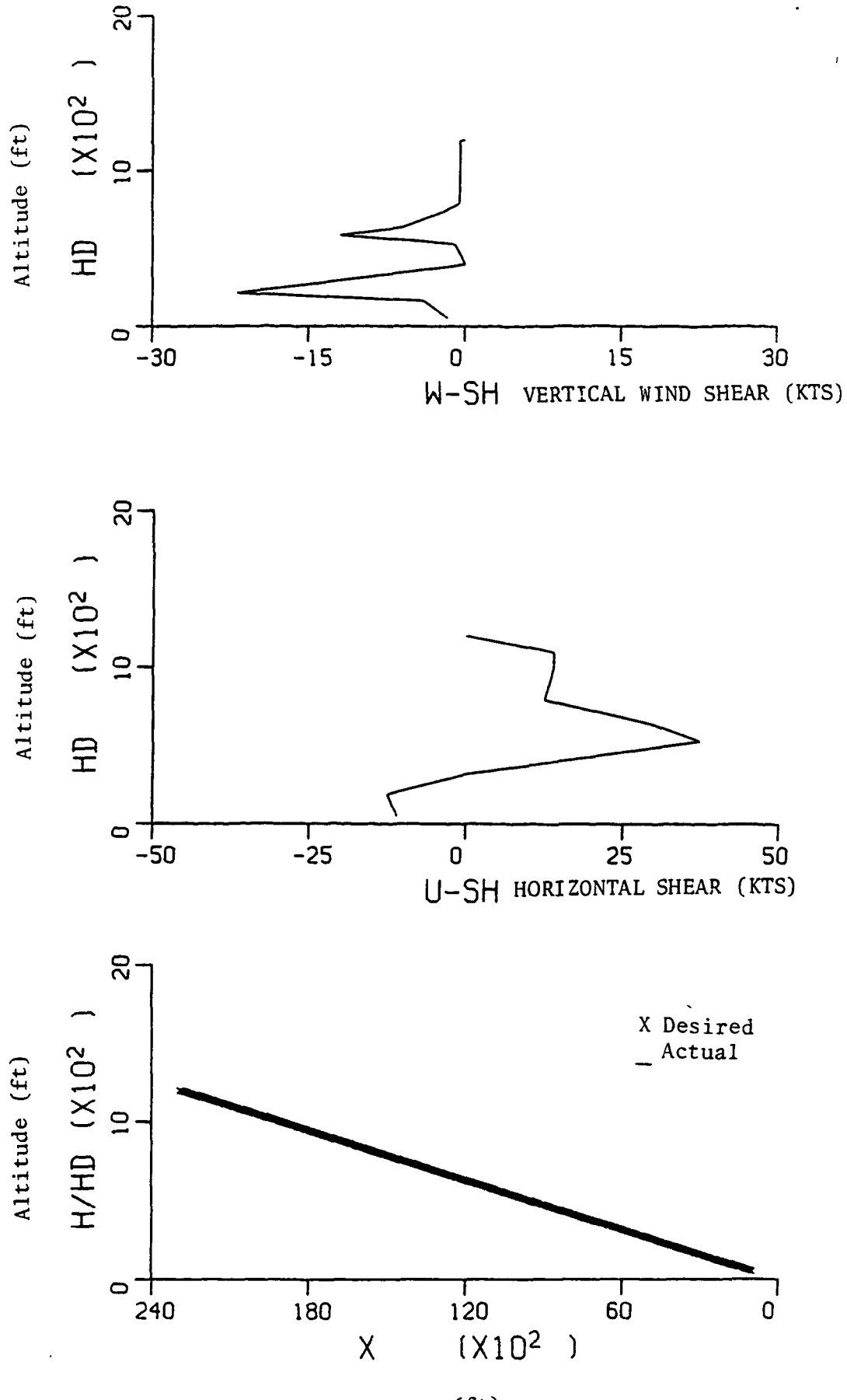

Figure 13. SIMULATION OF CONTROL SYSTEM 1 (FEEDBACK AND FEEDFORWARD) WITH THE KENNEDY SHEAR

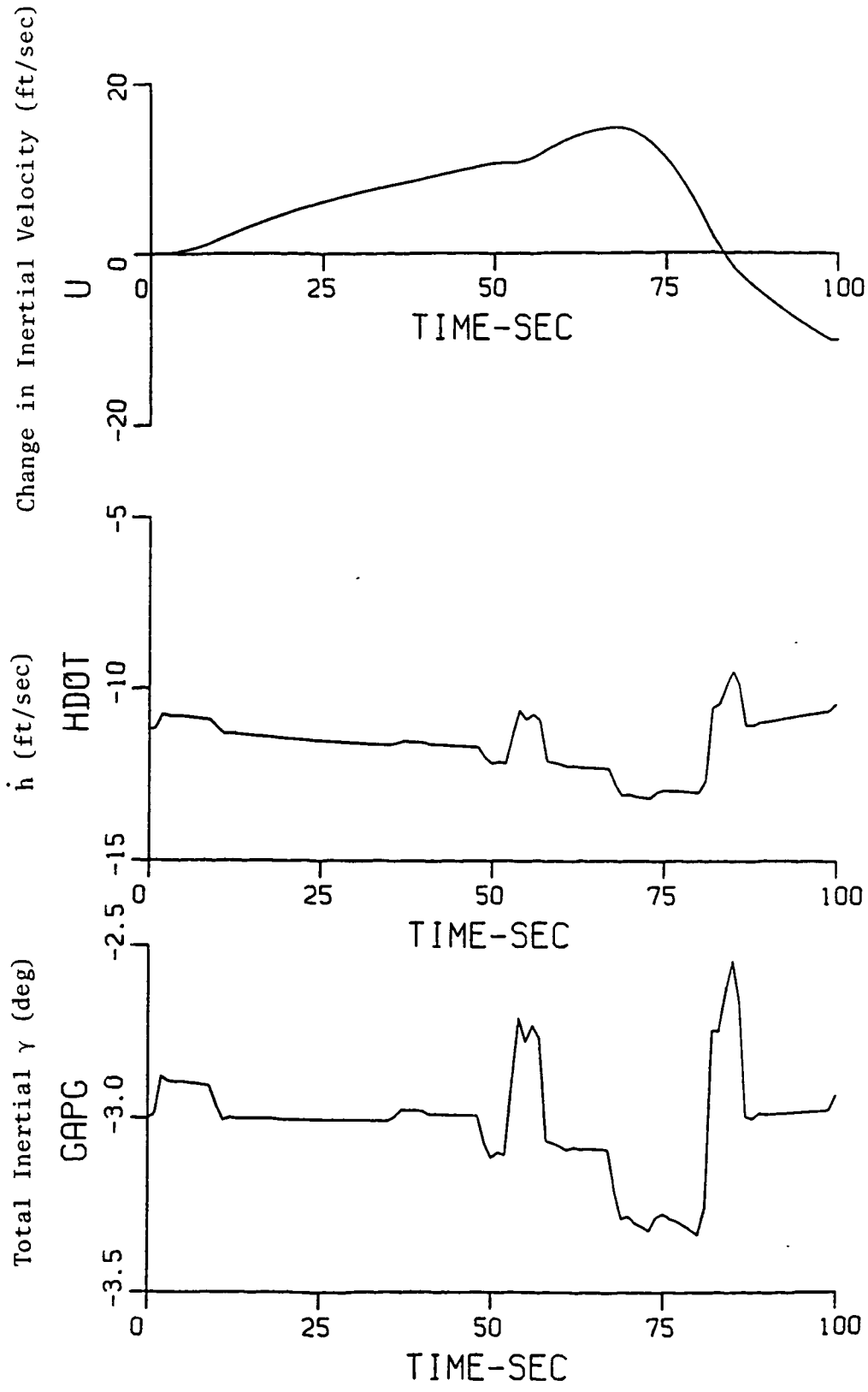

Figure 13. Cont'd SIMULATION OF CONTROL SYSTEM 1 (FEEDBACK AND FEEDFORWARD) WITH THE KENNEDY SHEAR

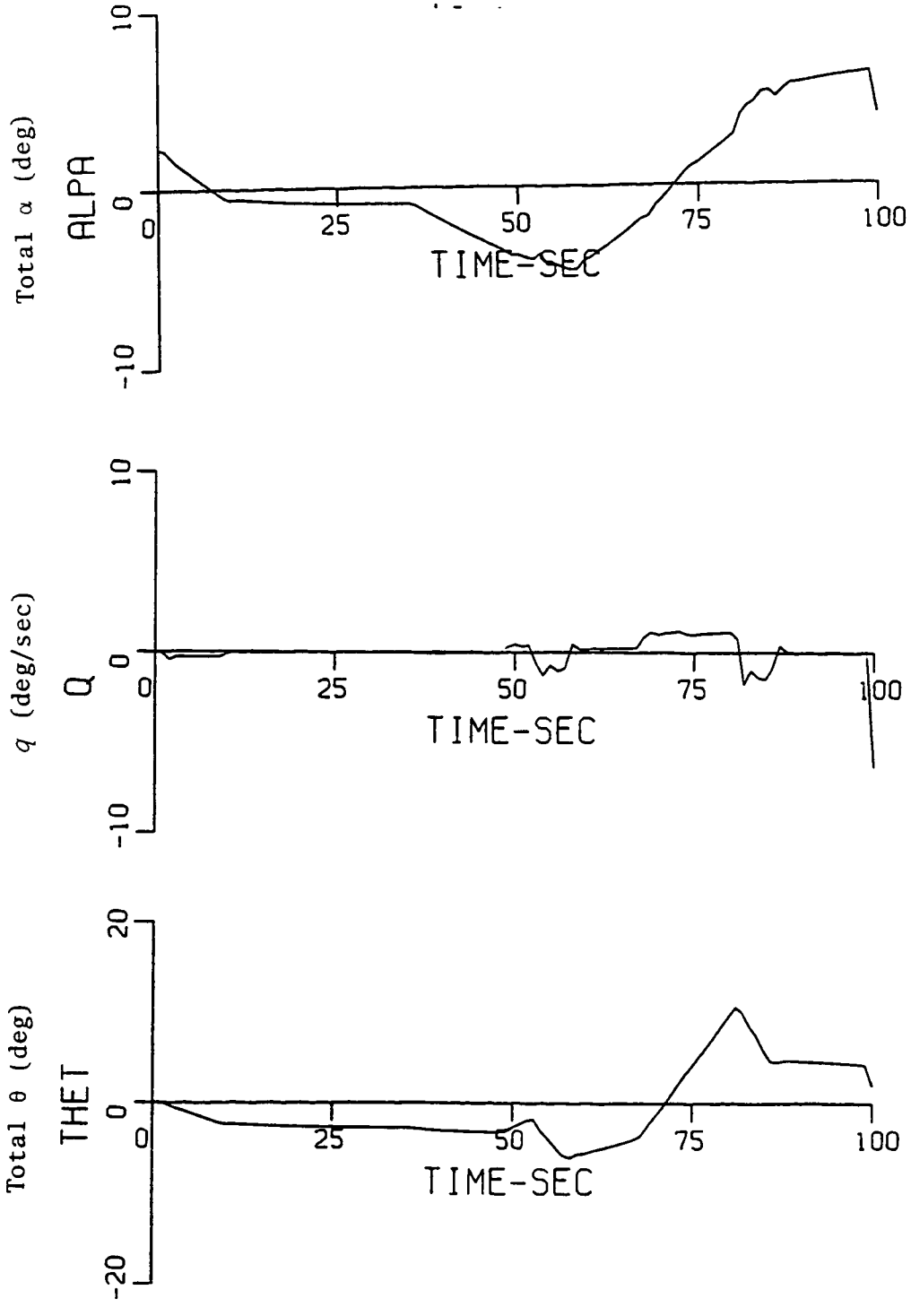

Figure 13. Cont'd SIMULATION OF CONTROL SYSTEM 1 (FEEDBACK AND FEEDFORWARD) WITH THE KENNEDY SHEAR

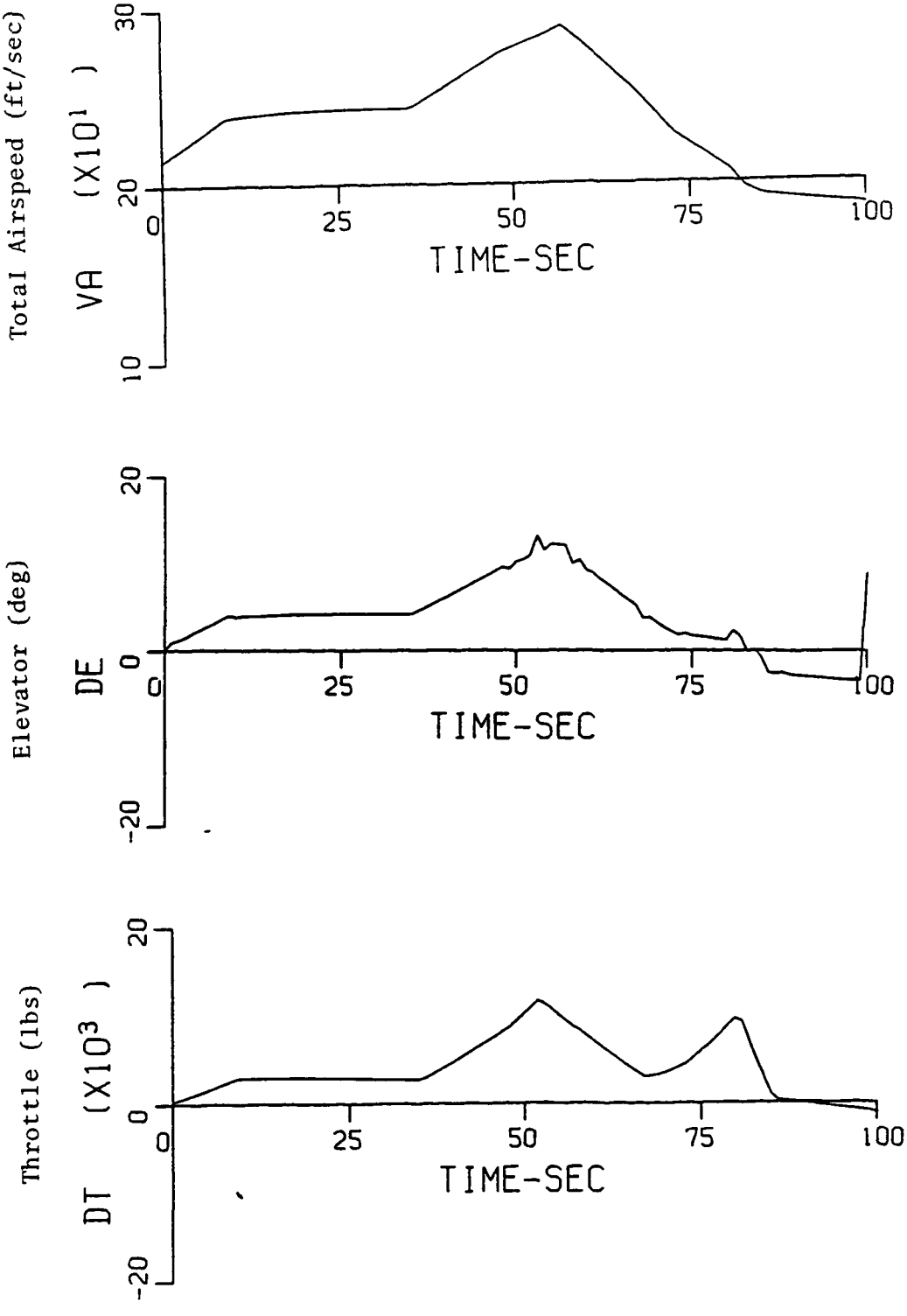

Figure 13. Cont'd SIMULATION OF CONTROL SYSTEM 1 (FEEDBACK AND FEEDFORWARD) WITH THE KENNEDY SHEAR

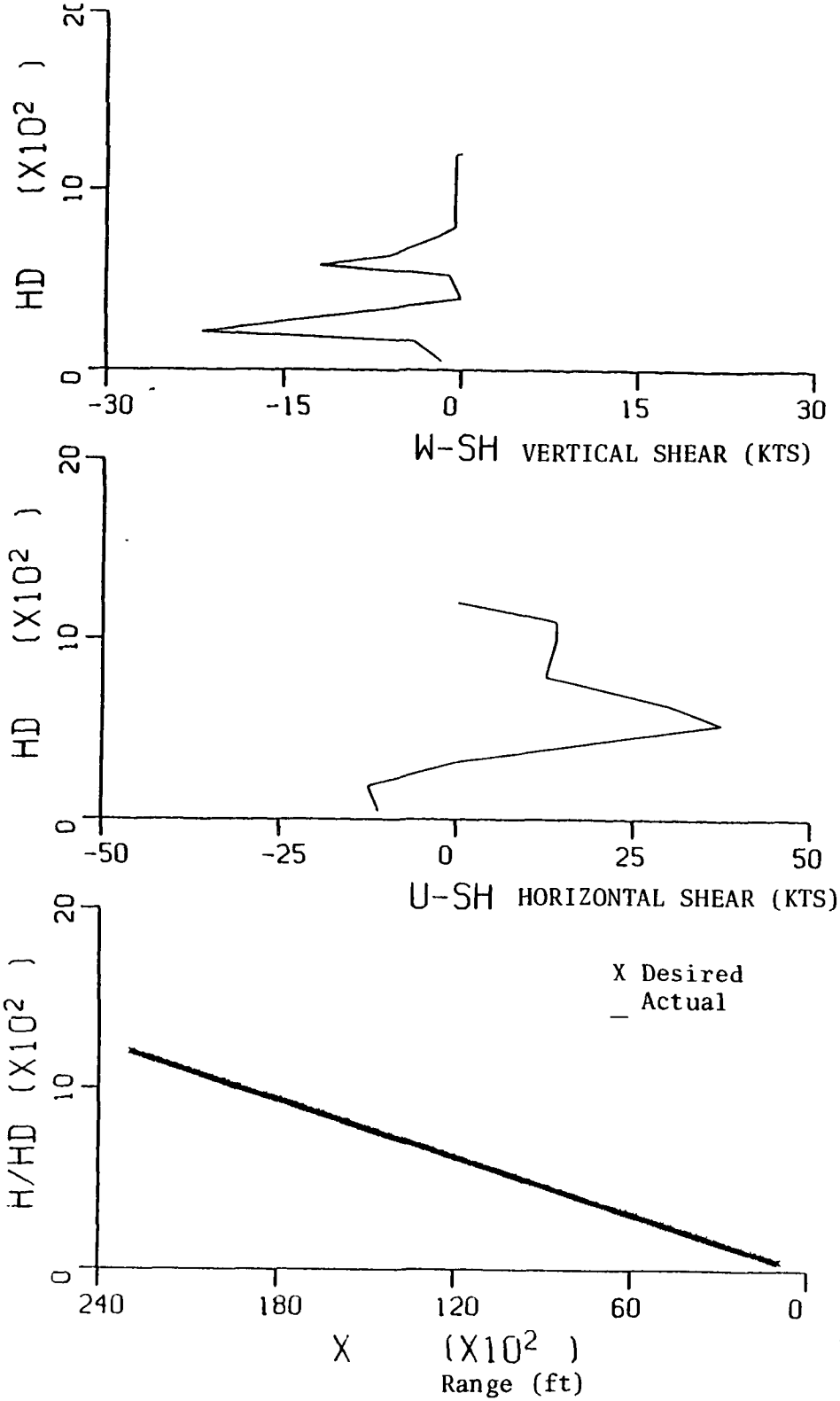

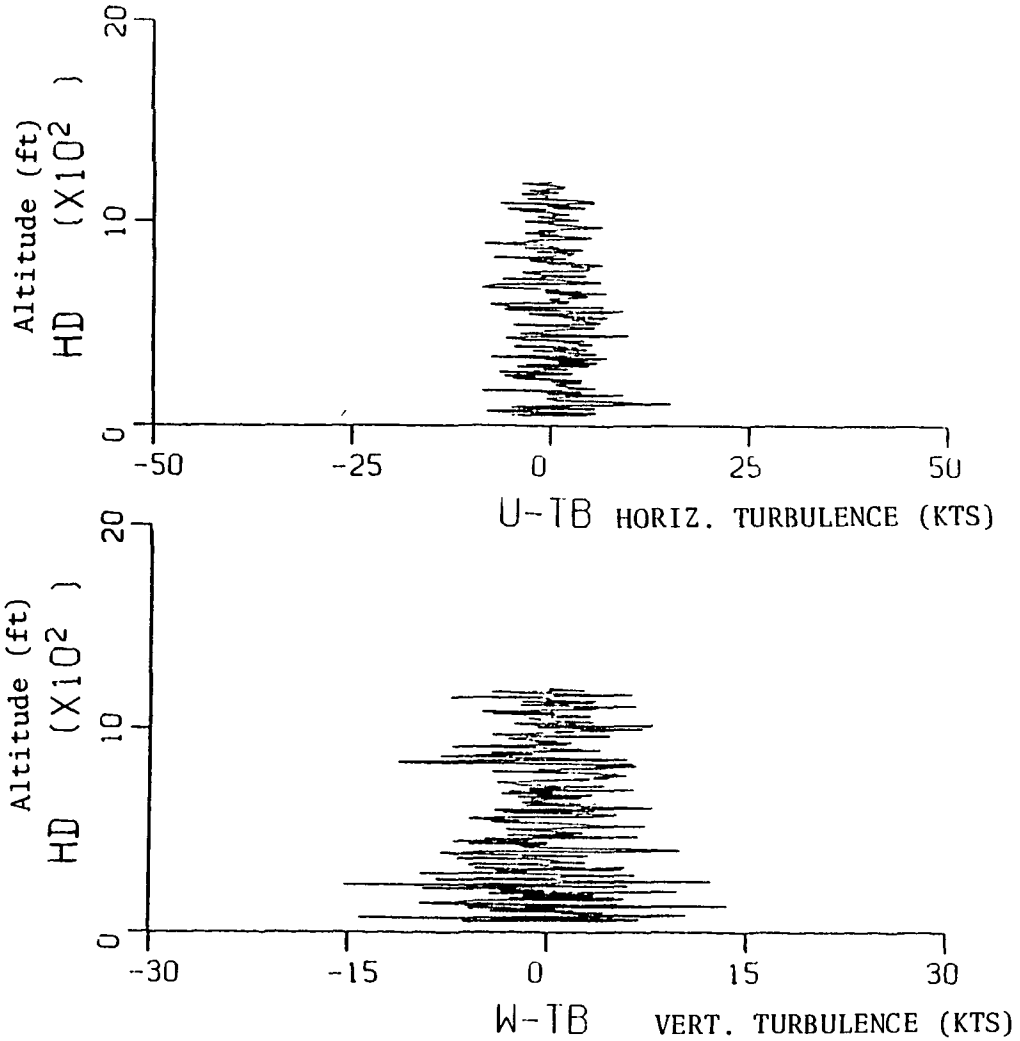

Figure 14. SIMULATION OF CONTROL SYSTEM 1 (FEEDBACK AND FEEDFORWARD) WITH KENNEDY SHEAR AND TURBULENCE

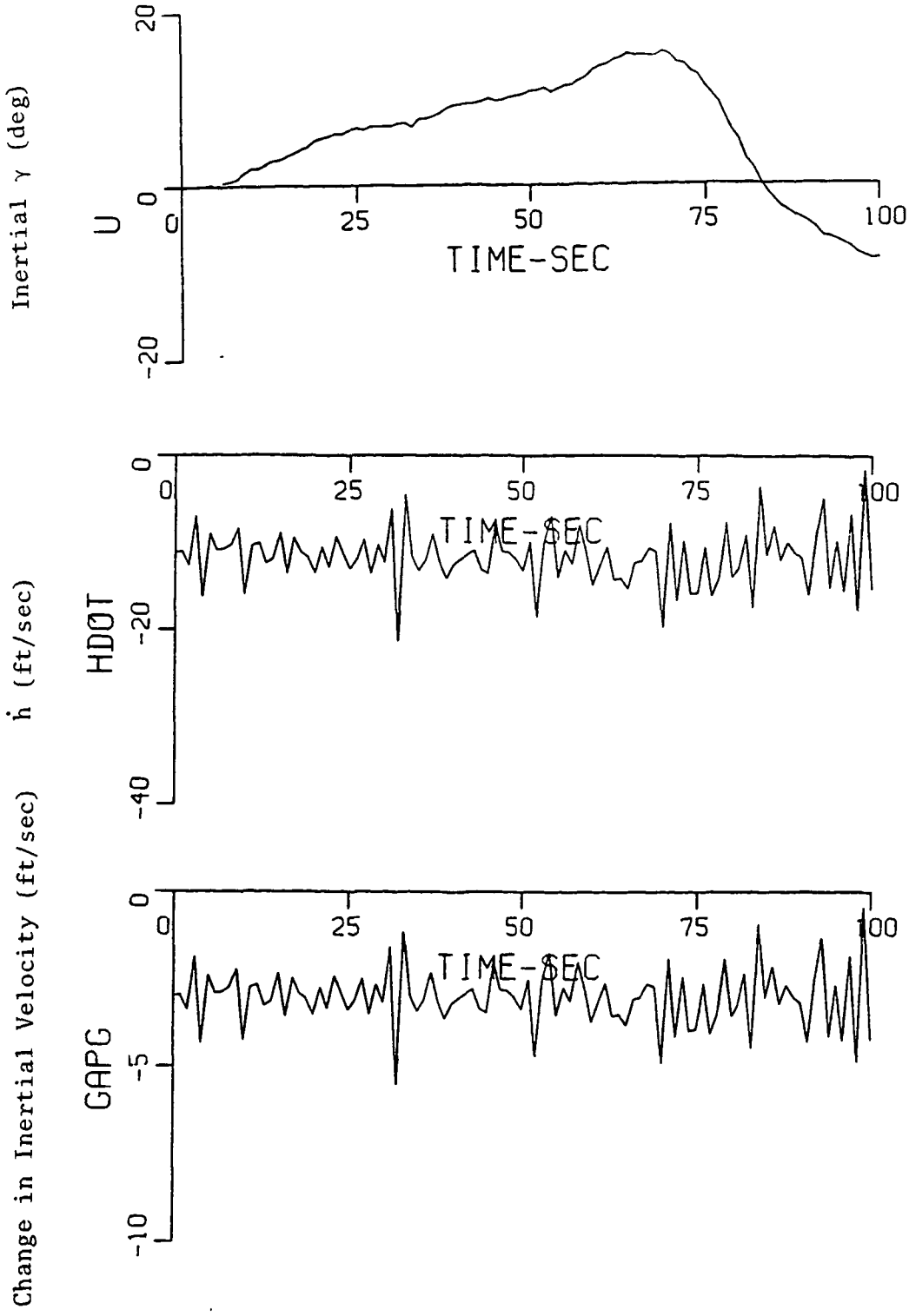

Figure 14. Cont'd SIMULATION OF CONTROL SYSTEM 1 (FEEDBACK AND FEEDFORWARD) WITH KENNEDY SHEAR AND TURBULENCE

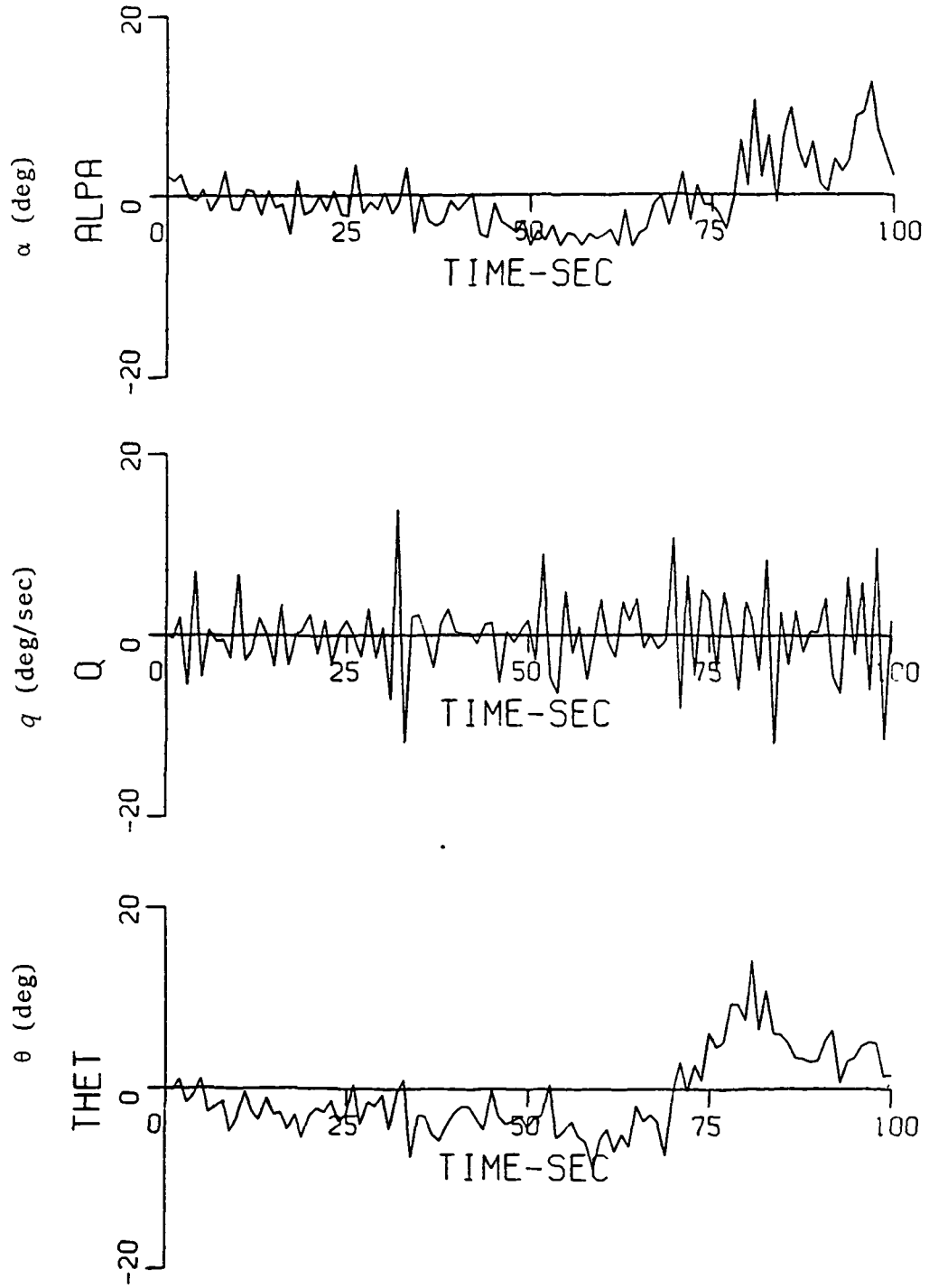

Figure 14. Cont'd SIMULATION OF CONTROL SYSTEM 1 (FEEDBACK AND FEEDFORWARD) WITH KENNEDY SHEAR AND TURBULENCE

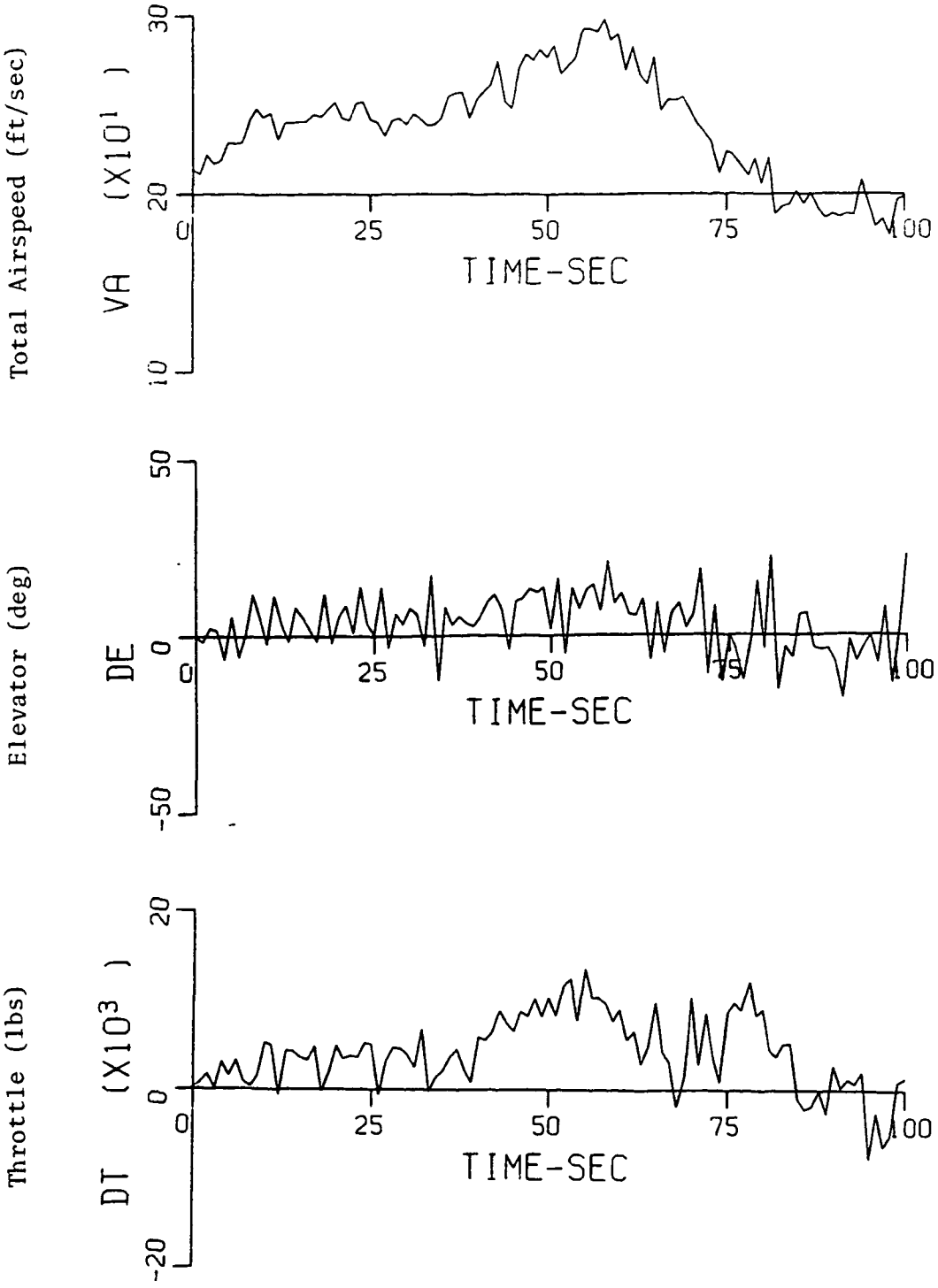

Figure 14. SIMULATION OF CONTROL SYSTEM 1 (FEEDBACK AND FEEDFORWARD) WITH KENNEDY SHEAR AND TURBULENCE
Cont'd

Simulation results of the control system with the severe Philadelphia T-25A shear and the Tower T-9A moderate shear are shown in Figures 15 and 16, respectively. As indicated by the time histories, the flight path angle is very well regulated. The performance is similar to the performance with the Kennedy shear.

Simulation results of control system 2 regulating the inertial velocity, altitude and altitude rate, and including the feedforward control for the three shear profiles are shown in Figures 17, 18 and 19, respectively. The flight path angle for all three cases is very well regulated.

Simulation time histories of control system 3 are shown in Figures 20 and 21. Figure 20 shows time histories of the altitude and airspeed regulation control system simulation and Figure 21 shows the simulation of the altitude, altitude rate, and airspeed regulation control system. Initially when the headwind is encountered, the throttle and the elevator are activated to minimize the deviation in airspeed and glide path. The throttle activity is decreased because of the headwind whereas control system 1 increased the throttle activity to minimize the deviation in inertial speed. The throttle activity is increased when the headwind turns to a tailwind and the severe down draft is encountered to minimize the deviation in the airspeed. In contrast, control system 1 decreased the throttle activity after getting past the severe down draft. The angle of attack increases to a maximum of about 5.3^{o} from its trim value. The thrust has increased to a maximum of about 21,000 lbs from the trim setting and the maximum elevator deflection is about 6.8^{o}. The flight path angle is well regulated. The inertial speed varies proportionately with the windspeed in an opposite sense in contrast to control system 1 simulation where the airspeed variation was proportional to the windspeed. The angle of attack excursion is smaller than that for control system 1. The elevator deflection is about half of the deflection for control system 1 whereas the maximum thrust is about two times more than that for control system 1. The performance of control system 3 regulating the airspeed, altitude and altitude rate is similar to the performance of the airspeed and altitude regulation system.

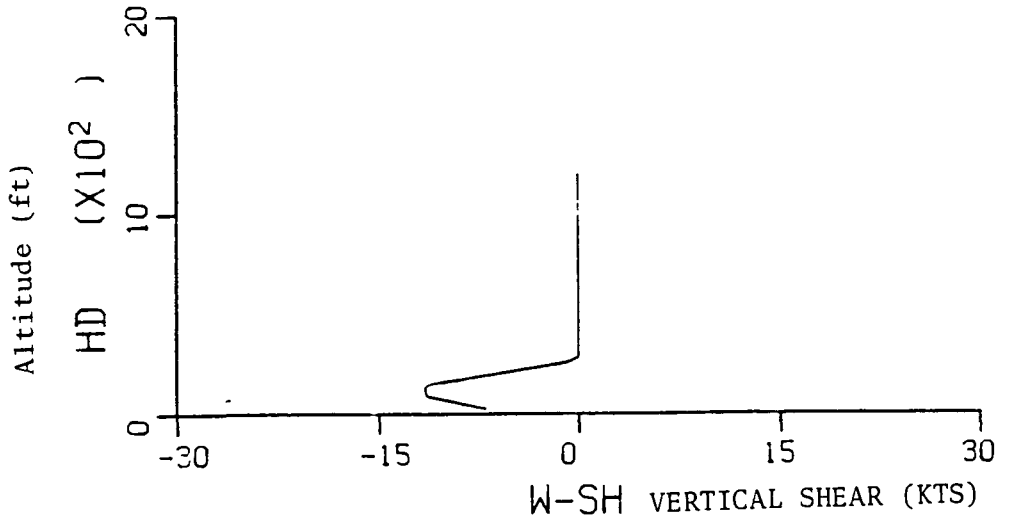

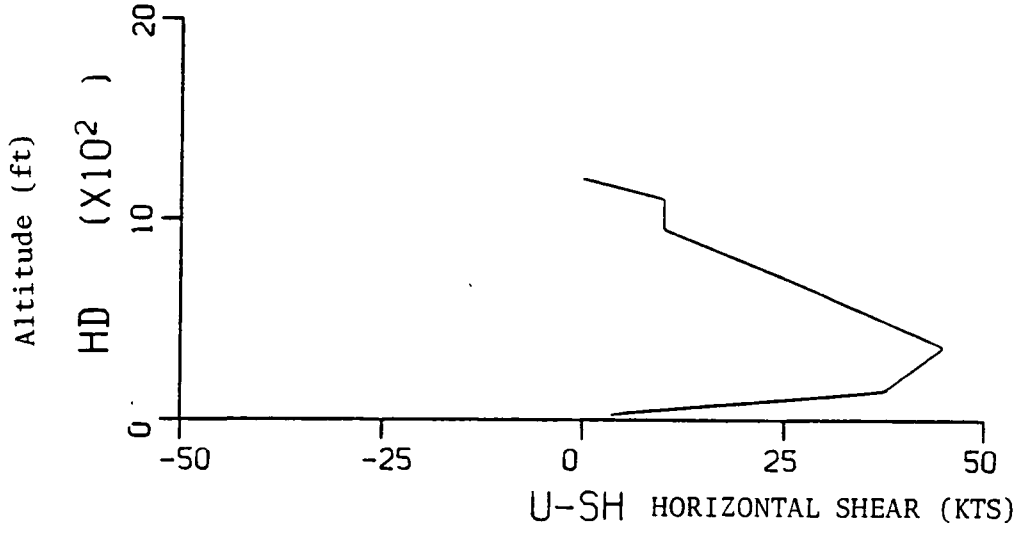

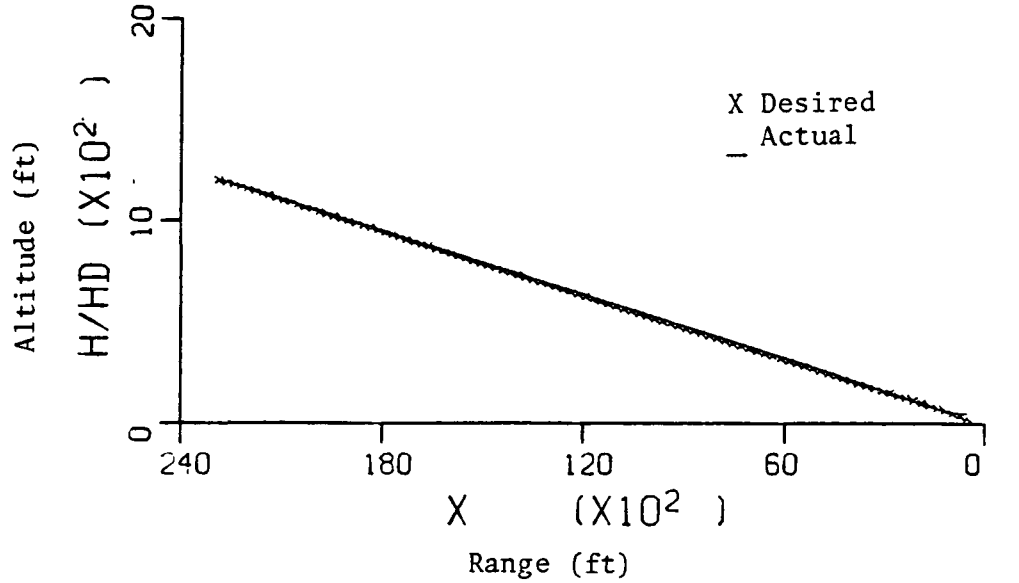

Figure 15. SIMULATION OF CONTROL SYSTEM 1 (FEEDBACK AND FEEDFORWARD) WITH THE PHILADELPHIA SEVERE SHEAR

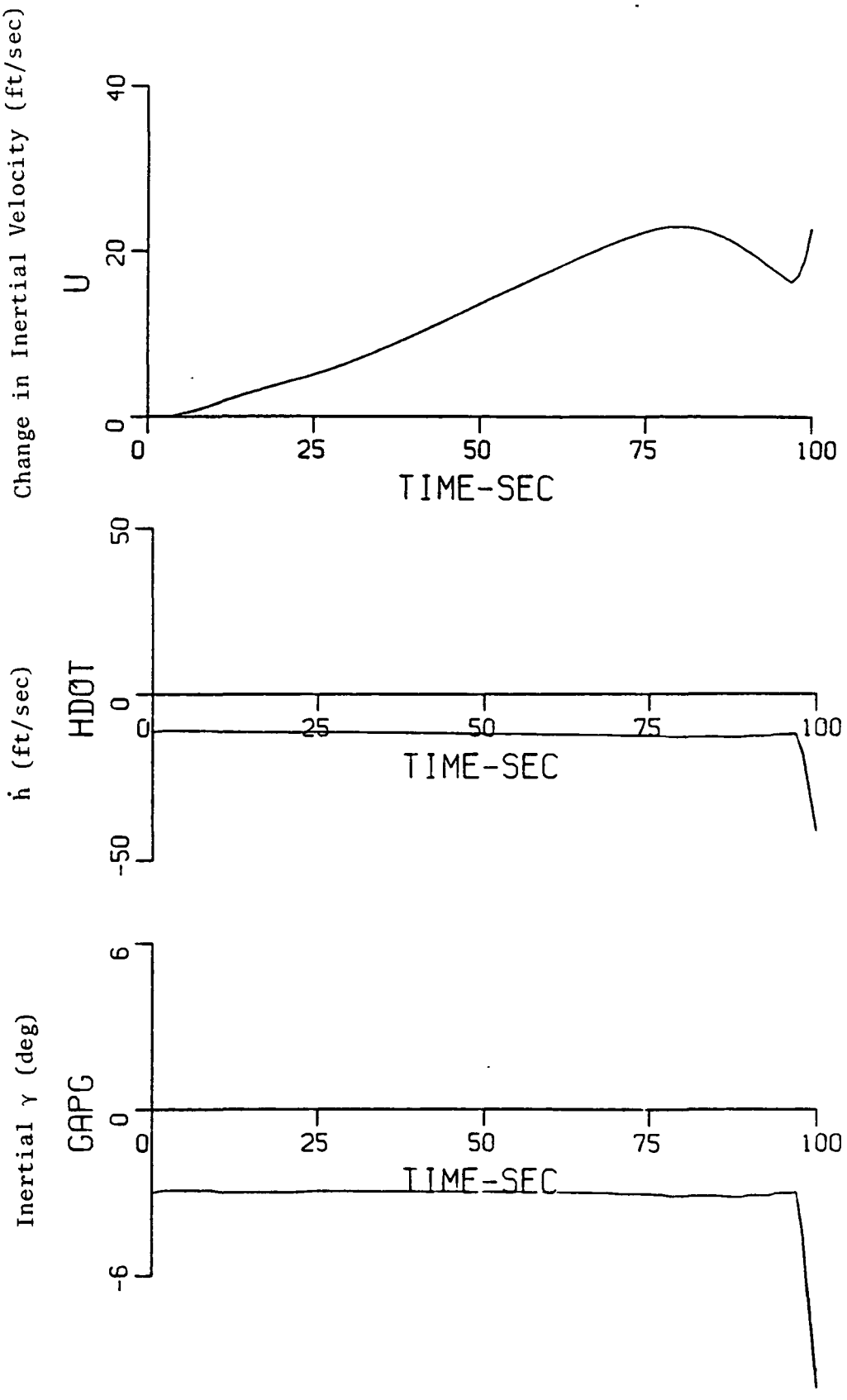

Figure 15. Cont'd SIMULATION OF CONTROL SYSTEM 1 (FEEDBACK AND FEEDFORWARD) WITH THE PHILADELPHIA SEVERE SHEAR

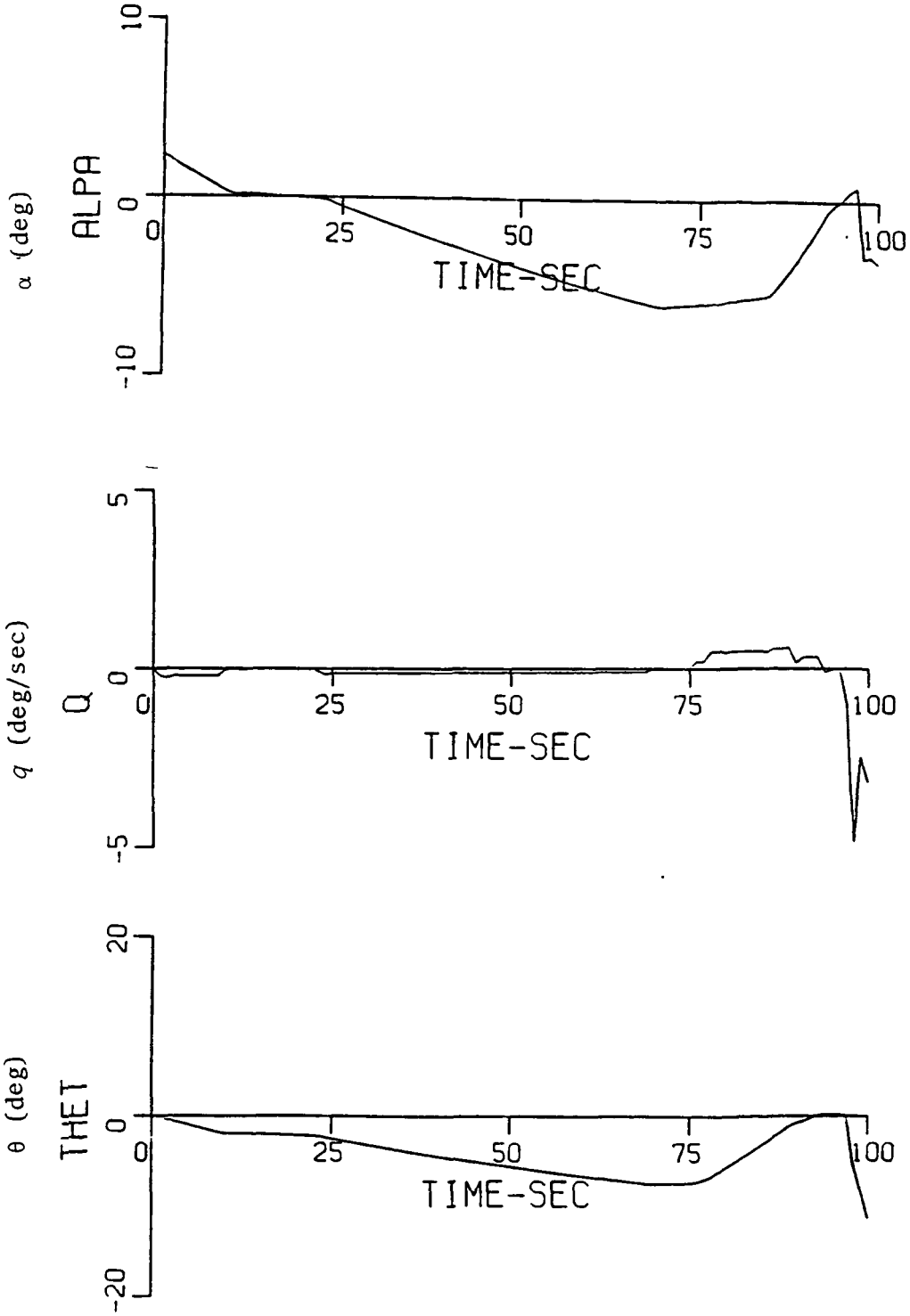

Figure 15. Cont'd SIMULATION OF CONTROL SYSTEM 1 (FEEDBACK AND FEEDFORWARD) WITH THE PHILADELPHIA SEVERE SHEAR

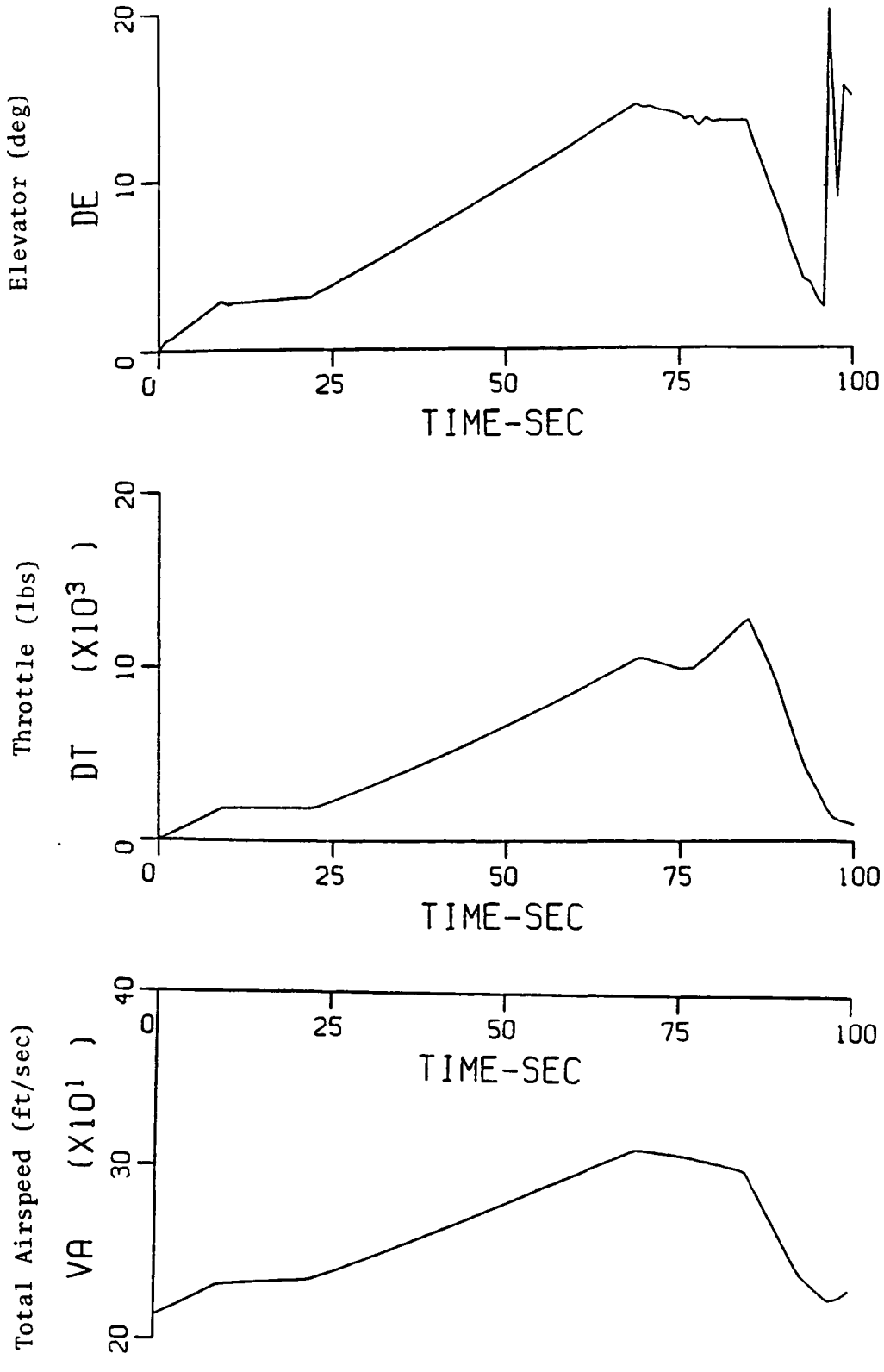

Figure 15. Cont'd SIMULATION OF CONTROL SYSTEM 1 (FEEDBACK AND FEEDFORWARD) WITH THE PHILADELPHIA SEVERE SHEAR

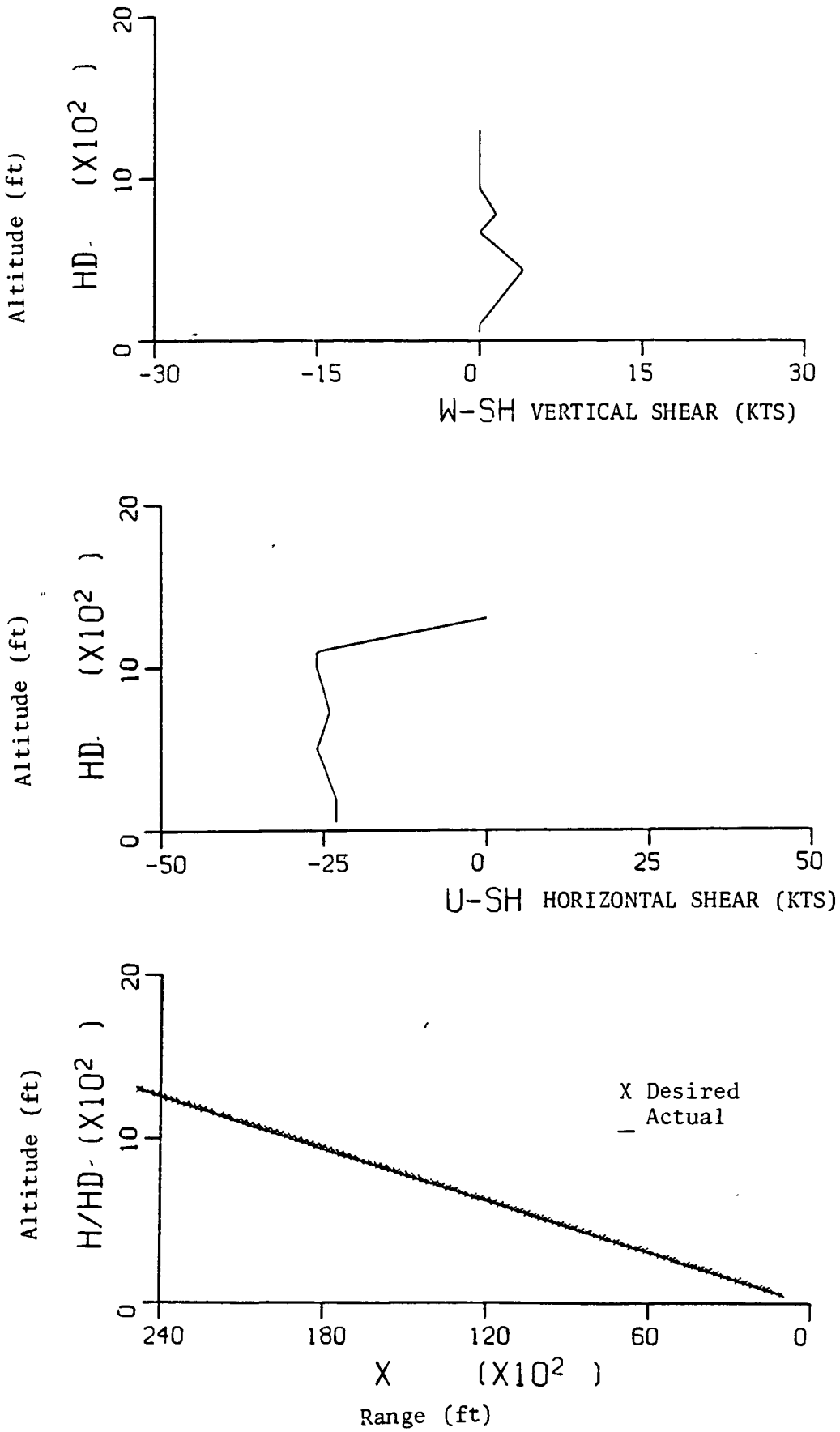

Figure 16. SIMULATION OF CONTROL SYSTEM 1 (FEEDBACK) WITH THE MODERATE SHEAR

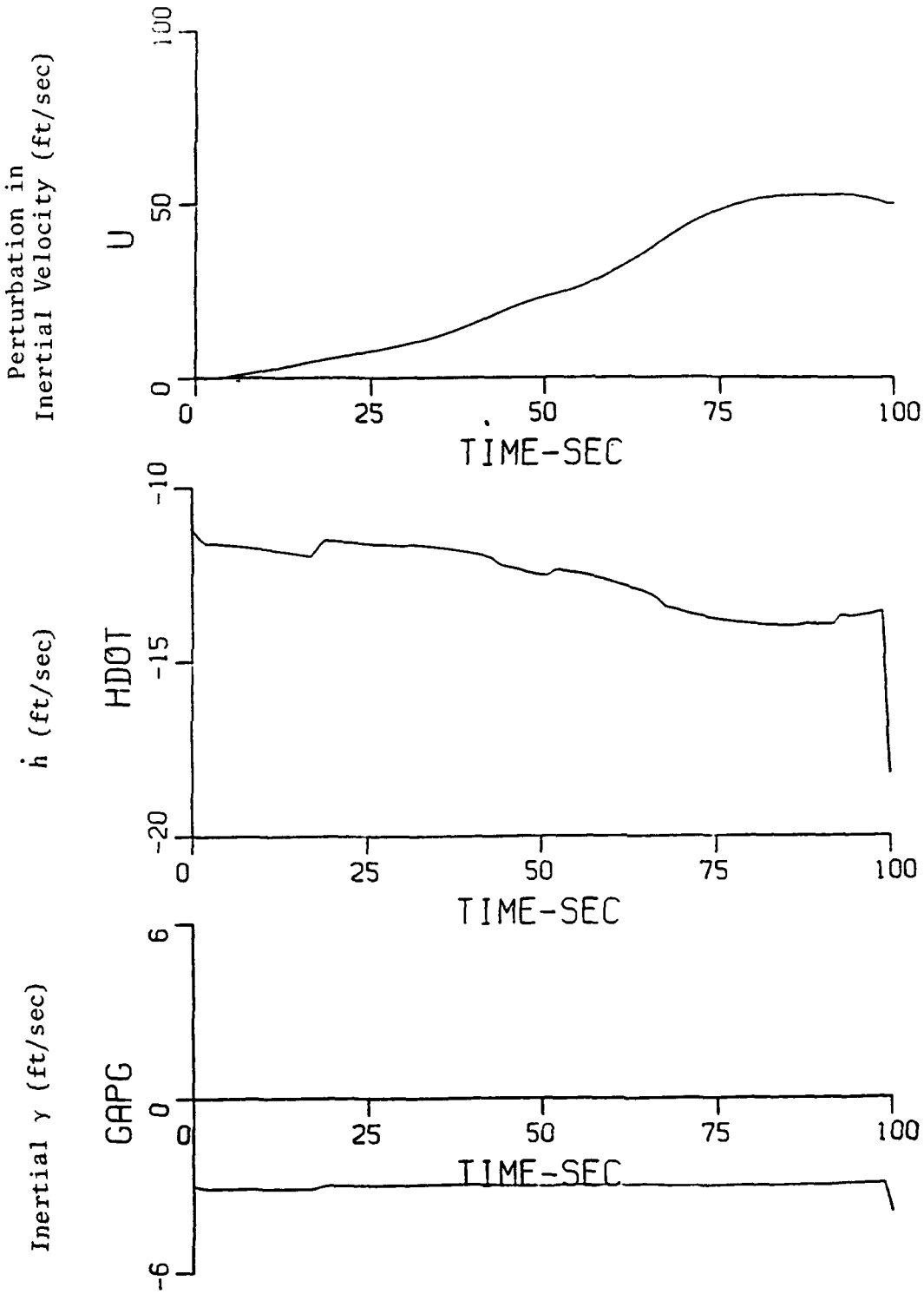

Figure 16. Cont'd SIMULATION OF CONTROL SYSTEM 1 (FEEDBACK) WITH THE MODERATE SHEAR

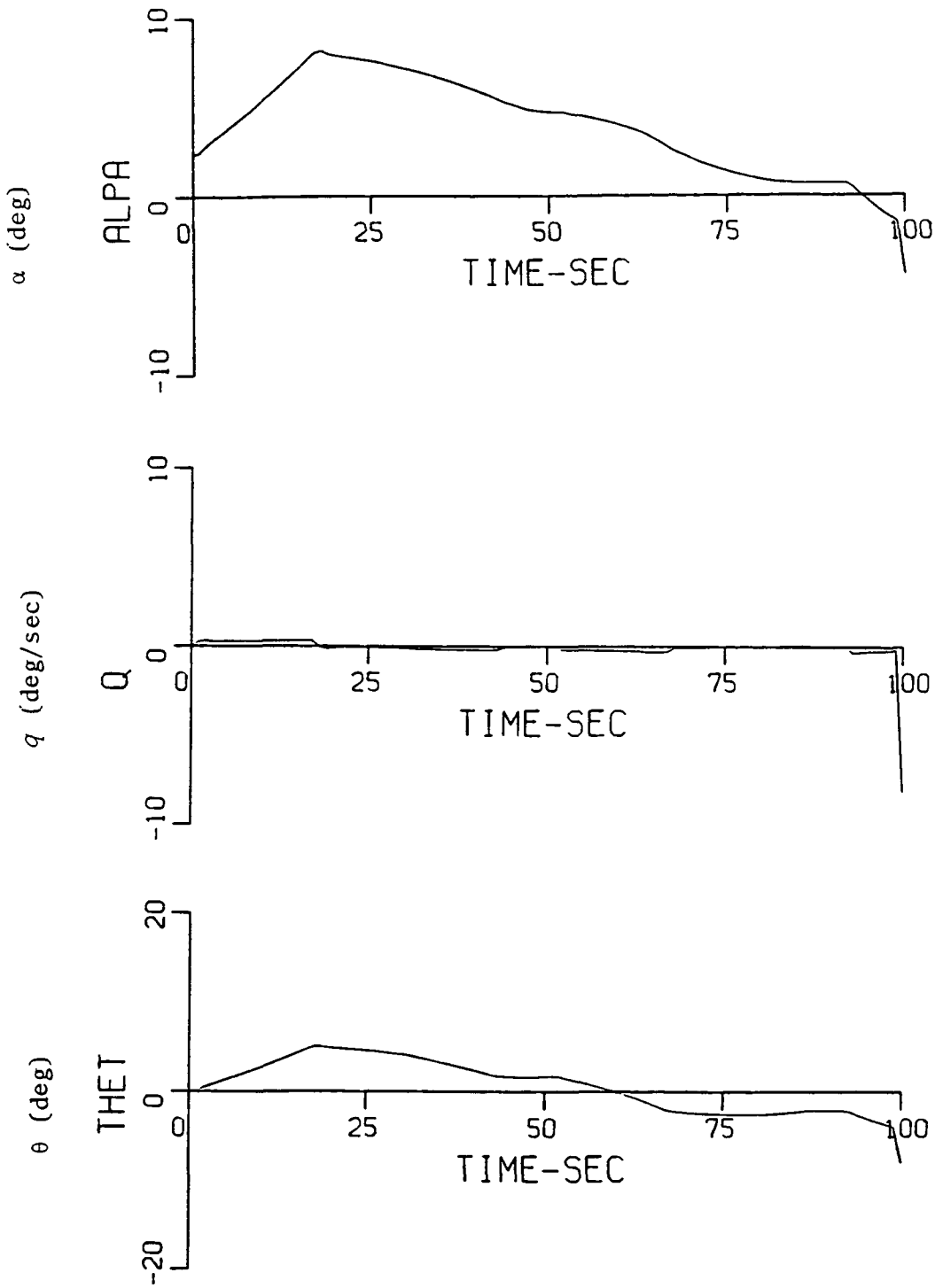

Figure 16. Cont'd SIMULATION OF CONTROL SYSTEM 1 (FEEDBACK) WITH THE MODERATE SHEAR

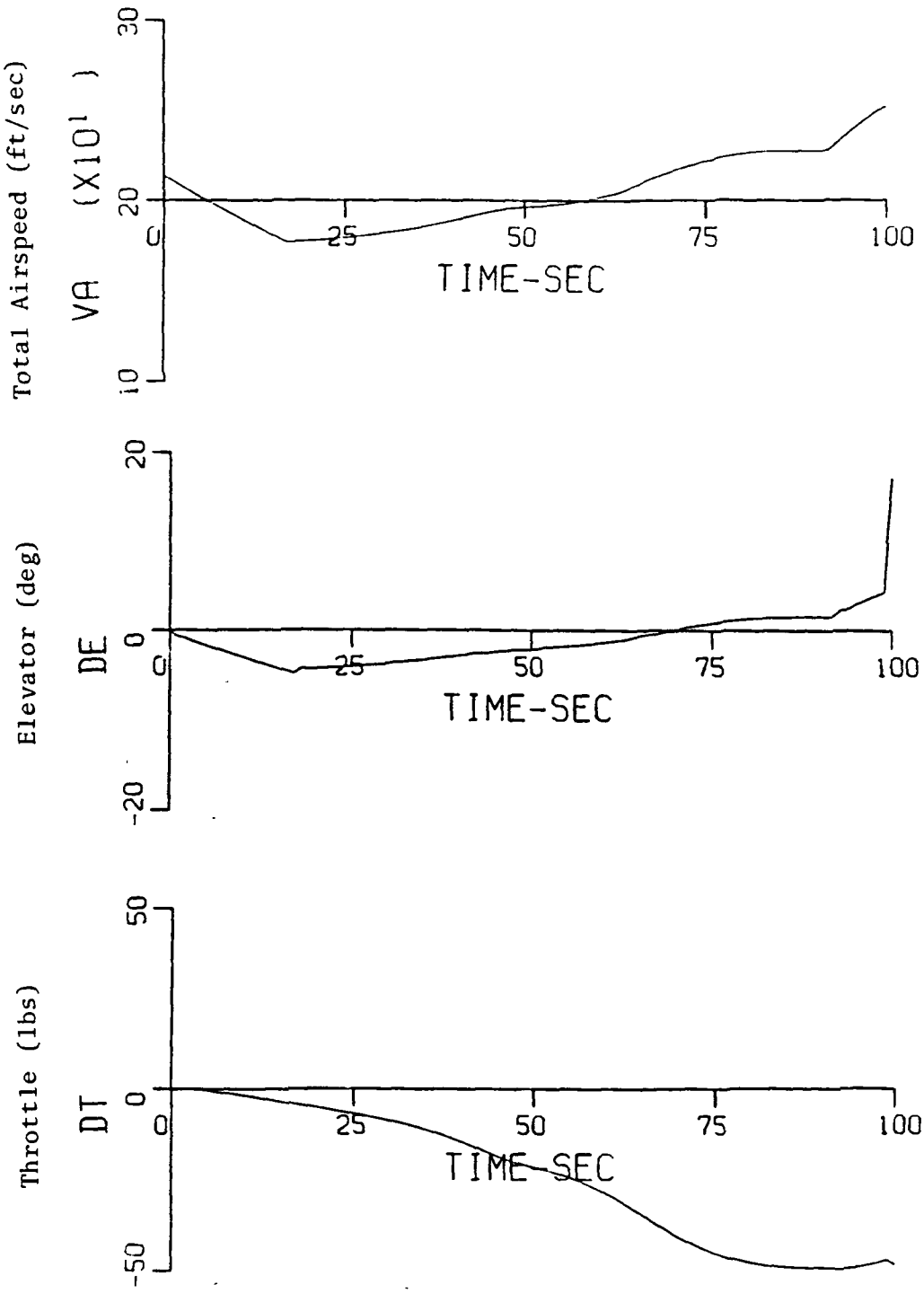

Figure 16. Cont'd SIMULATION OF CONTROL SYSTEM 1 (FEEDBACK) WITH THE MODERATE SHEAR

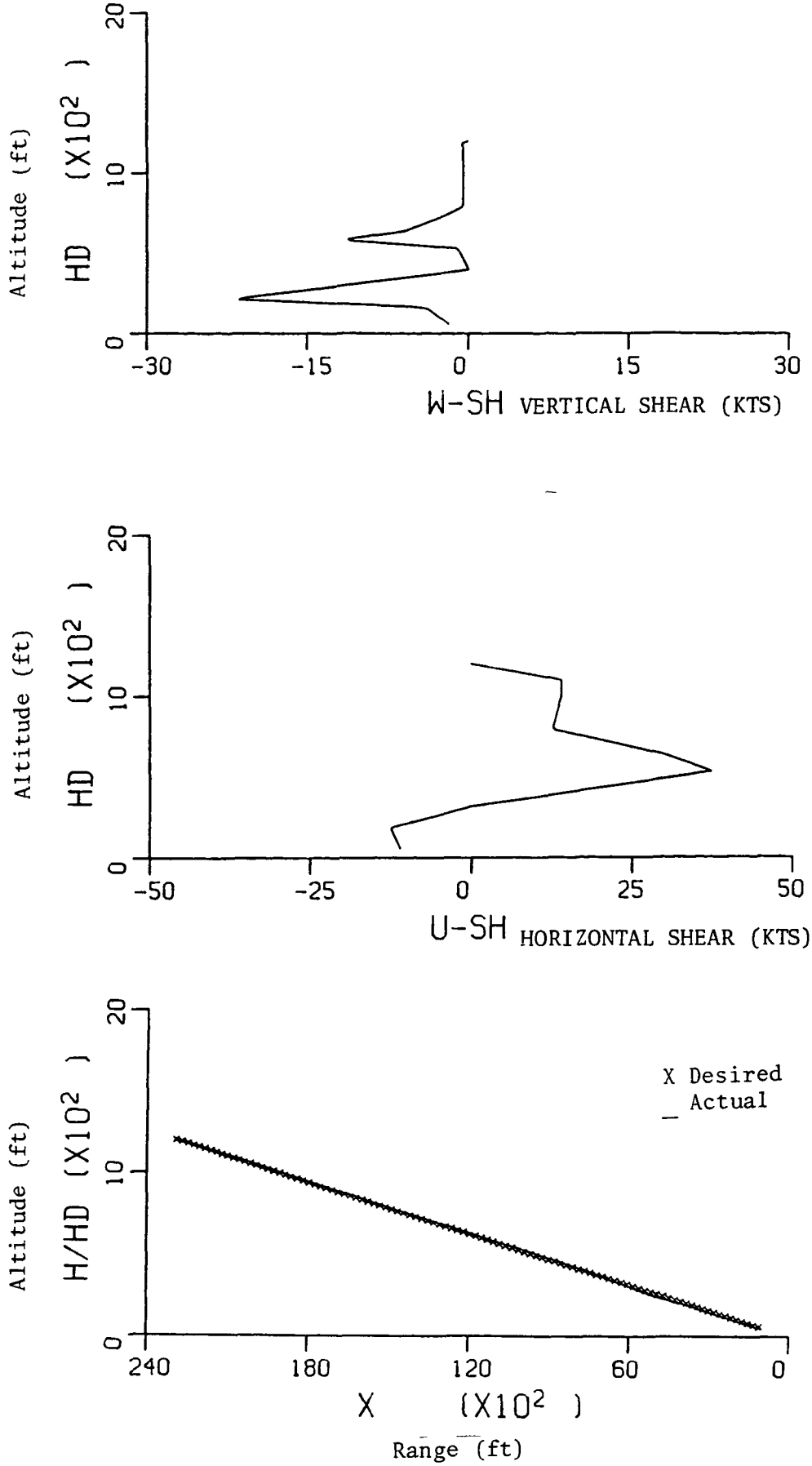

Figure 17. SIMULATION OF CONTROL SYSTEM 2 (FEEDBACK AND FEEDFORWARD) WITH THE SEVERE KENNEDY SHEAR

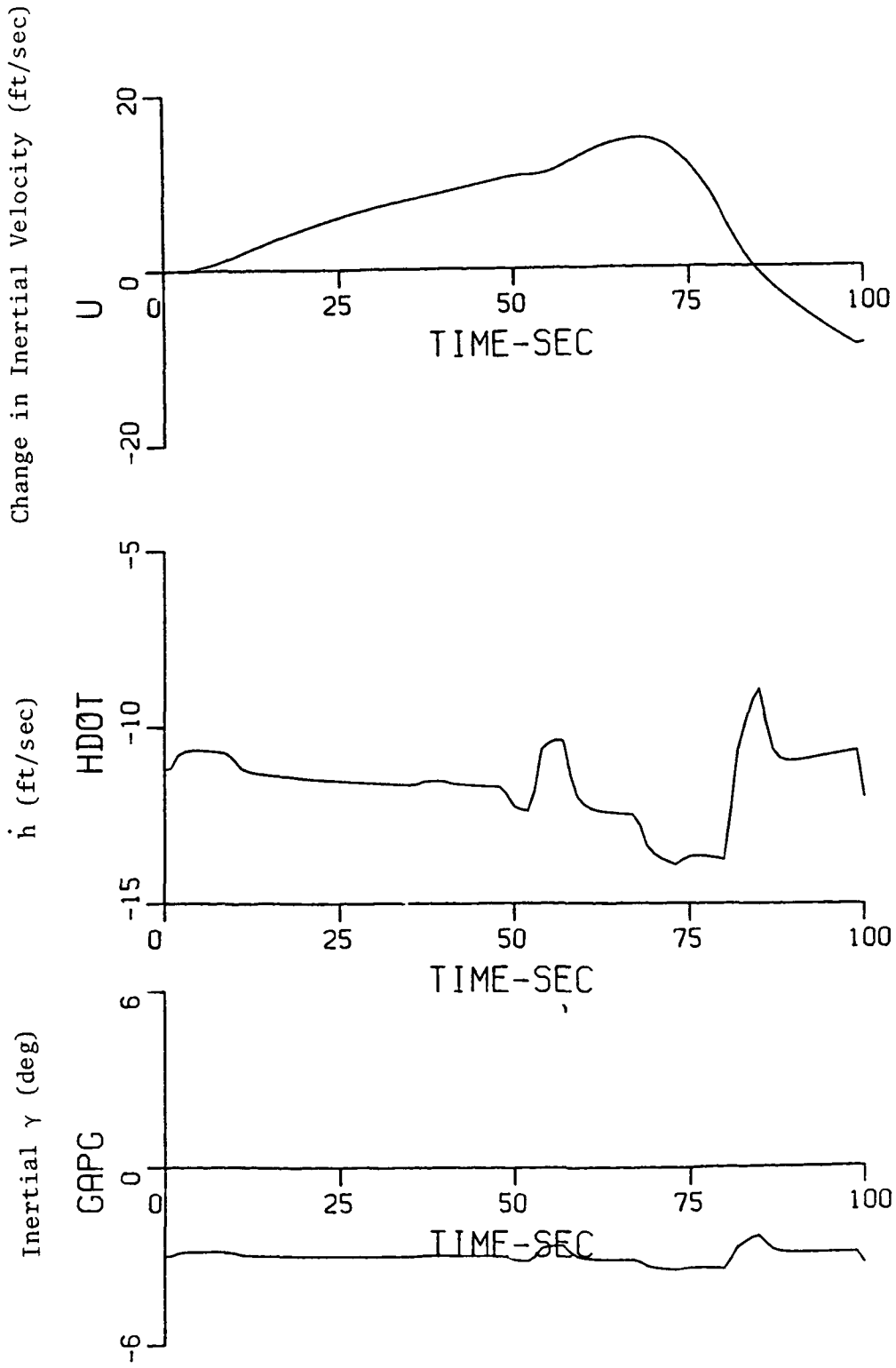

Figure 17. Cont'd SIMULATION OF CONTROL SYSTEM 2 (FEEDBACK AND FEEDFORWARD) WITH THE SEVERE KENNEDY SHEAR

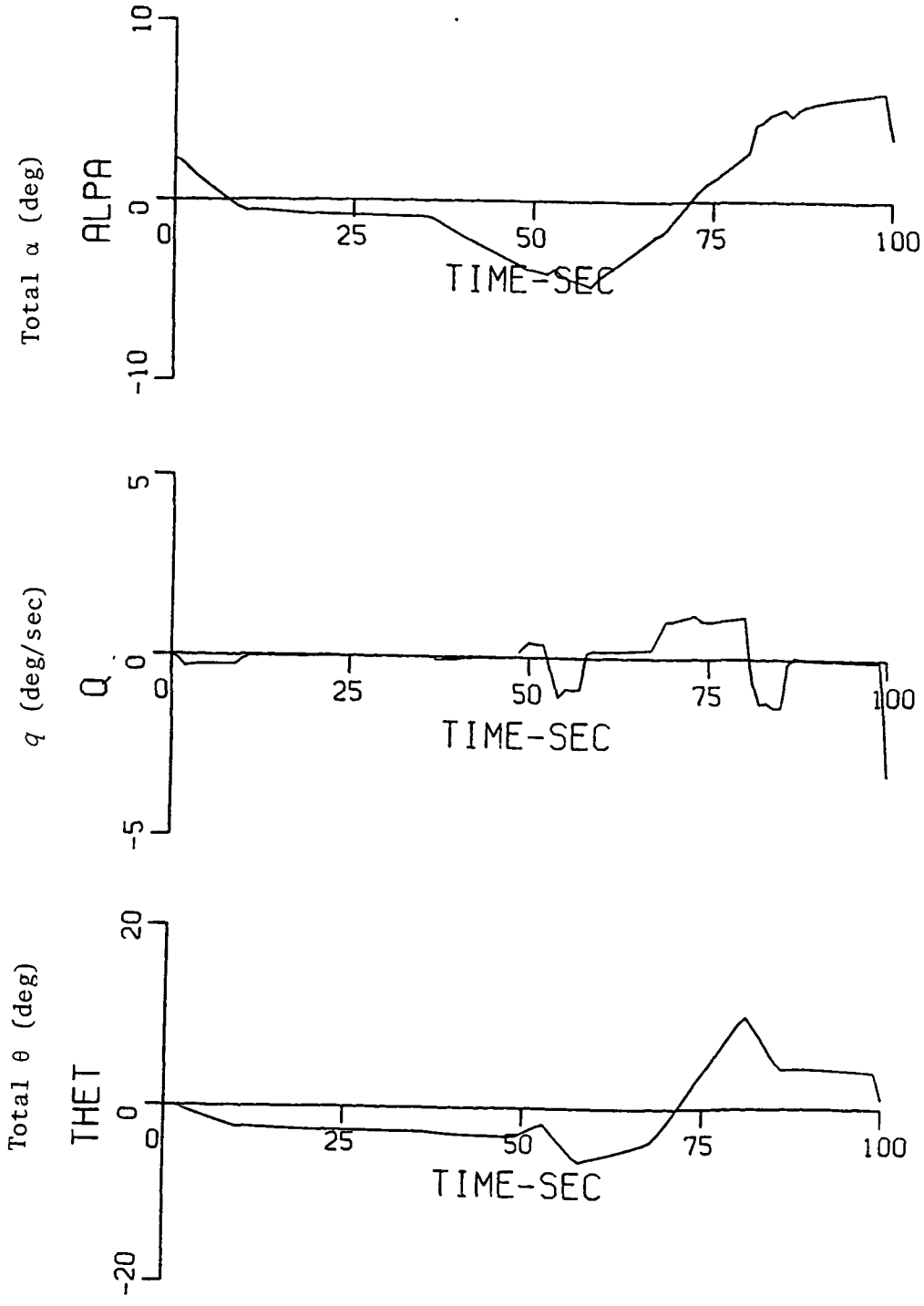

Figure 17. SIMULATION OF CONTROL SYSTEM 2 (FEEDBACK AND FEEDFORWARD) WITH THE SEVERE KENNEDY SHEAR
Cont'd

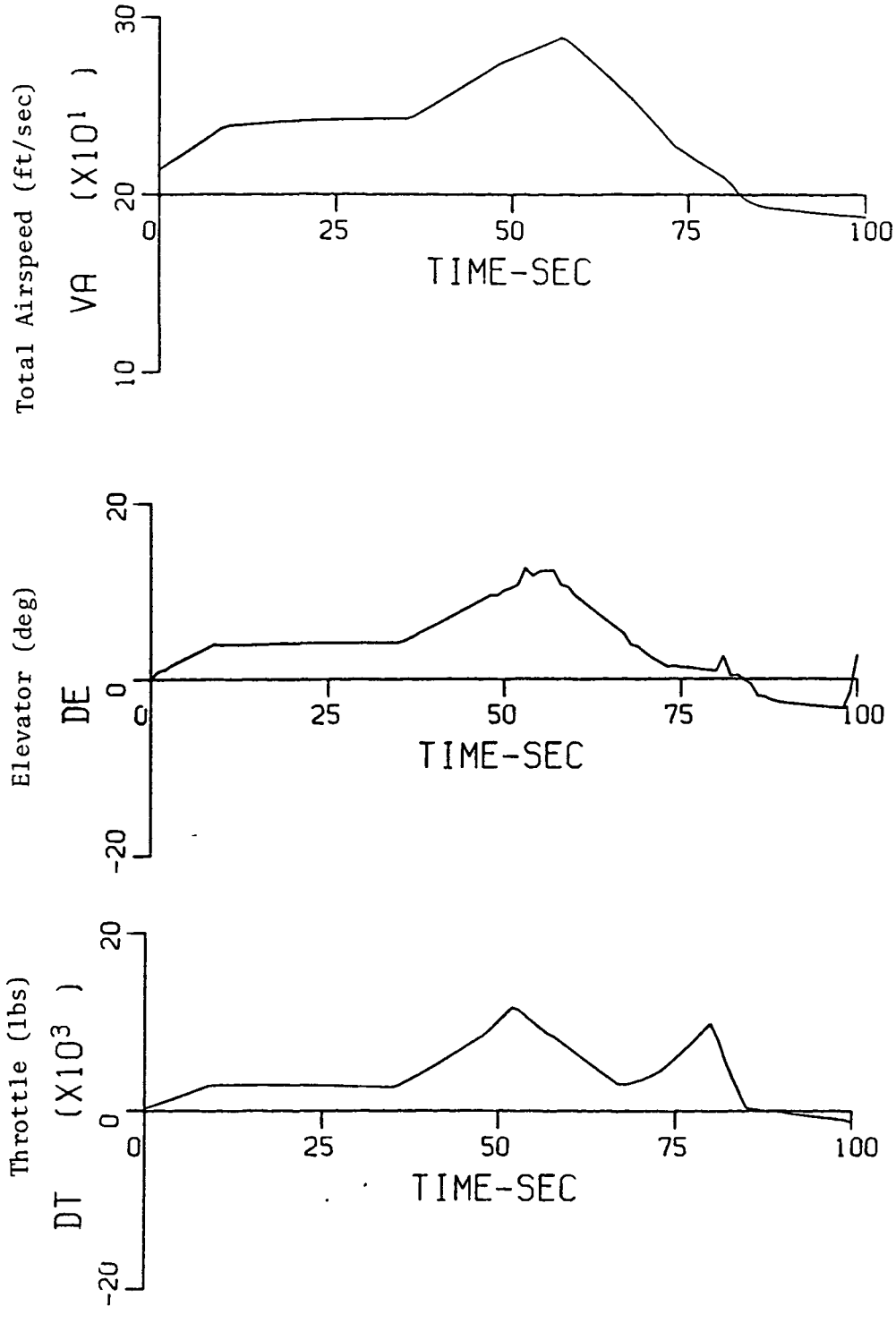

Figure 17. Cont'd SIMULATION OF CONTROL SYSTEM 2 (FEEDBACK AND FEEDFORWARD) WITH THE SEVERE KENNEDY SHEAR

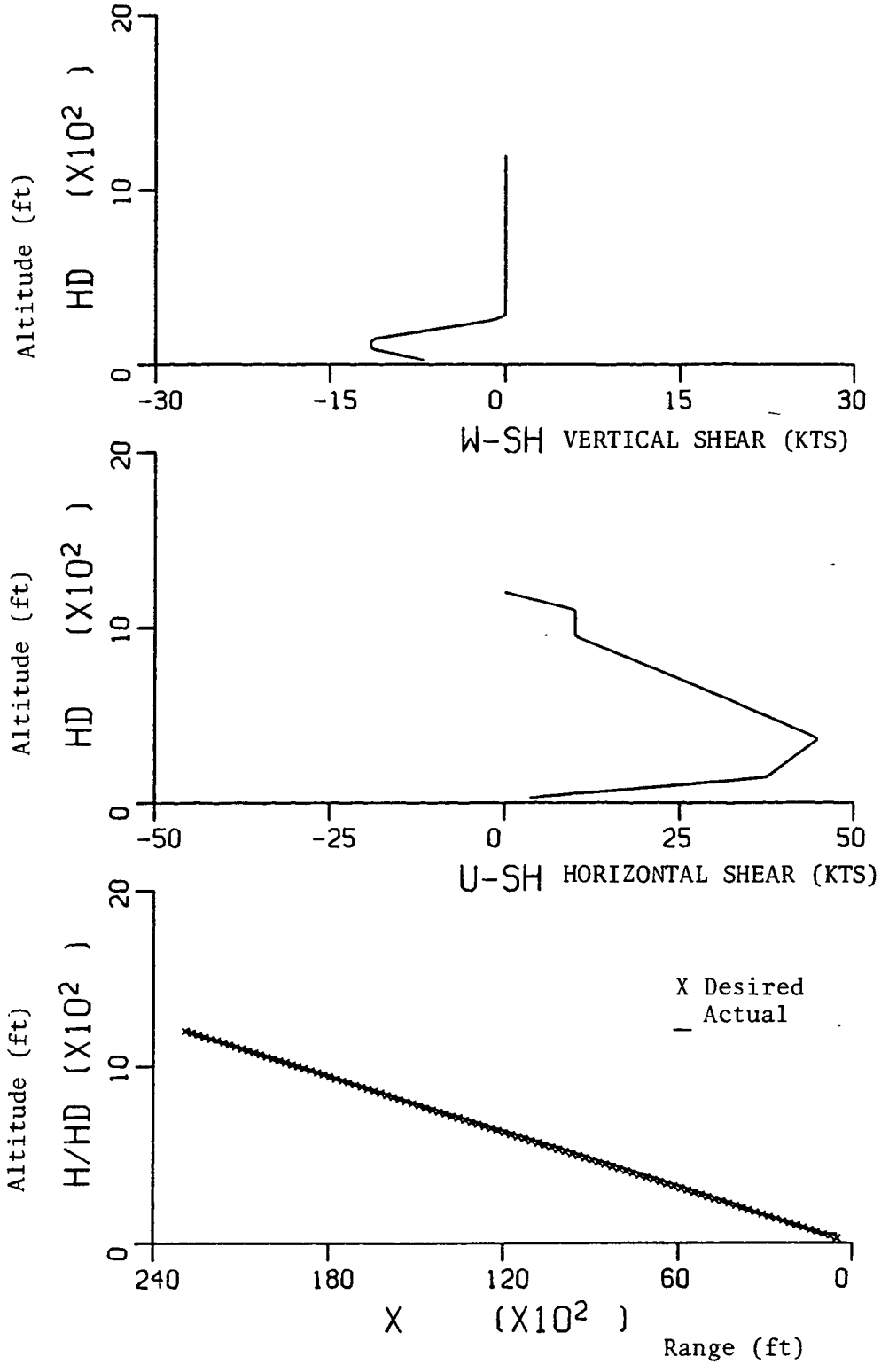

Figure 18. SIMULATION OF CONTROL SYSTEM 2 (FEEDBACK AND FEEDFORWARD) WITH THE PHILADELPHIA SEVERE SHEAR

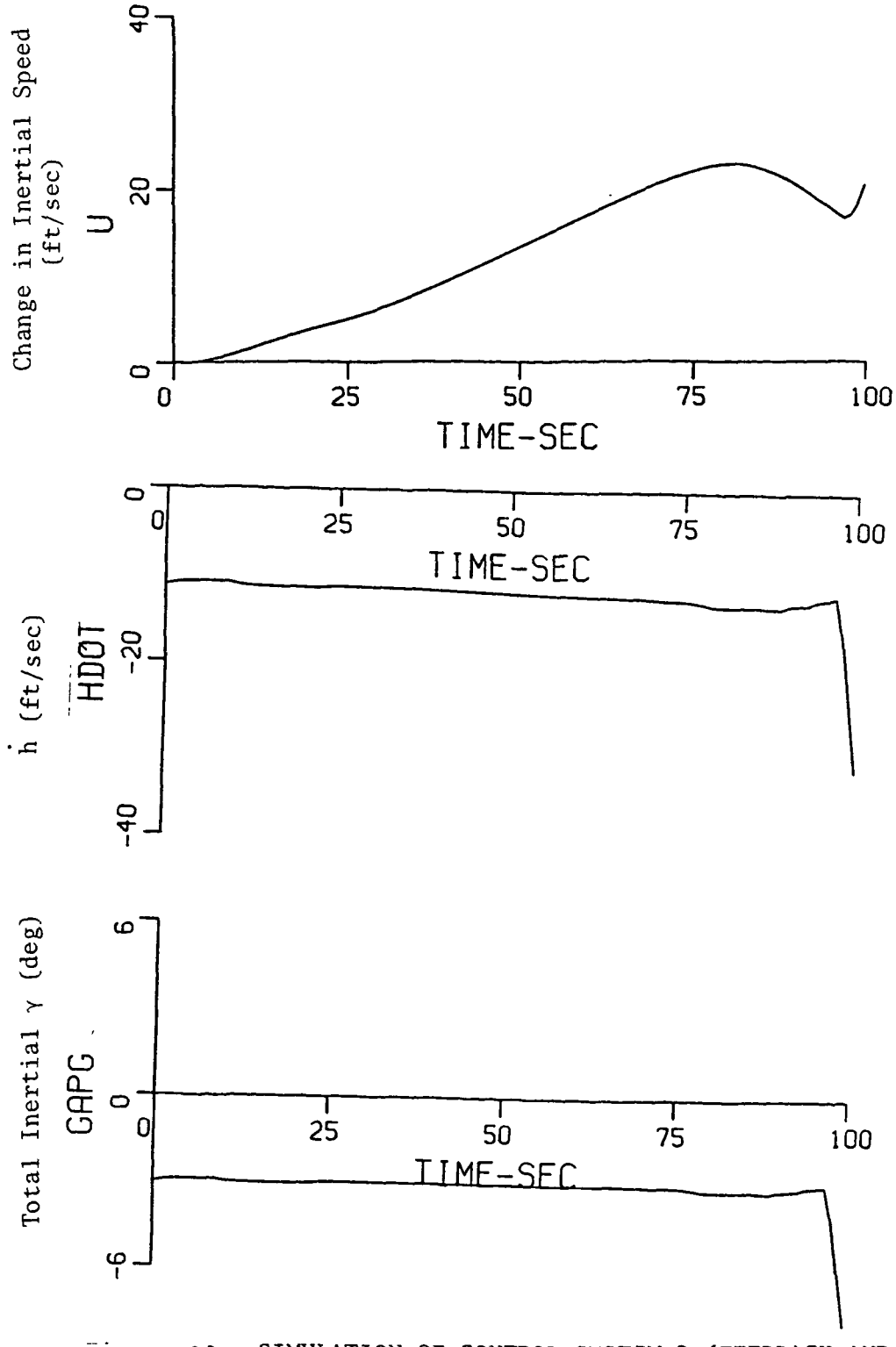

Figure 18. Cont'd SIMULATION OF CONTROL SYSTEM 2 (FEEDBACK AND FEEDFORWARD) WITH THE PHILADELPHIA SEVERE SHEAR

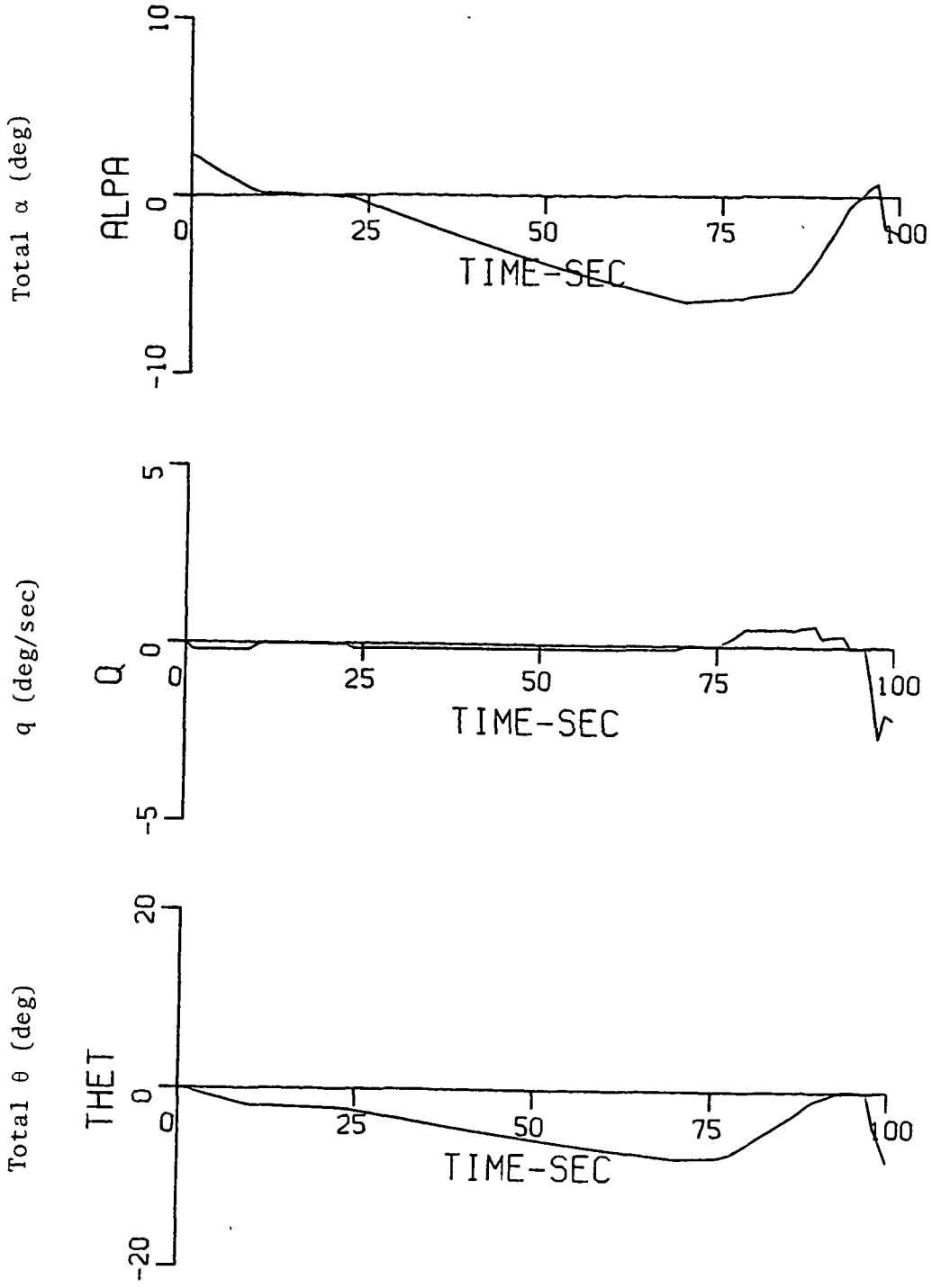

Figure 18. Cont'd SIMULATION OF CONTROL SYSTEM 2 (FEEDBACK AND FEEDFORWARD) WITH THE PHILADELPHIA SEVERE SHEAR

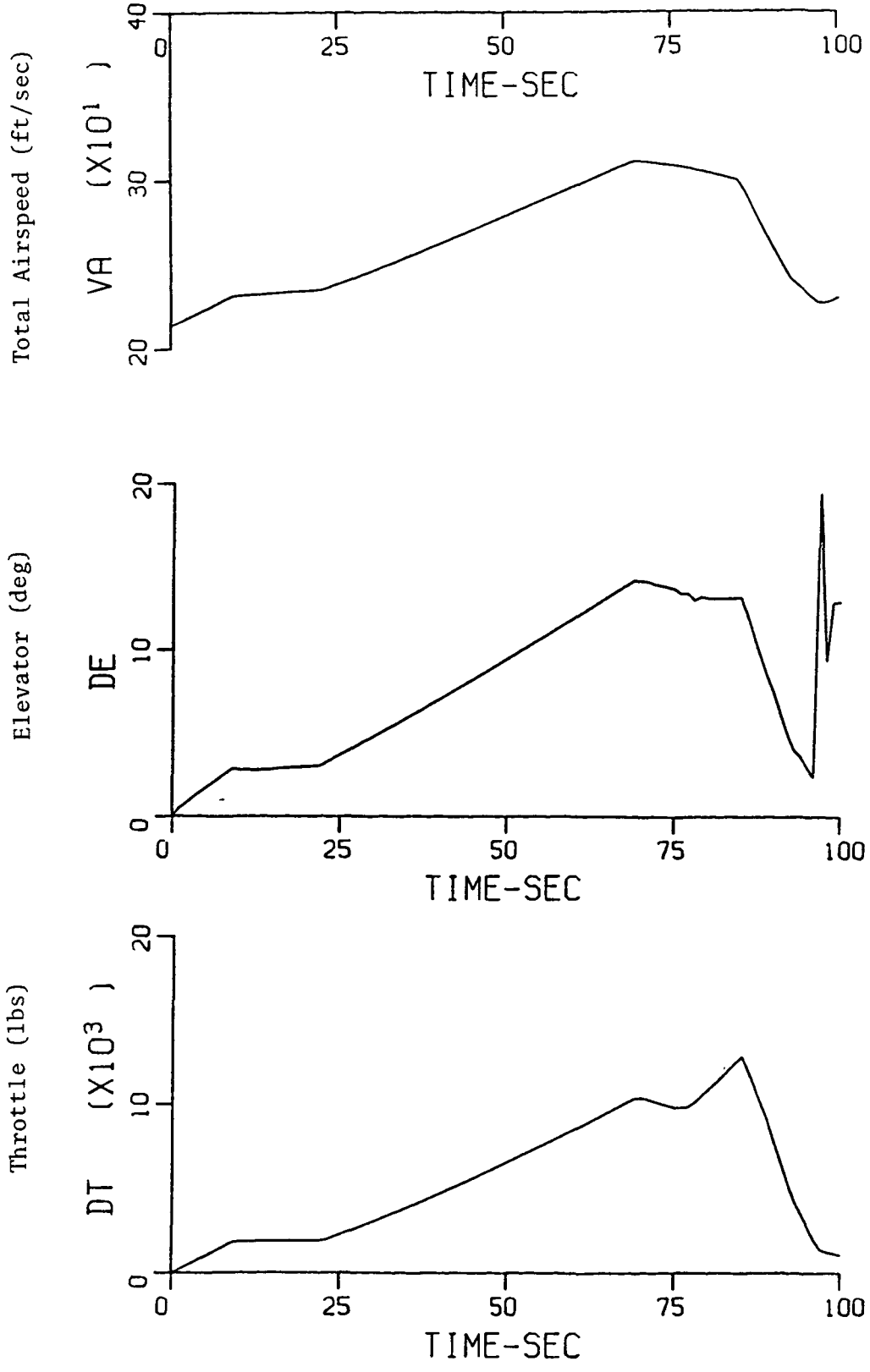

Figure 18. Cont'd SIMULATION OF CONTROL SYSTEM 2 (FEEDBACK AND FEEDFORWARD) WITH THE PHILADELPHIA SEVERE SHEAR

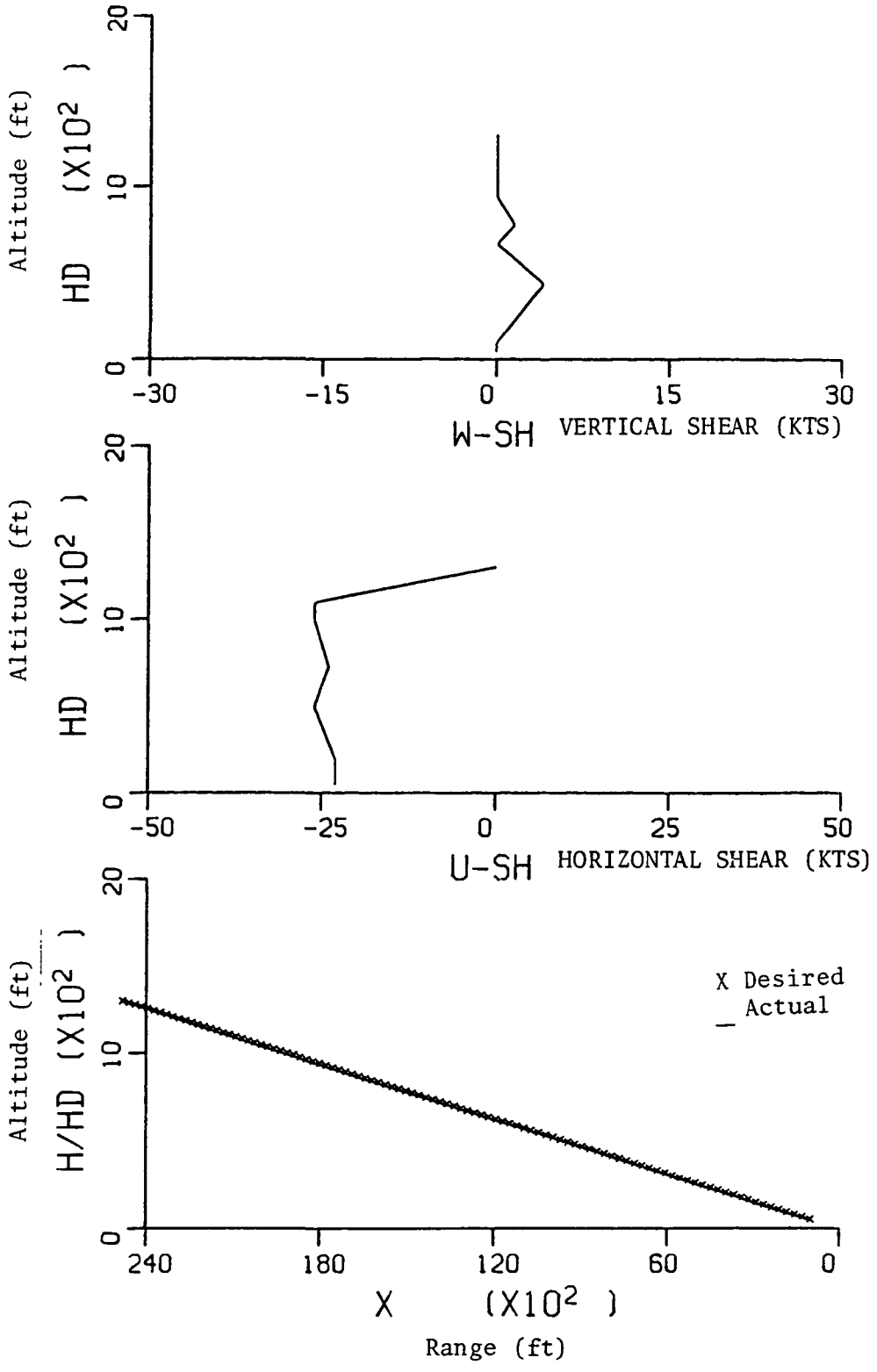

Figure 19. SIMULATION OF CONTROL SYSTEM 2 (FEEDBACK) WITH THE MODERATE SHEAR

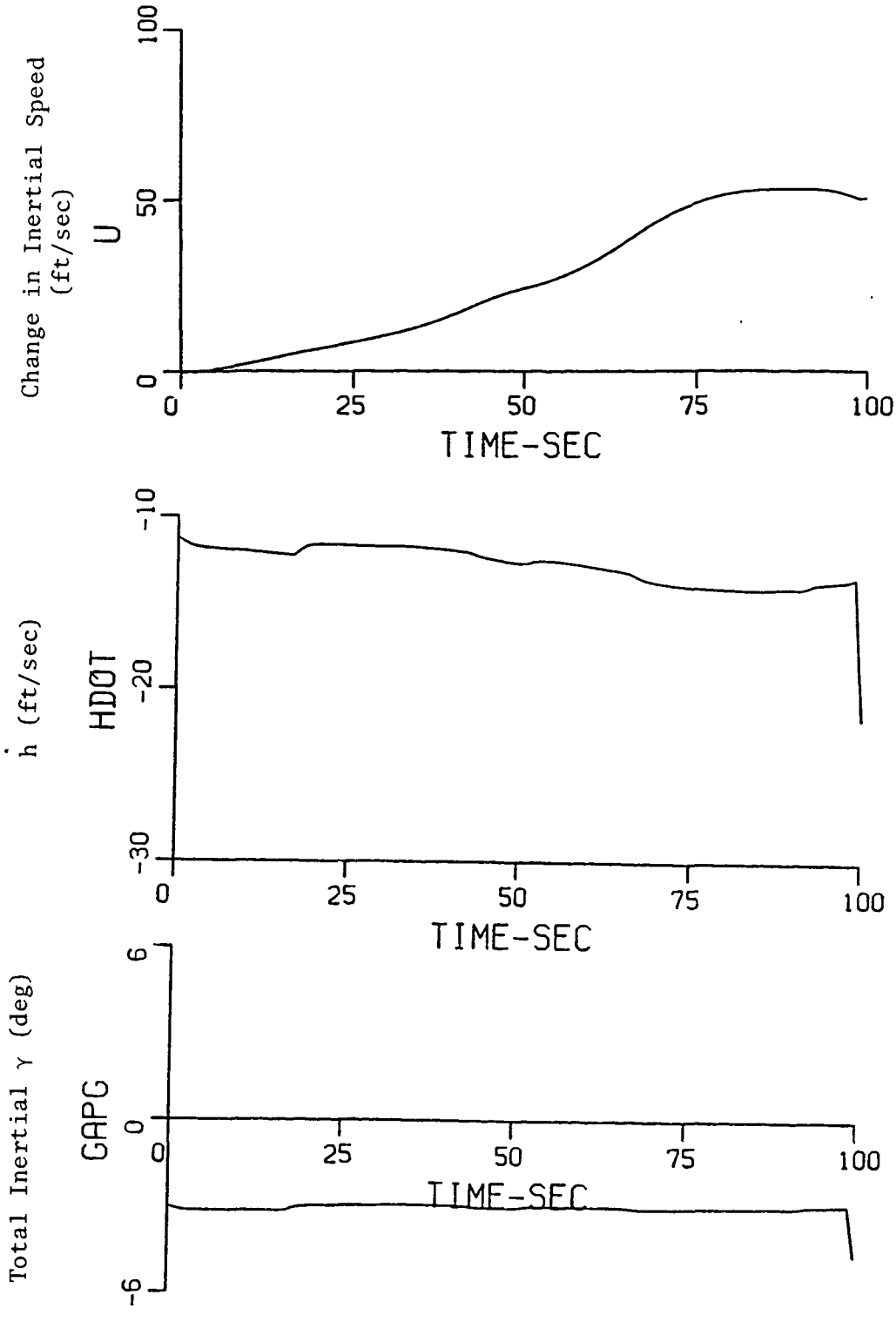

Figure 19. Cont'd SIMULATION OF CONTROL SYSTEM 2 (FEEDBACK) WITH THE MODERATE SHEAR

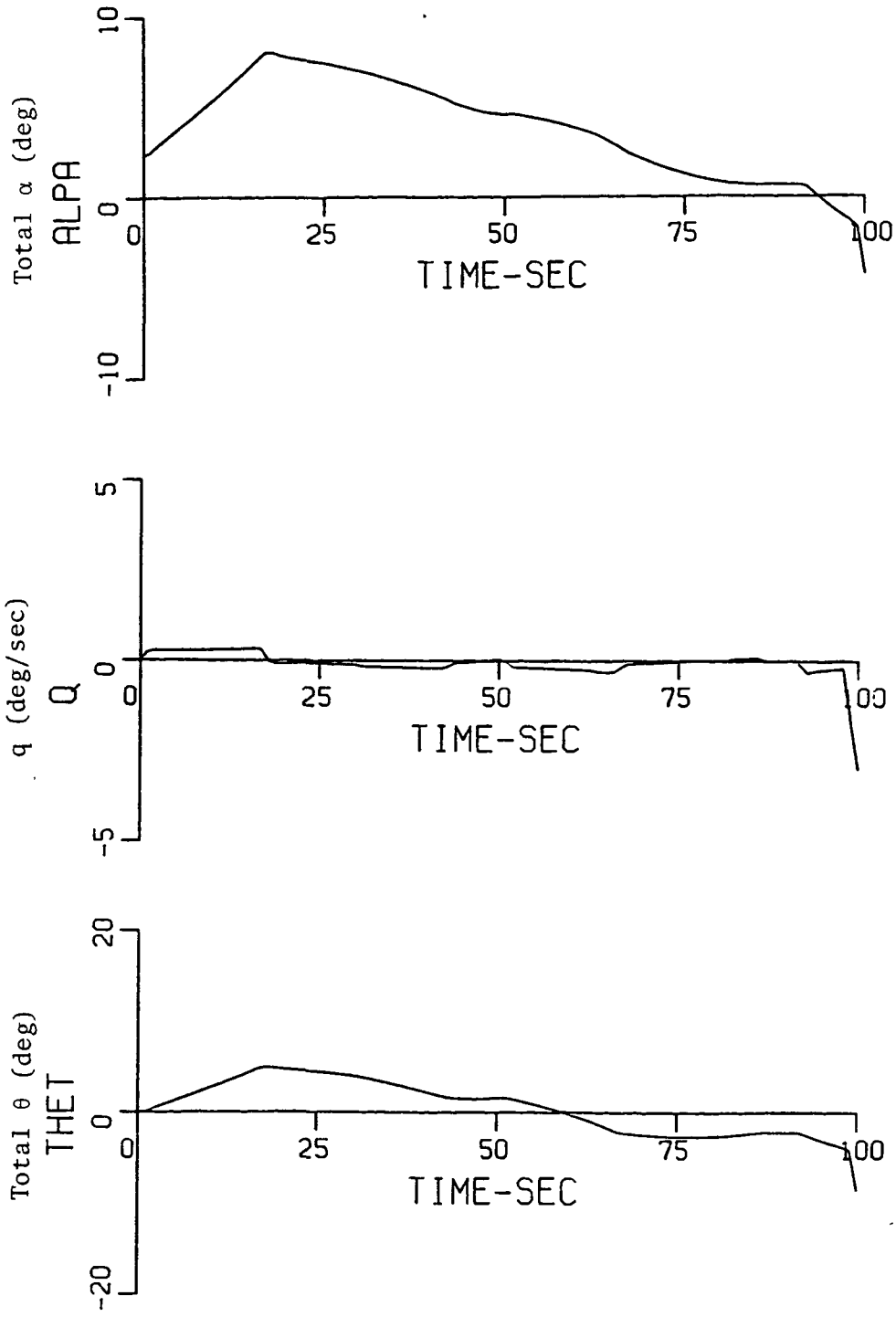

Figure 19. Cont'd SIMULATION OF CONTROL SYSTEM 2 (FEEDBACK) WITH THE MODERATE SHEAR

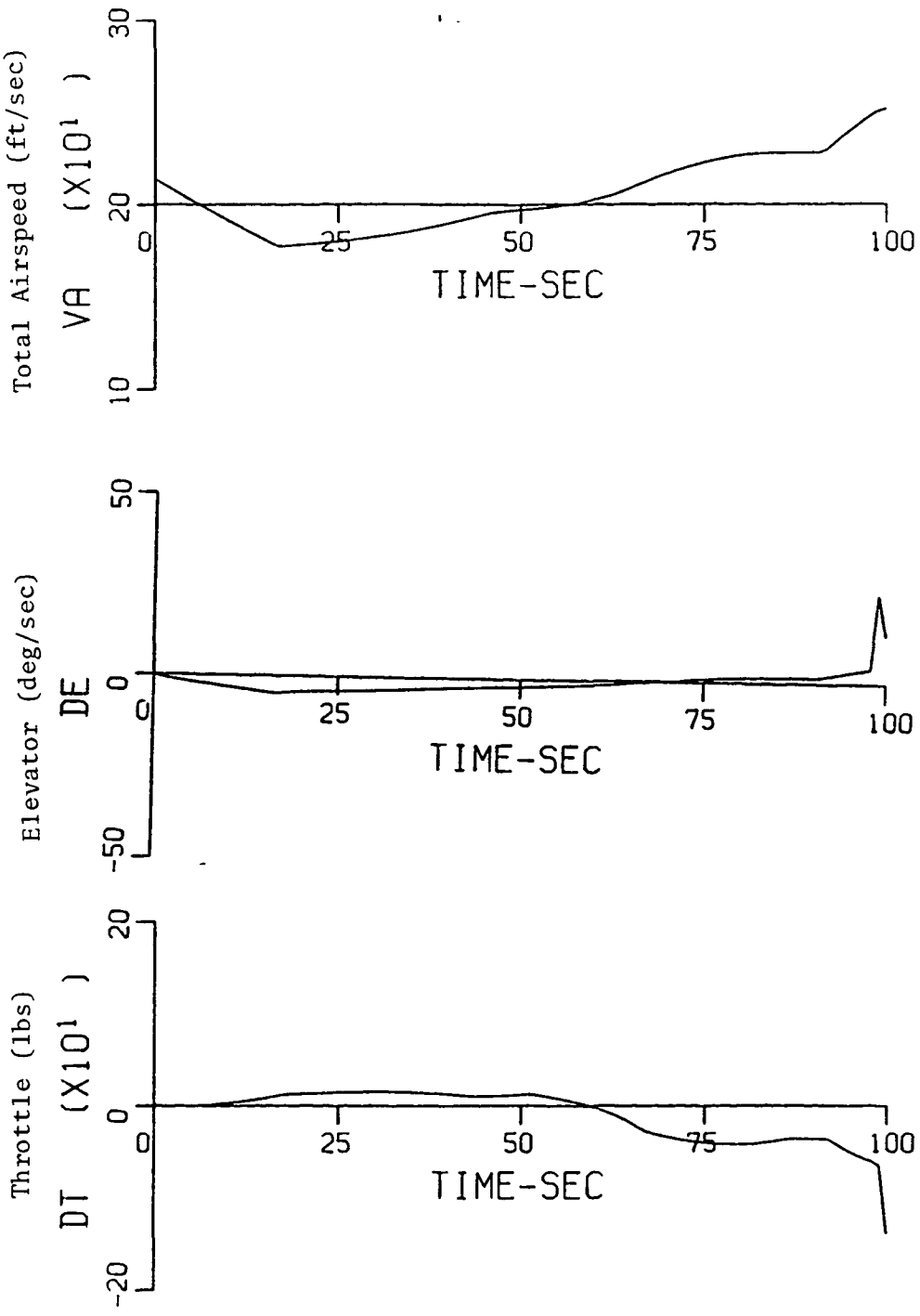

Figure 19. Cont'd SIMULATION OF CONTROL SYSTEM 2 (FEEDBACK) WITH THE MODERATE SHEAR

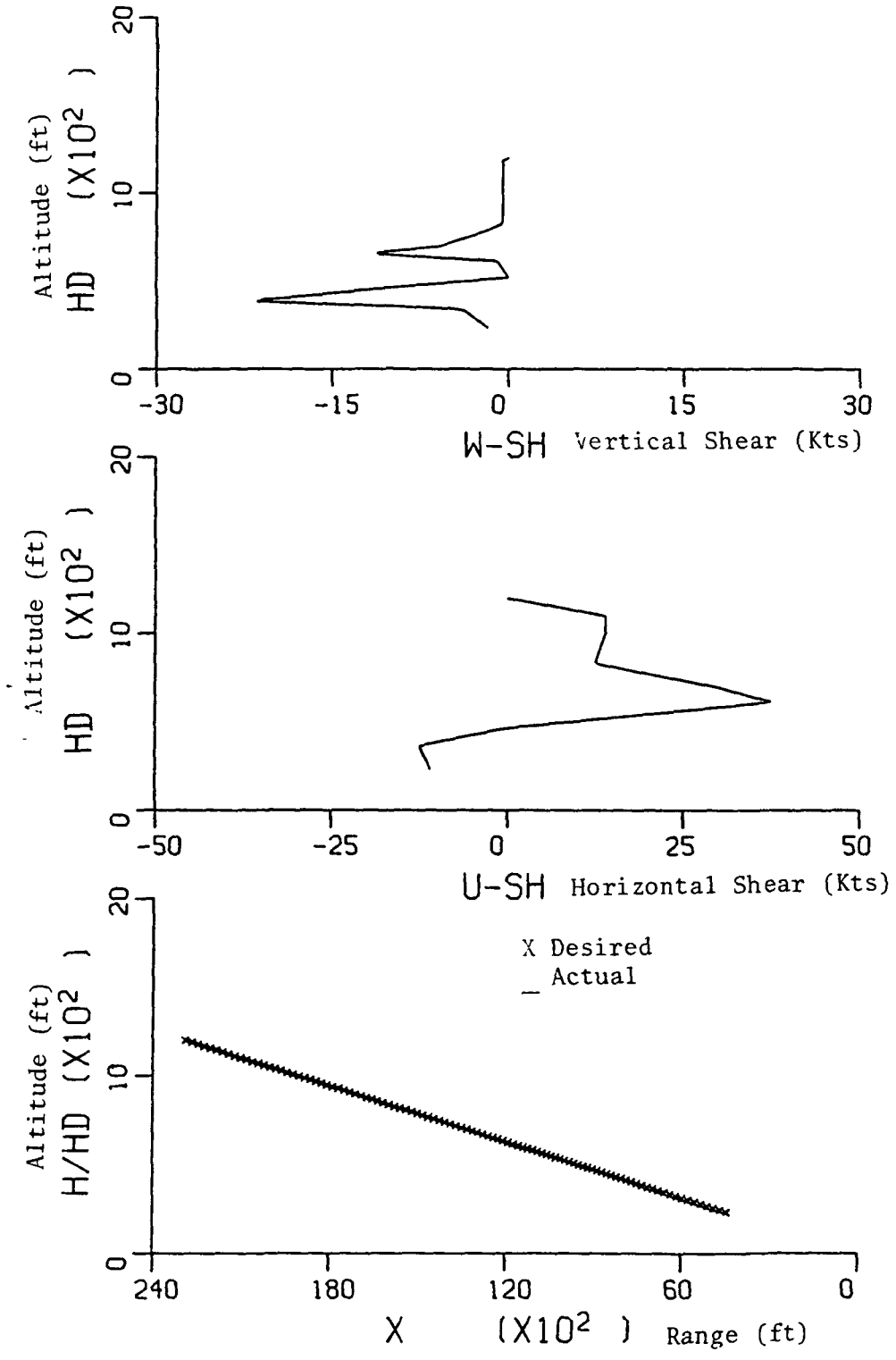

Figure 20. SIMULATION OF CONTROL SYSTEM 3 (ALTITUDE REGULATION) WITH KENNEDY SEVERE SHEAR

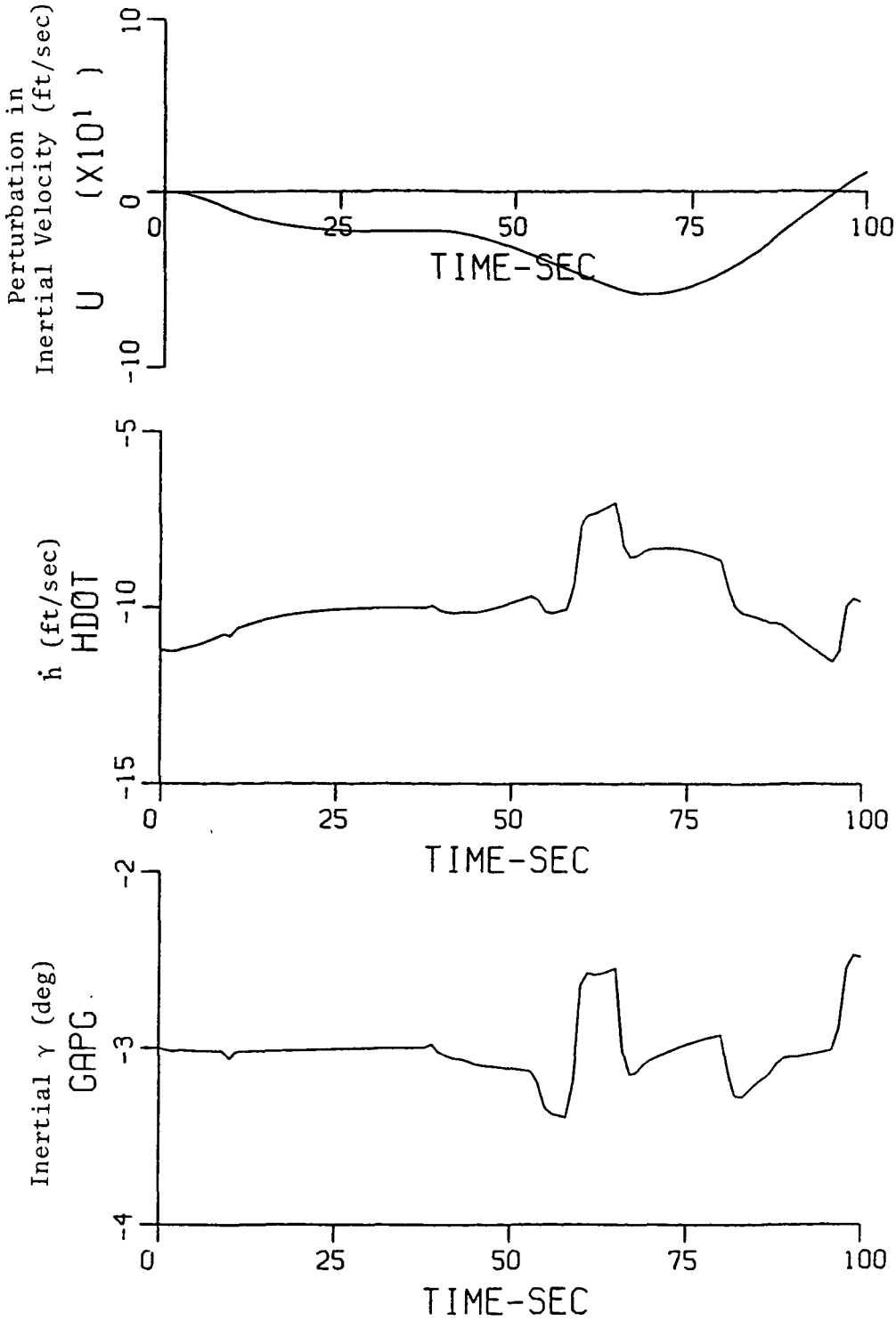

Figure 20. (Cont'd) SIMULATION OF CONTROL SYSTEM 3 (ALTITUDE REGULATION) WITH KENNEDY SEVERE SHEAR

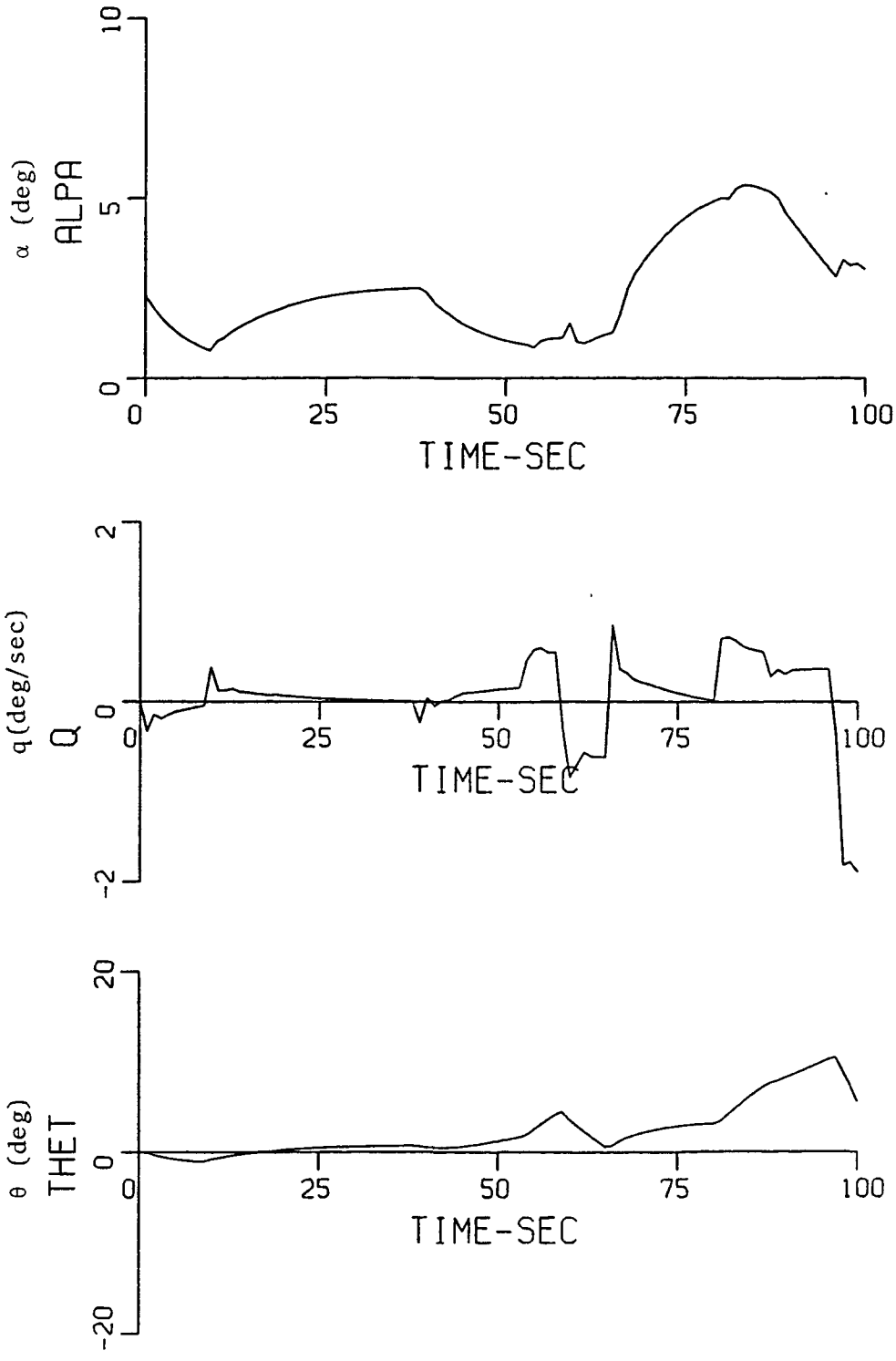

Figure 20. (Cont'd) SIMULATION OF CONTROL SYSTEM 3 (ALTITUDE REGULATION) WITH KENNEDY SEVERE SHEAR

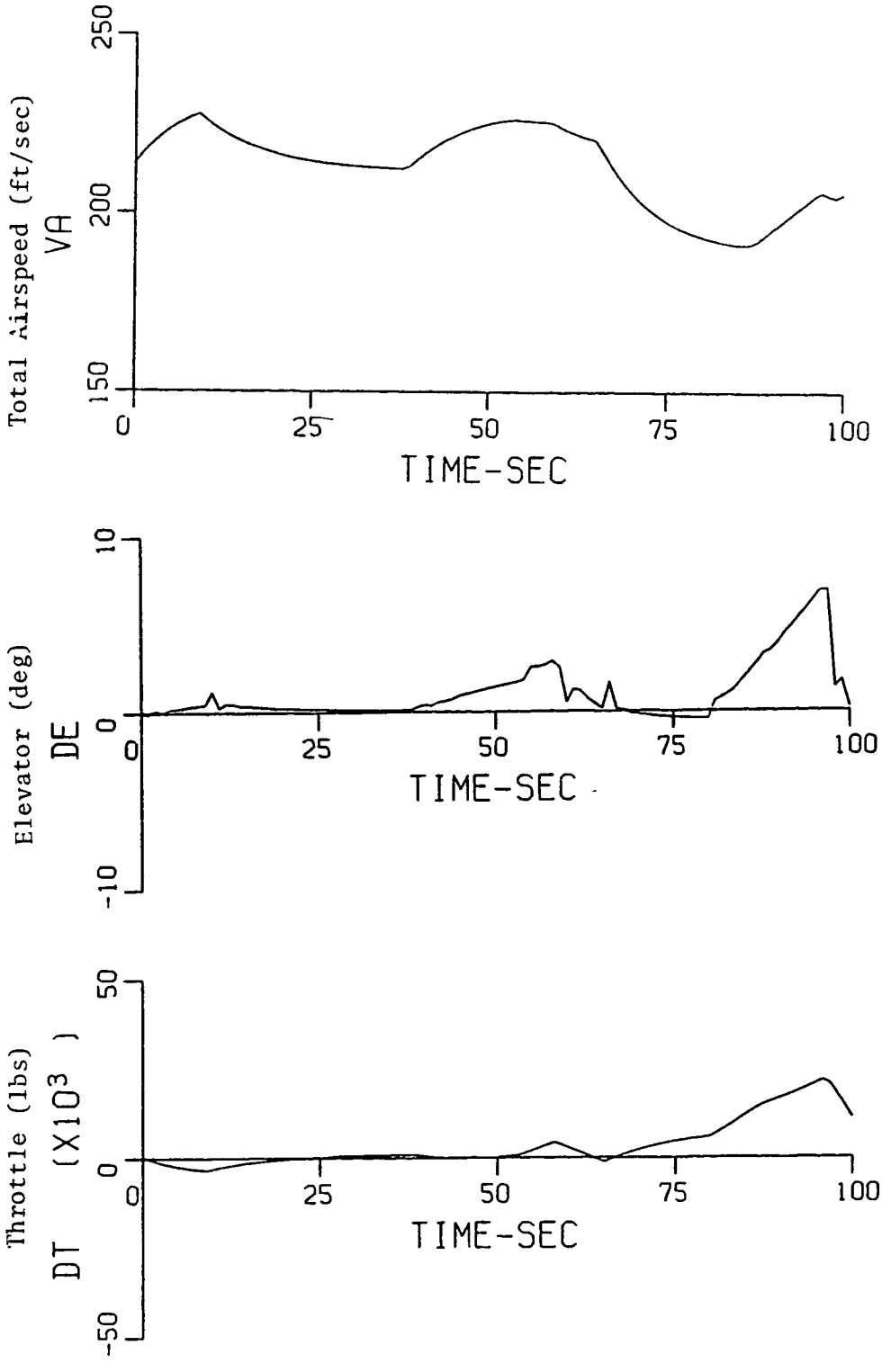

Figure 20. (Cont'd) SIMULATION OF CONTROL SYSTEM 3 (ALTITUDE REGULATION) WITH KENNEDY SEVERE SHEAR

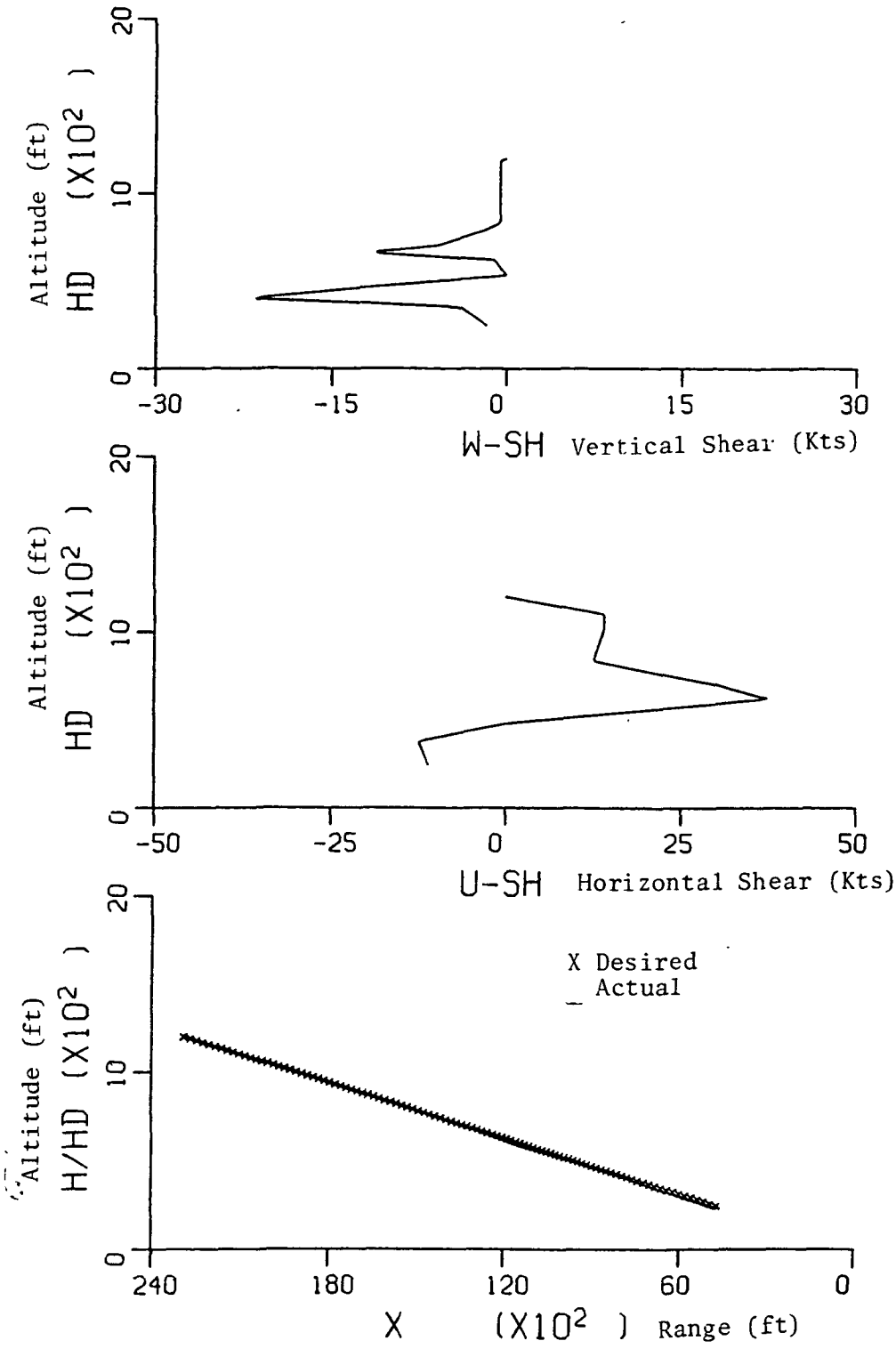

Figure 21. SIMULATION OF CONTROL SYSTEMS (ALTITUDE AND ALTITUDE RATE FEEDBACK) WITH THE KENNEDY SEVERE SHEAR

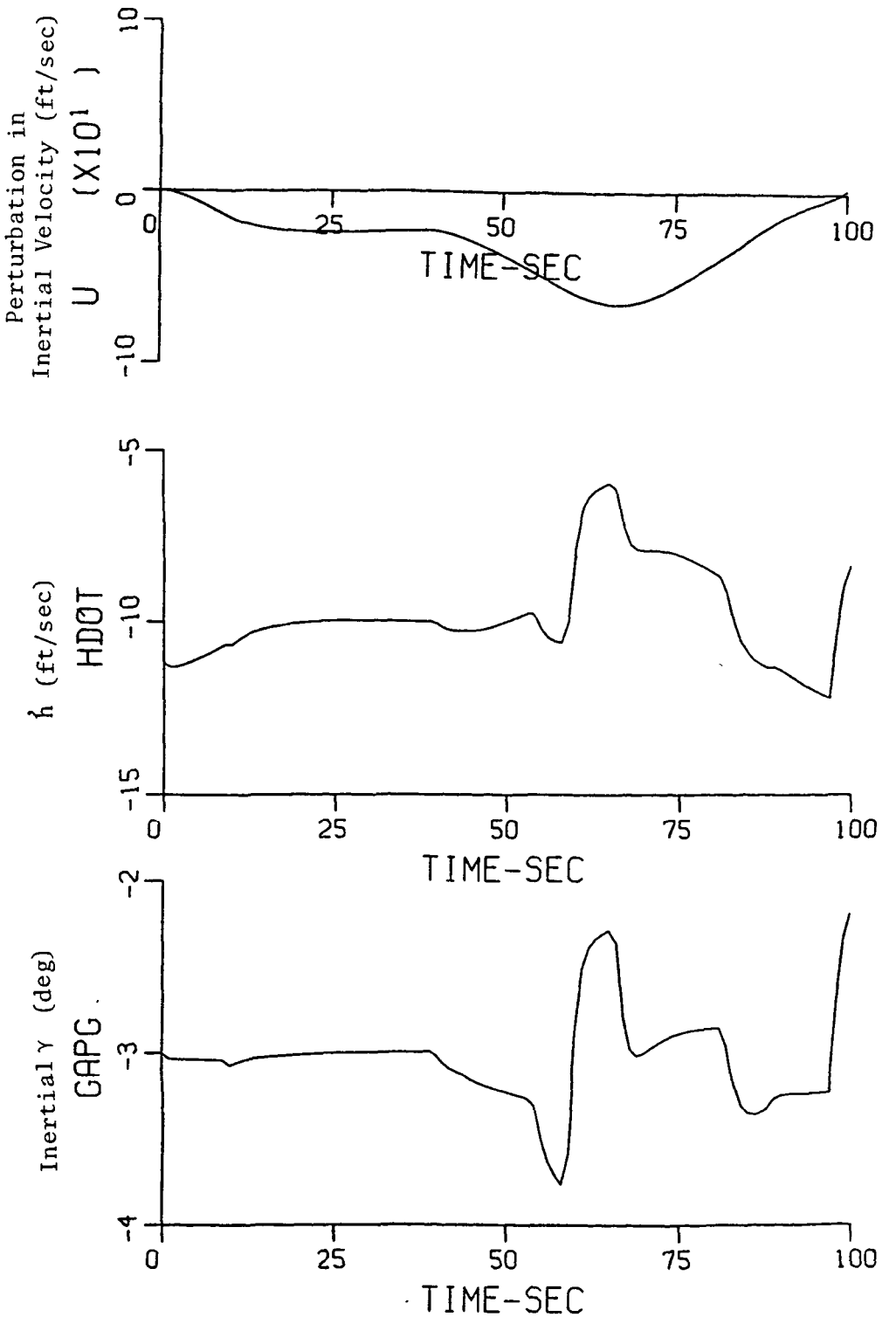

Figure 21. (Cont'd) SIMULATION OF CONTROL SYSTEMS (ALTITUDE AND ALTITUDE RATE FEEDBACK) WITH THE KENNEDY SEVERE SHEAR

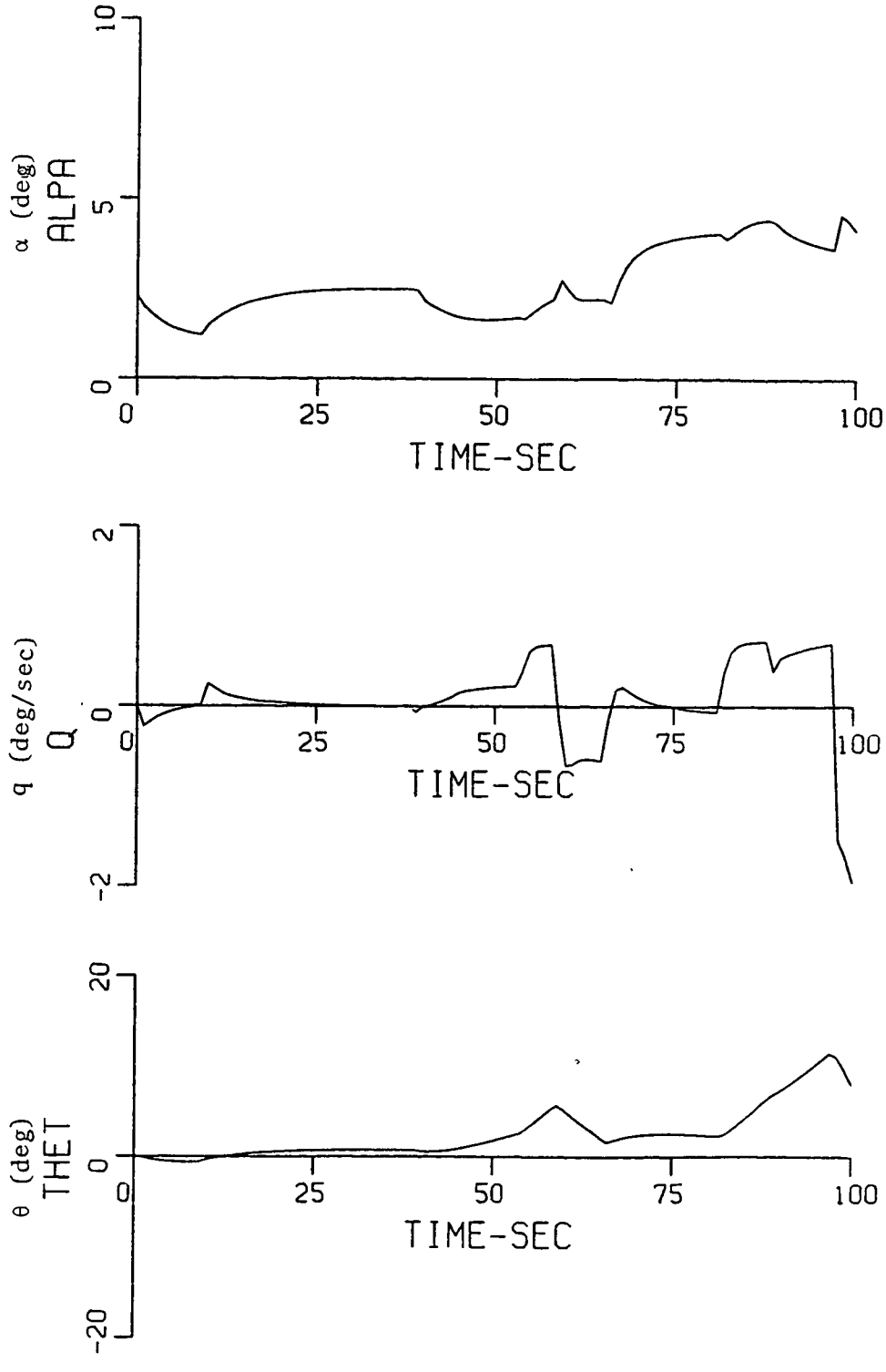

Figure 21. (Cont'd) SIMULATION OF CONTROL SYSTEMS (ALTITUDE AND ALTITUDE RATE FEEDBACK) WITH THE KENNEDY SEVERE SHEAR

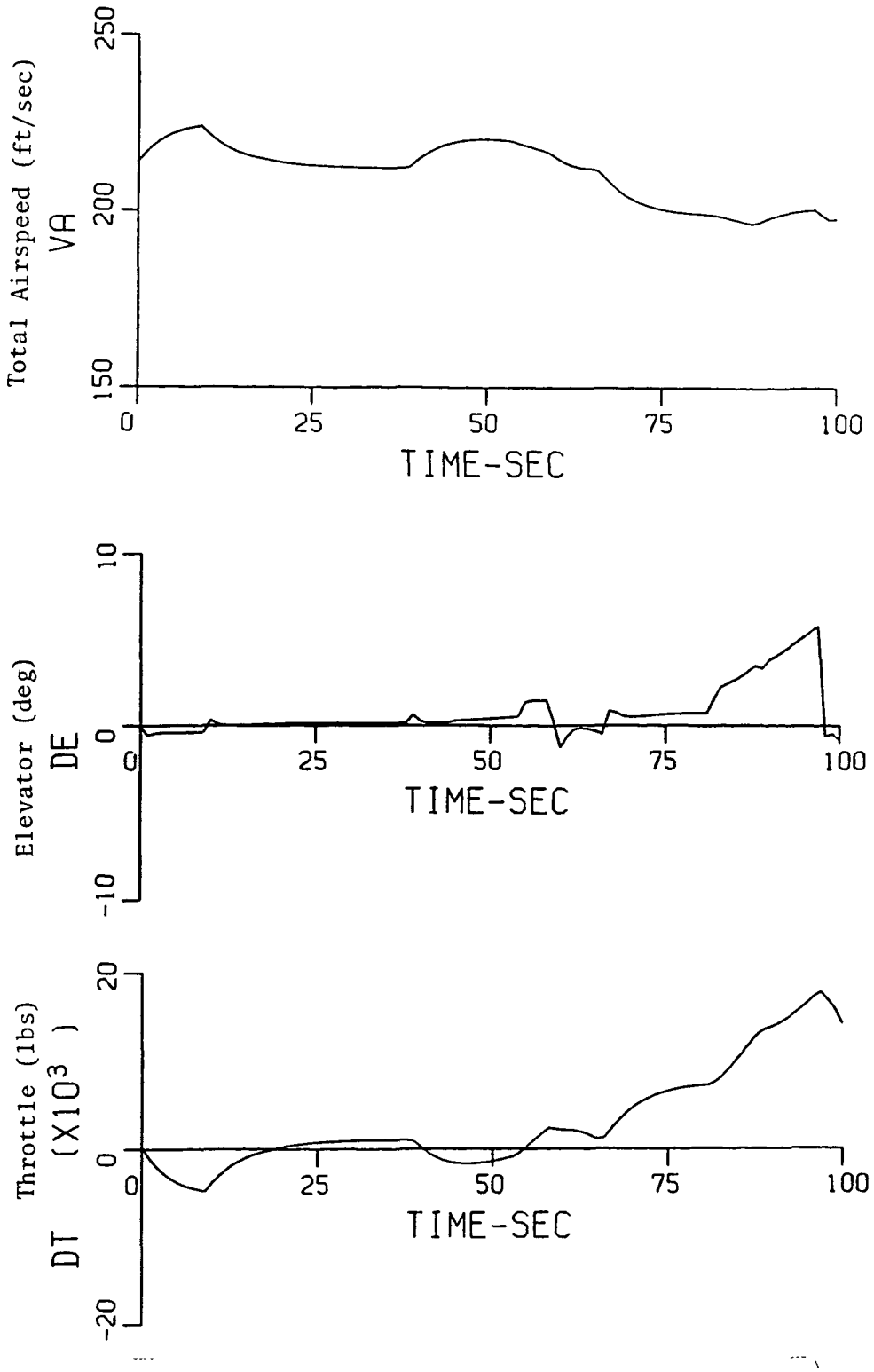

Figure 21. (Cont'd) SIMULATION OF CONTROL SYSTEMS (ALTITUDE AND ALTITUDE RATE FEEDBACK) WITH THE KENNEDY SEVERE SHEAR

The final simulation results shown are for control system 4. The time histories are shown in Figure 22. This control system regulates the airspeed through energy considerations. As with the control system 3, when the headwind is encountered, the throttle activity is decreased and when the headwind turns to tailwind and the down draft is encountered, the throttle activity is increased to minimize the deviation in airspeed. The flight path angle is well regulated. The angle of attack increases to a maximum of about 3^{o}. The thrust has increased to a maximum of 20,000 lbs from the trim setting and the maximum elevator deflection is about 5.6^{o} from the trim position. The angular motions and the control activity are smaller than that for control system 3.

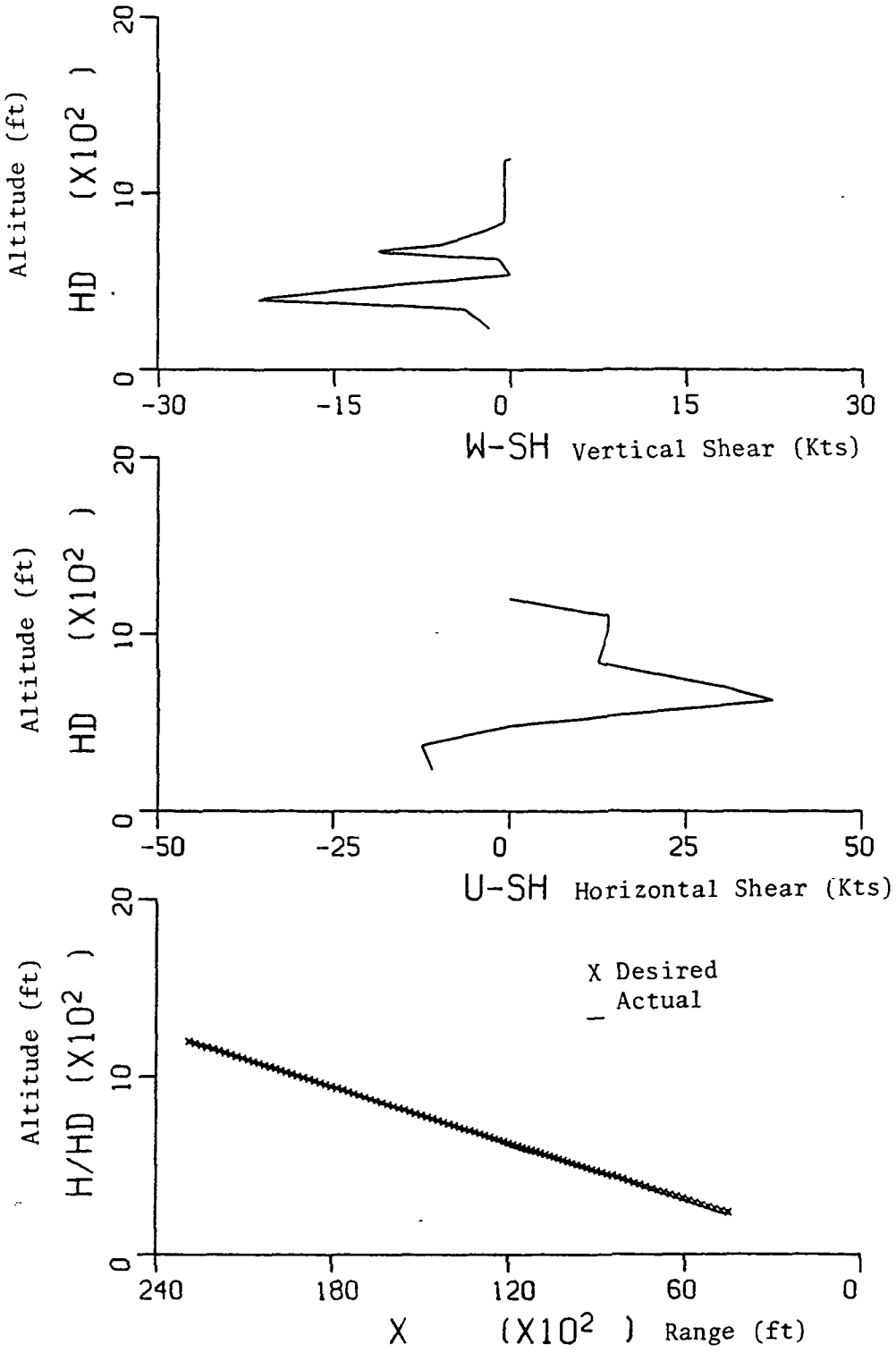

Figure 22. SIMULATION OF CONTROL SYSTEM 4

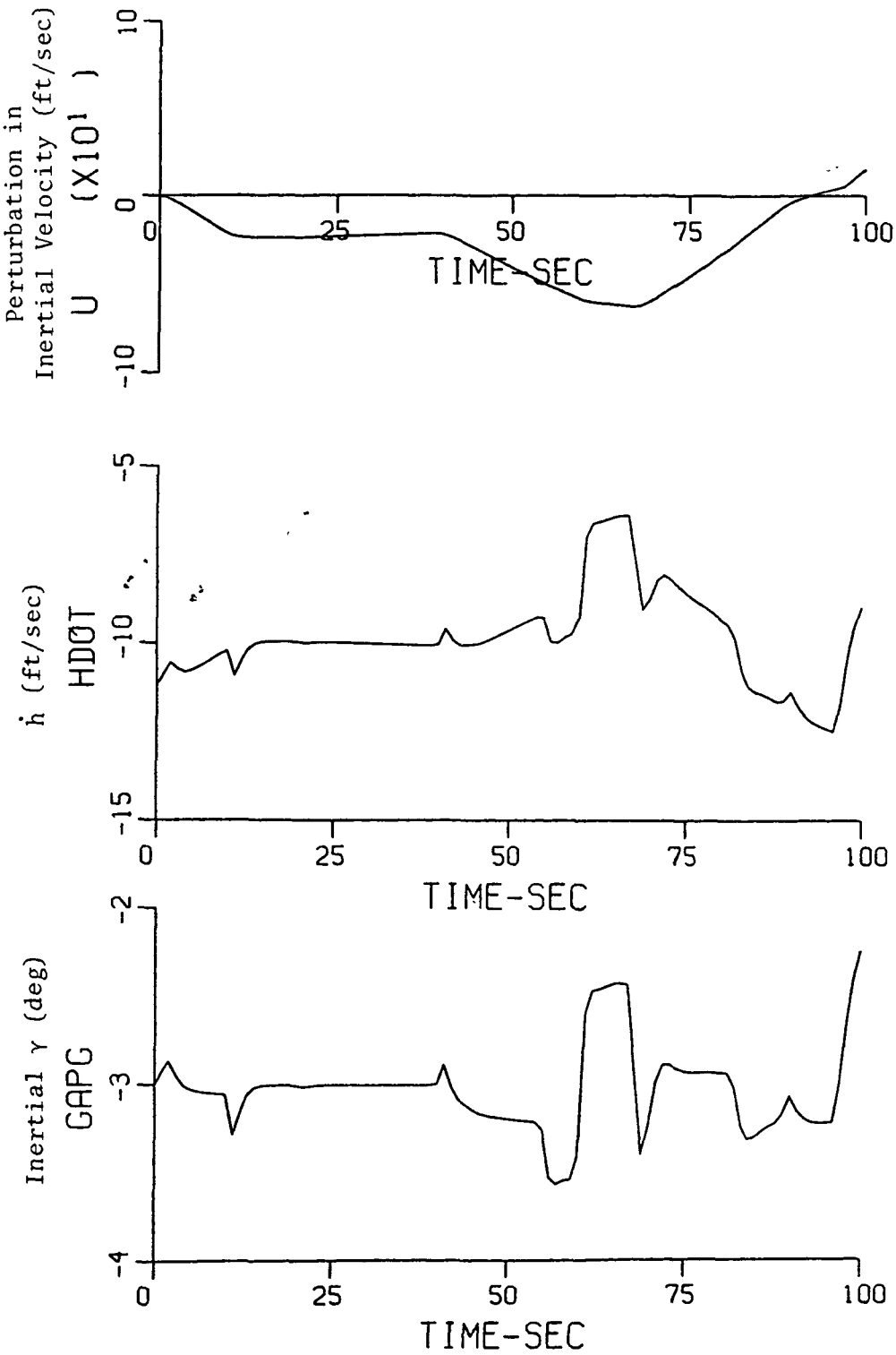

Figure 22. SIMULATION OF CONTROL SYSTEM 4
(Cont'd)

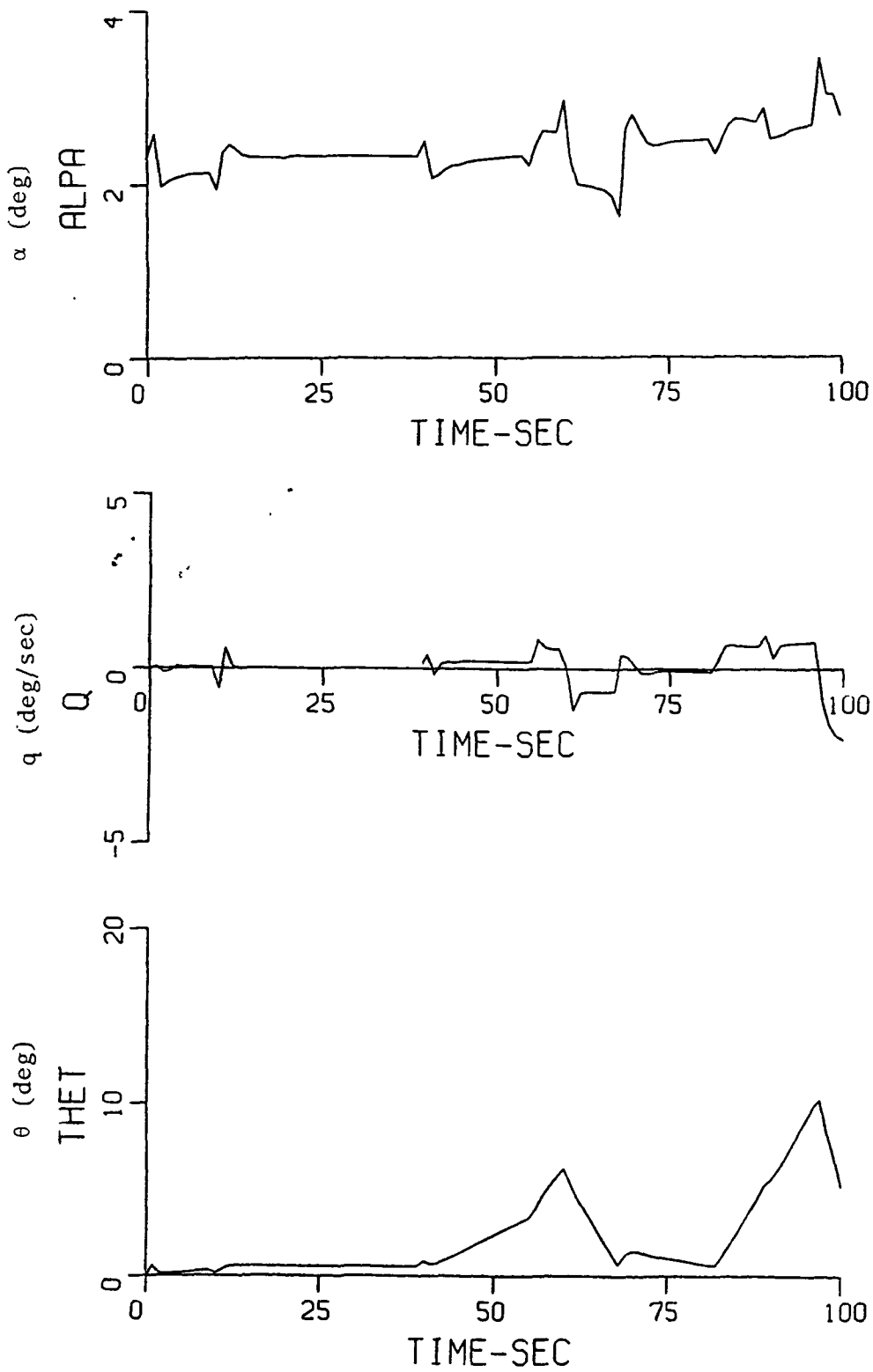

Figure 22. SIMULATION OF CONTROL SYSTEM 4 (Cont'd)

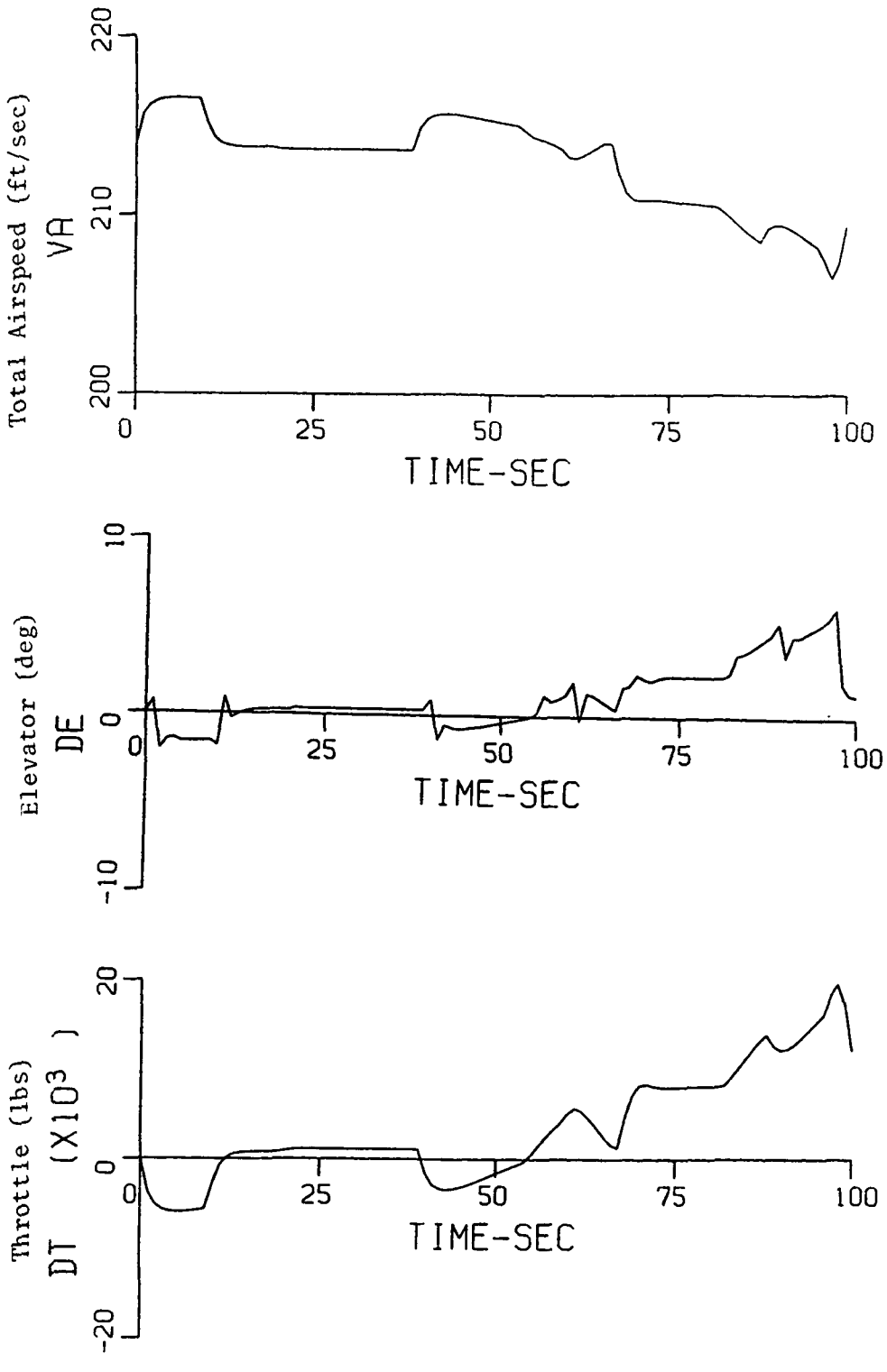

Figure 22. SIMULATION OF CONTROL SYSTEM 4
(Cont'd)

Section 5
CONCLUSIONS AND RECOMMENDATIONS

5.1 CONCLUSIONS

The research performed in this program was done in response to a need to develop automatic control methods that would enable an aircraft to safely fly through a severe wind shear and turbulence environment. As demonstrated in this report, there are many different concepts and criteria associated with shear and gust alleviation, and the total list of possible ways to do it are far from exhausted.

The objective of this study program was to demonstrate feasibility in a preliminary way. Basic studies were performed such as inertial or ground speed regulation compared to airspeed regulation. The purpose was to determine the control law differences in the concepts, the control power requirements and the basic safety of flight parameters, such as angle of attack excursions of the aircraft as it flew through the shear environment. It was shown that regulation with respect to airspeed or groundspeed is conceptually the same; depending upon the variable used in the control law, the aircraft can be regulated with respect to either with equal effectiveness. This applies, of course, only with respect to the horizontal shear. Vertical motions of the aircraft must be regulated with respect to ground.

Basically, then, this program involved the study of criteria definition for the gust and wind shear problem. It was not found to be difficult to formulate a performance index that would produce a shear alleviation control law, either with respect to inertial speed or airspeed. One of the better criteria involved the use of an expression for total energy in the performance index. This produced a control law that was , in many ways, directly related to the kind of behavior inherently expected of a gust/shear alleviation system.

The total energy probe was shown to be a reasonable approach to an implementation of a gust/shear alleviation system. Total energy can be expressed

as a state variable and, therefore, not only expresses a very good criteria for shear alleviation, but the energy probe output also becomes part of the feedback control law.

For the most part, optimal control methods were used to obtain both criteria and control laws for the solution of the shear/gust problem. In general, these control laws are quite complex, requiring feedback from all of the states to each of the controllers. A theoretical contribution of the research reported upon involves the development of robust observers. The application of these methods should result in simplified control laws involving requirements for fewer sensors.

5.2 RECOMMENDATIONS

1. The research results reported upon in this report demonstrate the feasibility of automatic gust and shear alleviation systems for commercial aircraft such as a Boeing 737. In order to more realistically verify the direct suitability of the systems defined,it will be necessary to demonstrate their usefulness on a simulation that more realistically reproduces the actual environment. Among the more important nonlinear and dynamical effects that should be added are:

a) Throttle and control surface servo dynamic behavior. The nonlinear engine response characteristics are probably the most important effects not included in the simulation of the present study.

b) Aerodynamic nonlinearities.

c) The energy probe mathematical model should be more accurately represented.

d) Sensor dynamics and other characteristics such as biases, misalignments and noise, if determinable, should be added to the system simulation.

e) Other turbulence models, such as the Tomlinson representation of turbulence, should be tested.

2. One of the important findings of the present program is the conclusion that the spoilers of the example aircraft are of limited effectiveness and control power. The use of flaps as active devices for gust/shear alleviation should be explored.

3. The investigation of suitable performance indices or criteria should be continued, the possibilities are far from exhaused. In particular, the use of energy rate, $\dot{E}$, should be investigated.

4. Several theoretical areas show potential in producing more effective and more realistic gust alleviation systems. The realistic problems of instrumentation should be included in a further investigation of direct gust alleviation methods. As now formulated, the integral performance criteria only indirectly express alleviation criteria, the minimization is with respect to the control inputs rather than the environmental disturbances.

5. More emphasis should be placed on the use of the energy probe in terms of criteria definition, control law mechanization and environmental disturbance sensing.

6. A sensitivity analysis of off-nominal flight conditions should be conducted to verify the robustness of the control system design. In particular, the final control system configuration should be capable of accommodating both frontside and backside power-required operation.

Section 6
REFERENCES

1. Ellis, D. W. and Keenan, M. G.: "Development of Wind S r Models and Determination of Wind Shear Hazards," Report No. FAA-RD-79-119, SRI International, Menlo Park, California, January 1978

2. "Military Specifications: Flying Qualities of Piloted Airplanes," MIL-F-8785C, 5 November 1980

3. Nicks, O. W.: "A Simple Total Energy Sensor," NASA-TM-X-73928, 1976

4. Ostroff, A. J., Hueschen, R. M., Hellbaum, R. F. and Creedon, J. F.: "Flight Evaluation of a Simple Total Energy-Rate System With Potential Wind Shear Application," NASA Technical Paper 1854, May 1981.

5. Gera, J.: "Longitudinal Stability and Control in Wind Shear with Energy Height Rate Feedback," NASA TM 81828, November 1980.

6. Lebacqz, J. V., Radford, R. and Beilman, J. L.: "An Experimental Investigation of Control-Display Requirements for a Jet-Lift VTOL Aircraft in the Terminal Area," Calspan Report No. AK-5985-F-1, July 1978.

7. Rynaski, E. G.: "Gust Alleviation-Criteria and Control Laws," AIAA Atmospheric Flight Mechanics Conference, Boulder, Colorado, 6-8 August 1979.

8. Rynaski, E. G., Andrisani II, D. and Eulrich, B. J.: "Gust Alleviation Using Direct Turbulence Measurements," AIAA Atmospheric Flight Mechanics Conference, Boulder, Colorado, 6-8 August 1979.

9. Rynaski, E. G., Adnrisani II, D. and Weingarten, N.: "Active Control for the Total In-Flight Simulator," NASA Contractor Report 2118, April 1979.

10. Rynaski, E. G. and Whitbeck, R. F.: "The Theory and Application of Linear Optimal Control," Calspan Report No. IH-1943-F-1, AFFDL-TR-65-28, October 1965.

11. Luenberger, D. G.: "Observers for Multivariable Systems," IEEE Transactions on Automatic Control, Vol. AC-11, April 1966.

12. Rynaski, E. G., Whitbeck, R. F. and Wierwille, W. W.: "Optimal Control of a Flexible Launch Vehicle," Calspan Report No. IH-2089-F-1, July 1966.

Appendix A

EQUATIONS OF MOTION AND WIND MODEL
EQUATIONS FOR SIMULATION

This appendix gives the equations of motion of the TCV airplane used in control system design and the wind model equations for use in the simulation. The linearized aircraft equations of motion used in this study are represented in body axis by the following equations:

$$\dot{x} = Fx + Gu + J u_g$$

$$x = \begin{bmatrix} \Delta u_{PG} \\ \Delta w_{PG} \\ q \\ \Delta\theta \end{bmatrix} \quad u = \begin{bmatrix} \delta_t \\ \delta_e \\ \delta_{sp} \end{bmatrix} \quad u_g = \begin{bmatrix} u_w \\ w_w \end{bmatrix} \qquad \text{(A-1)}$$

u_w and w_w are the wind shear and turbulence along the X and Z body axes, respectively with the sign convention that headwind and updraft are positive.

The matrices are defined in terms of the dimensional derivatives as follows:

$$F = \begin{bmatrix} X_u & X_w & X_q - W_o & -g\cos\theta_o \\ Z_u & Z_w & Z_q + U_o & -g\sin\theta_o \\ M_u & M_w & M_q & M_\theta \\ 0 & 0 & 1 & 0 \end{bmatrix}$$

$$G = \begin{bmatrix} X_{\delta_t} & X_{\delta_e} & X_{\delta_{sp}} \\ Z_{\delta_t} & Z_{\delta_e} & Z_{\delta_{sp}} \\ M_{\delta_t} & M_{\delta_e} & M_{\delta_{sp}} \\ 0 & 0 & 0 \end{bmatrix} \qquad J = \begin{bmatrix} X_u & X_w \\ Z_u & Z_w \\ M_u & M_w \\ 0 & 0 \end{bmatrix} \qquad \text{(A-2)}$$

The expression for $\Delta\dot{h}$ is determined as follows:

$$\begin{aligned} \dot{h} &= u_{PG} \sin\theta - w_{PG} \cos\theta \\ \dot{h}_o &= U_o \sin\theta_o - W_o \cos\theta_o \end{aligned} \qquad \text{(A-3)}$$

$$u_{PG} = U_o + \Delta u_{PG}, w_{PG} = W_o + \Delta w_{PG}, \quad \theta = \theta_o + \Delta\theta$$

where u_{PG} and w_{PG} are total inertial velocities along the X and Z body axes, respectively; U_o, W_o and θ_o are trim values.

$$\Delta\dot{h} = \dot{h} - \dot{h}_o = u_{PG} \sin\theta - w_{PG} \cos\theta - (U_o \sin\theta_o - W_o \cos\theta_o) \qquad \text{(A-4)}$$

using small angle approximations, the expression for $\Delta\dot{h}$ reduces to

$$\Delta\dot{h} = \sin\theta_o \, \Delta u_{PG} - \cos\theta_o \, \Delta w_{PG} + (U_o \cos\theta_o + W_o \sin\theta_o)\Delta\theta \qquad \text{(A-5)}$$

The expression for $\Delta\ddot{h}$ is obtained by differentiating Equation (A-5) and is given as

$$\begin{aligned} \Delta\ddot{h} = {} & (X_u \sin\theta_o - Z_u \cos\theta_o)\Delta u_{PG} + (X_w \sin\theta_o - Z_w \cos\theta_o)\Delta w_{PG} \\ & [X_q \sin\theta_o - Z_q \cos\theta_o]q + (X_{\delta_t} \sin\theta_o - Z_{\delta_t} \cos\theta_o)\delta_t + \\ & (X_{\delta_e} \sin\theta_o - Z_{\delta_e} \cos\theta_o)\delta_e \end{aligned} \qquad \text{(A-6)}$$

Only the δ_t and δ_e controls are considered.

The rate of change of energy deviation is defined as follows:

$$\begin{aligned} E &= \dot{h} + \frac{u_{PA}^2}{2g} \\ E_c &= h_c + \frac{U_o^2}{2g} \end{aligned} \qquad \text{(A-7)}$$

where u_{PA} is the total airspeed along the X-axis. Since U_o, the trim airspeed, is constant

$$\Delta\dot{E} = \dot{E} - \dot{E}_c = \Delta\dot{h} + \frac{u_{PA}\,\dot{u}_{PA}}{g} \qquad \text{(A-8)}$$

The equations of motion (A-1) represent the perturbation in air or inertial speed in the absence of wind disturbance. Using the approximation $u_{PA} \simeq U_o$, the $\Delta\dot{E}$ equation can be written as

$$\Delta\dot{E} = \left(\frac{U_o}{g} X_u + \sin\theta_o\right)\Delta u_{PA} + \left(\frac{U_o}{g} X_w - \cos\theta_o\right)\Delta w_{PA} + \frac{U_o}{g}(X_q - W_o)q + W_o \sin\theta_o \Delta\theta + \frac{U_o}{g} X_{\delta_t}\delta_t + \frac{U_o}{g} X_{\delta_e}\delta_e \qquad \text{(A-9)}$$

NUMERICAL VALUES OF STABILITY AND CONTROL DERIVATIVES

Units

Δu_{PG}, Δw_{PG} - ft/sec
q, $\Delta\theta$ - deg/sec, deg
δ_t - lbs.
δ_e - degrees

Flight Condition

U_o = 213.9 ft/sec
W_o = 8.63 ft/sec
θ_o = -.69 deg
γ_o = -3^o

Derivative	Value
X_u	.0376
X_w	.106
X_q	0
X_{δ_t}	.00038
X_{δ_e}	.0065
$X_{\delta_{sp}}$	-4.37×10^{-5}
Z_u	-.278
Z_w	-.711

Derivative	Value
Z_q	0
Z_{δ_t}	-2.99 E-7
Z_{δ_e}	-.162
$Z_{\delta_{sp}}$	8.12×10^{-4}
M_u	-.011
M_w	-.361
M_q	-.523
M_θ	-3.27 E-4
M_{δ_t}	3.61 E-4
M_{δ_e}	-1.215
$M_{\delta_{sp}}$	.12

Turbulence Simulation Equations

The transfer functions of the turbulence are given as

$$T_{u_g}(s) = \sigma_u \sqrt{\frac{2\,L_u}{\pi V_0}} \; \frac{1}{1 + \frac{L_u}{V_0} s} \; w_1$$

$$T_{w_g}(s) = \sigma_w \sqrt{\frac{L_w}{\pi V_0}} \; \frac{1 + \frac{\sqrt{3}\,L_w}{V_0} s}{\left(1 + \frac{L_w}{V} s\right)^2} \; w_2 \qquad \text{(A-10)}$$

where w_1 and w_2 are two independent white noise sources.

The time domain equations, using the phase variable representation, can be written straightforwardly as

$$u_g(t) = -\frac{V}{L_u} u_g(t) + \frac{V}{L_u} \sigma_u \sqrt{\frac{2L_u}{AV}}\, w_1(t)$$

$$\begin{bmatrix} \dot{x}_1(t) \\ \dot{x}_2(t) \end{bmatrix} = \begin{bmatrix} 0 & 1 \\ -\frac{V^2}{L_w^2} & -\frac{2V}{L_w} \end{bmatrix} \begin{bmatrix} x_1(t) \\ x_2(t) \end{bmatrix} + \begin{bmatrix} 0 \\ 1 \end{bmatrix} w_2(t)$$

$$w_g(t) = \begin{bmatrix} \sigma_w \sqrt{\frac{L_w}{AV}} \frac{V^2}{L_w^2} & \sigma_w \sqrt{\frac{L_w}{AV}} \sqrt{\frac{3V}{L_w}} \end{bmatrix} \begin{bmatrix} x_1 \\ x_2 \end{bmatrix}$$

(A-11)

The turbulence signals generated from these equations have significant low frequency content. In this study the wind shear represents the low frequency wind disturbence. Consequently during the simulation of the control system, the turbulence signals generated from Eq.(A-11) were filtered to remove the low frequency content using the following filter:

$$H(s) = \frac{.8(s + .25)}{(s + 3.12)(s + 10)} \qquad \text{(A-12)}$$

where the frequencies are in the units of radians.

The three windshear profiles useddin this study are shown in Figures A-1, A-2 and A-3.

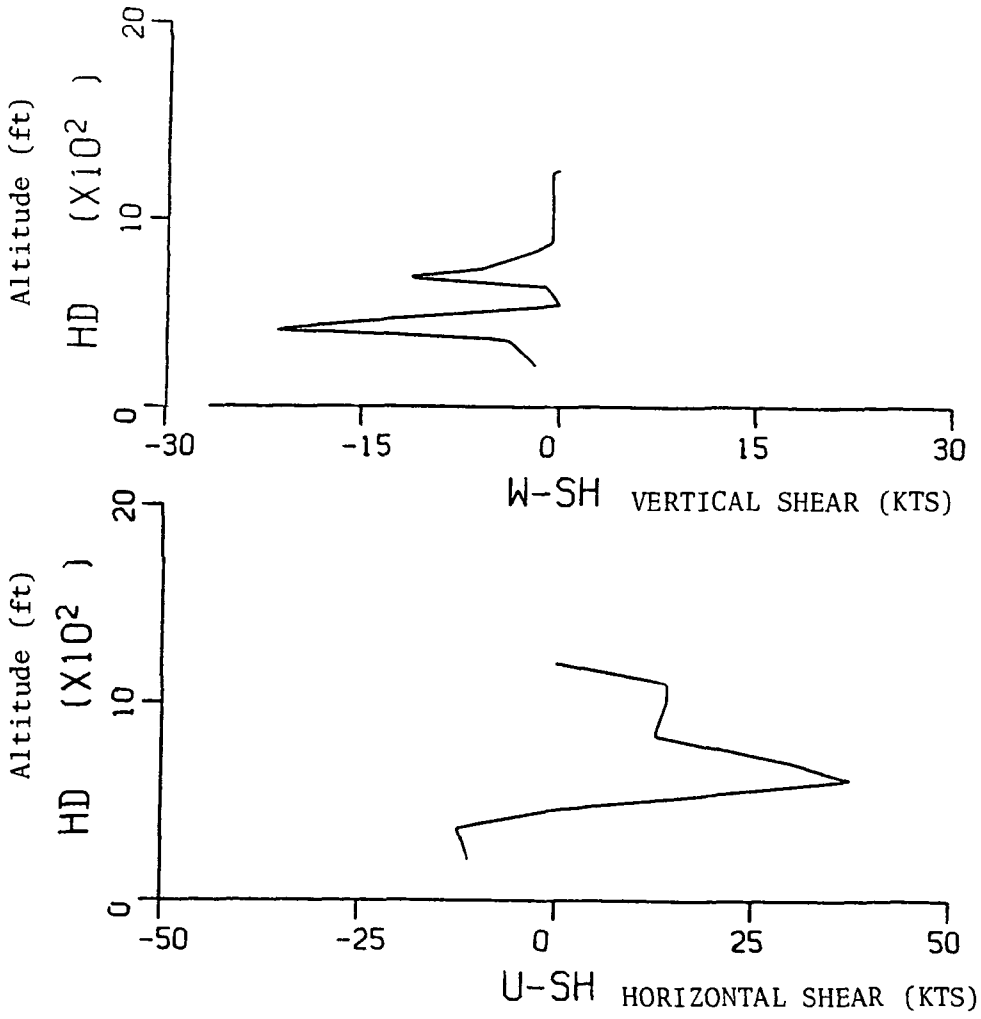

Figure A-1. KENNEDY INCIDENT (TOC) SEVERE SHEAR PROFILE

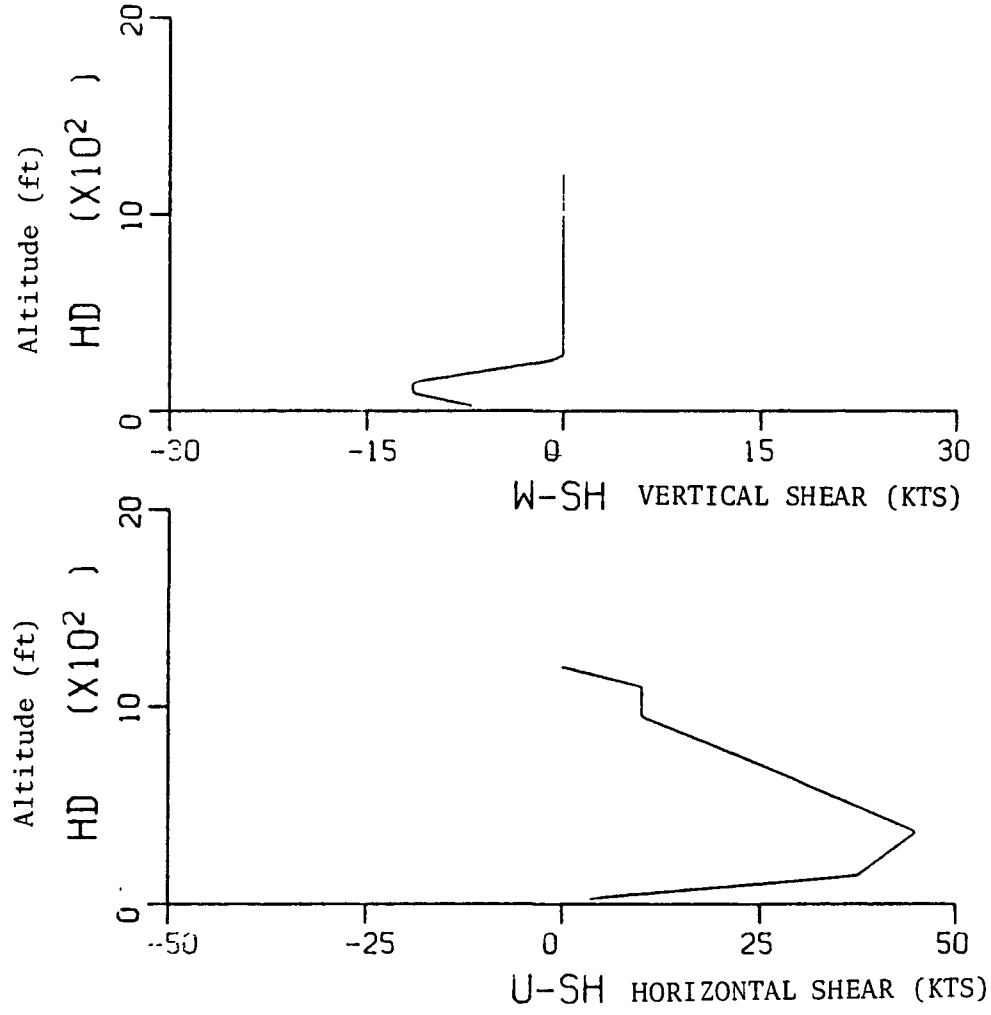

Figure A-2. PHILADELPHIA (T-25A) SEVERE SHEAR PROFILE

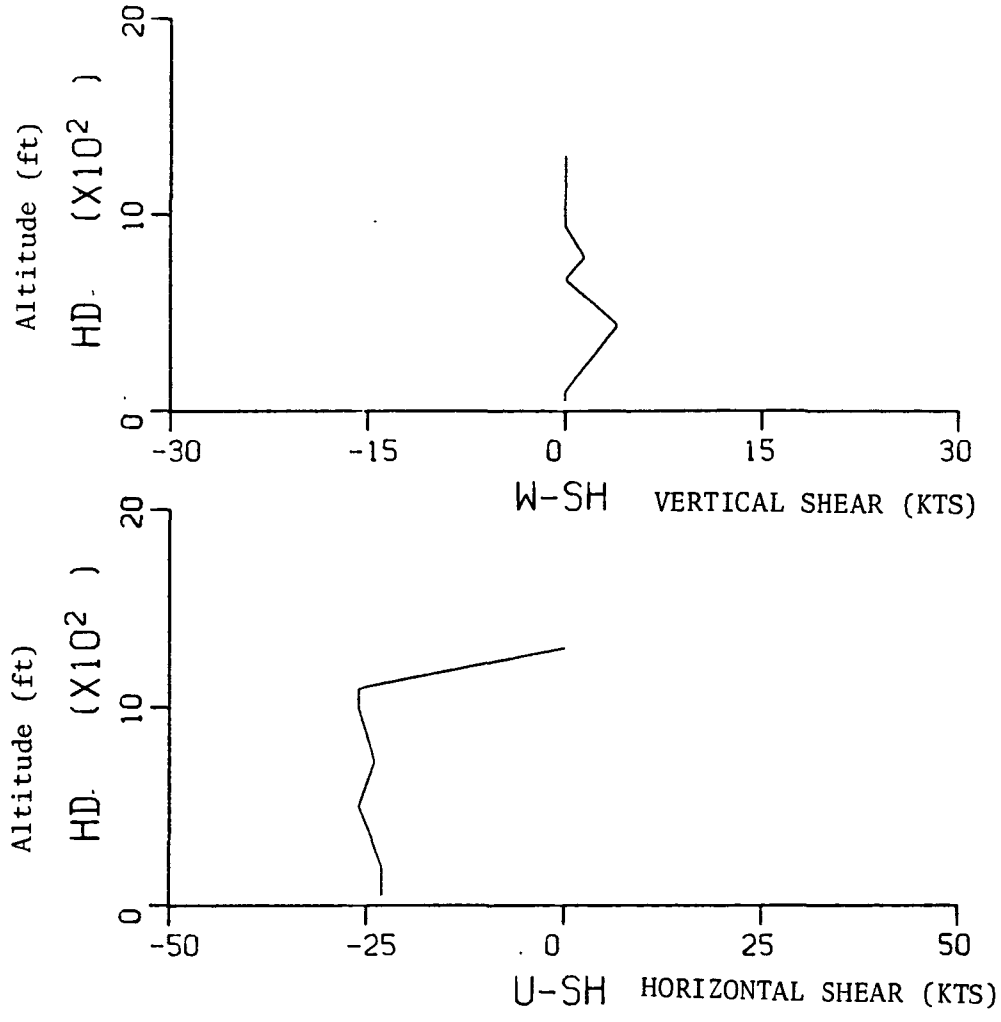

Figure A-3. MODERATE T-9A SHEAR PROFILE

Appendix B

CONTROL SYSTEM GAINS AND TRANSFER FUNCTIONS

This appendix gives the weighting factors used in the performance index, the gain matrix, and the transfer functions for each control system.

Open Loop

$$\dot{x} = Fx + Gu$$
$$y = Ax$$

$$x = \begin{bmatrix} \Delta u_{PG} \\ \Delta w_{PG} \\ q \\ \Delta\theta \\ \Delta h \\ \Delta\dot{h} \\ \Delta E \end{bmatrix} \qquad u = \begin{bmatrix} \delta_t \\ \delta_e \end{bmatrix} \qquad y = \Delta\gamma = \Delta\theta - \frac{w_{PG}}{U_o}$$

Units

Δu_{PG}, w_{PG}, $\Delta\dot{h}$ - ft/sec

q, $\Delta\theta$ - rad/sec, rad

Δh, ΔE - ft

δ_e - deg

δ_t - lbs

MATRIX F

-3.76250D-02	1.06280D-01	-8.62890D+00	-3.21670D+01	0.0	0.0	0.0
-2.78430D-01	-7.10810D-01	2.13830D+02	4.19940D-01	0.0	0.0	0.0
-2.02440D-04	-6.27090D-03	-5.23080D-01	-3.26760D-04	0.0	0.0	0.0
0.0	0.0	1.00000D+00	0.0	0.0	0.0	0.0
-1.20400D-02	-9.99900D-01	0.0	2.13800D+02	0.0	0.0	0.0
2.78860D-01	7.09500D-01	9.53000D-02	-3.26000D-02	0.0	0.0	0.0
-2.61980D-01	-2.93900D-01	-5.73210D+01	1.19200D-01	0.0	0.0	0.0

MATRIX G

3.78530D-04	6.53460D-03
-2.99670D-07	-1.61930D-01
6.26270D-06	-2.11870D-02
0.0	0.0
0.0	0.0
-4.25800D-06	1.61840D-01
2.51500D-03	4.31000D-02

Note: The last row of the F and G matrices represents the $\Delta\dot{E}$ equation. The elements of these rows were computed from Eq.(A-8) using the stability and control derivatives supplied by NASA. The coefficient of $\Delta\theta$ (element F(7,4)) in Eq.(A-9) is negative for the particular flight condition considered, whereas the coefficient computed from Eq.(8) is positive. This discrepancy is because of the approximations involved in linearization of the nonlinear aerodynamic equations in obtaining the stability and control derivatives, which were used in computing the coefficients of Eq.(A-8), and should have little effect on the control law design for system 4.

MATRIX A

0.0	-4.67700D-03	0.0	1.00000D+00	0.0	0.0

```
********** CH. EQ. **********
 1.00000D+00  1.27151D+00  1.78731D+00  9.47109D-02  5.16616D-02  0.0          0.0          0.0

     REAL           IMAG          -2*Z*W          0**2           ZETA          OMEGA          TAU

   0.0                                                                                      0.0
   0.0                                                                                      0.0
   0.0                                                                                      0.0
  -1.67370D-02    1.72713D-01   -3.34740D-02    3.01100D-02    9.64545D-02    1.73522D-01
  -6.19020D-01    1.15437D+00   -1.23804D+00    1.71576D+00    4.72581D-01    1.30987D+00
```

NUMERATORS OF TRANSFER FUNCTIONS /DT

********** U /DT **********

3.78530D-04 4.12992D-04 5.50866D-04 -1.41890D-04 0.0 0.0 0.0

REAL	IMAG	-2*Z*W	O**2	ZETA	OMEGA	TAU
-6.53406D-01	1.14469D+00	-1.30681D+00	1.73725D+00	4.95738D-01	1.31805D+00	-4.63456D+00
2.15770D-01						0.0
0.0						0.0
0.0						0.0
0.0						

********** W /DT **********

-2.99670D-07 1.23359D-03 -3.45872D-06 5.61246D-05 0.0 0.0 0.0

REAL	IMAG	-2*Z*W	O**2	ZETA	OMEGA	TAU
4.11650D+03						-2.42925D-04
1.39637D-03	2.13296D-01	2.79273D-03	4.54970D-02	-6.54648D-03	2.13300D-01	0.0
0.0						0.0
0.0						0.0
0.0						

********** Q /DT **********

6.26270D-06 4.61247D-06 9.59338D-07 0.0 0.0 0.0 0.0

REAL	IMAG	-2*Z*W	O**2	ZETA	OMEGA	TAU
-3.68250D-01	1.32571D-01	-7.36499D-01	1.53183D-01	9.40887D-01	3.91386D-01	0.0
0.0						0.0
0.0						0.0
0.0						0.0
0.0						

********** THET/DT **********

6.26270D-06 4.61247D-06 9.59338D-07 0.0 0.0 0.0

REAL	IMAG	-2*Z*W	O**2	ZETA	OMEGA	TAU
-3.68250D-01	1.32571D-01	-7.36499D-01	1.53183D-01	9.40887D-01	3.91386D-01	0.0
0.0						0.0
0.0						0.0
0.0						

NUMERATORS OF TRANSFER FUNCTIONS /DT

********** H /DT **********

-4.25786D-06 1.00525D-04 9.82973D-04 1.50696D-04 0.0 0.0

REAL	IMAG	-2*Z*W	O**2	ZETA	OMEGA	TAU
3.10751D+01						-3.21801D-02
-7.30997D+00						1.36799D-01
-1.55805D-01						6.41828D+00
0.0						0.0
0.0						0.0

********** HDT /DT **********

-4.25800D-06 1.00527D-04 9.83025D-04 1.50698D-04 1.59722D-09 0.0 0.0

REAL	IMAG	-2*Z*W	O**2	ZETA	OMEGA	TAU
3.10749D+01						-3.21803D-02
-7.31016D+00						1.36796D-01
-1.55789D-01						6.41896D+00
-1.05996D-05						9.43436D+04
0.0						0.0
0.0						0.0

********** E /DT **********

2.51500D-03 2.73980D-03 3.76070D-03 4.04580D-05 1.50721D-04 0.0 0.0

REAL	IMAG	-2*Z*W	O**2	ZETA	OMEGA	TAU
-5.54487D-01	1.08120D+00	-1.10897D+00	1.47645D+00	4.56334D-01	1.21509D+00	
9.79597D-03	2.01231D-01	1.95919D-02	4.05899D-02	-4.86227D-02	2.01469D-01	
0.0						0.0
0.0						0.0

********** GAMA/DT **********

1.40156D-09 4.93195D-07 4.62865D-06 6.96843D-07 0.0 0.0 0.0

REAL	IMAG	-2*Z*W	O**2	ZETA	OMEGA	TAU
-3.42246D+02						2.92188D-03
-9.49224D+00						1.05349D-01
-1.53045D-01						6.53404D+00
0.0						0.0
0.0						0.0
0.0						0.0

NUMERATORS OF TRANSFER FUNCTIONS /DE

********** U /DE **********

6.53460D-03 1.73674D-01 3.23410D-01 4.50836D-01 0.0 0.0 0.0

REAL	IMAG	-2*Z*W	O**2	ZETA	OMEGA	TAU
-2.46859D+01						4.05090D-02
-9.45826D-01	1.37848D+00	-1.89165D+00	2.79480D+00	5.65765D-01	1.67177D+00	
0.0						0.0
0.0						0.0
0.0						0.0

********** W /DE **********

-1.61930D-01 -4.62303D+00 -2.34448D-01 -1.89040D-01 0.0 0.0 0.0

REAL	IMAG	-2*Z*W	O**2	ZETA	OMEGA	TAU
-2.85002D+01						3.50875D-02
-2.46819D-02	2.00879D-01	-4.93637D-02	4.09617D-02	1.21952D-01	2.02390D-01	
0.0						0.0
0.0						0.0
0.0						0.0

********** Q /DE **********

-2.11870D-02 -1.48430D-02 -1.14143D-03 0.0 0.0 0.0 0.0

REAL	IMAG	-2*Z*W	O**2	ZETA	OMEGA	TAU
-6.12631D-01						1.63230D+00
-8.79386D-02						1.13716D+01
0.0						0.0
0.0						0.0
0.0						0.0
0.0						0.0

********** THET/DE **********

-2.11870D-02 -1.48430D-02 -1.14143D-03 0.0 0.0 0.0

REAL	IMAG	-2*Z*W	O**2	ZETA	OMEGA	TAU
-6.12631D-01						1.63230D+00
-8.79386D-02						1.13716D+01
0.0						0.0
0.0						0.0
0.0						0.0

NUMERATORS OF TRANSFER FUNCTIONS /DE

********** H /DE **********
1.61835D-01 9.06967D-02 -2.94290D+00 -6.04443D-02 0.0 0.0

REAL	IMAG	-2*Z*W	O**2	ZETA	OMEGA	TAU
-4.54411D+00						2.20065D-01
4.00421D+00						-2.49737D-01
-2.05266D-02						4.87174D+01
0.0						0.0
0.0						0.0

********** HDT /DE **********
1.61840D-01 9.06958D-02 -2.94307D+00 -6.04520D-02 -5.26808D-06 0.0 0.0

REAL	IMAG	-2*Z*W	O**2	ZETA	OMEGA	TAU
-4.54417D+00						2.20062D-01
4.00429D+00						-2.49732D-01
-2.04404D-02						4.89226D+01
-8.75179D-05						1.14262D+04
0.0						0.0
0.0						0.0

********** E /DE **********
4.31000D-02 1.31514D+00 2.23853D+00 5.19179D-02 -6.04608D-02 0.0 0.0

REAL	IMAG	-2*Z*W	O**2	ZETA	OMEGA	TAU
-2.87059D+01						3.48360D-02
-1.76745D+00						5.65788D-01
-1.87674D-01						5.32840D+00
1.47325D-01						-6.78773D+00
0.0						0.0
0.0						0.0

********** GAMA/DE **********
7.57347D-04 4.34914D-04 -1.37465D-02 -2.57288D-04 0.0 0.0 0.0

REAL	IMAG	-2*Z*W	O**2	ZETA	OMEGA	TAU
-4.54842D+00						2.19857D-01
3.99286D+00						-2.50447D-01
-1.87060D-02						5.34588D+01
0.0						0.0
0.0						0.0
0.0						0.0

Single control system (elevator)

Performance index to regulate inertial speed and altitude

$$V = \frac{1}{2}\int_0^\infty (1000\Delta u_{PG}^2 + 100\ \Delta h^2 + \delta_e^2)dt$$

Control law

$$\delta_e = [5.72 \quad 8.61 \quad -5.31 \quad -45.6 \quad -10]\begin{bmatrix}\Delta u_{PG}\\ \Delta w_{PG}\\ q\\ \Delta\theta\\ \Delta h\end{bmatrix}$$

Units

Δu_{PG}, Δw_{PG} - ft/sec

q, $\Delta\theta$, δ_e - deg/sec, deg, deg

Δh - ft

********** CH. EQ. **********
1.00000D+00 6.36613D+00 2.12215D+01 3.81367D+01 3.34144D+01 6.04443D-01

REAL	IMAG	-2*Z*W	O**2	ZETA	OMEGA	TAU
-1.22883D+00	2.24404D+00	-2.45765D+00	6.54573D+00	4.80298D-01	2.55846D+00	
-1.94500D+00	1.10236D+00	-3.89000D+00	4.99822D+00	8.69986D-01	2.23567D+00	
-1.84749D-02						5.41275D+01

NUMERATORS OF TRANSFER FUNCTIONS /DE

********** U /DE **********
6.53450D-03 1.73674D-01 3.23410D-01 4.50836D-01 0.0

REAL	IMAG	-2*Z*W	O**2	ZETA	OMEGA	TAU
-2.46859D+01						4.05090D-02
-9.15826D-01	1.37848D+00	-1.89165D+00	2.79480D+00	5.65765D-01	1.67177D+00	
0.0						0.0

********** W /DE **********
-1.61930D-01 -4.62303D+00 -2.34448D-01 -1.89040D-01 0.0

REAL	IMAG	-2*Z*W	O**2	ZETA	OMEGA	TAU
-2.85002D+01						3.50875D-02
-2.46819D-02	2.00879D-01	-4.93637D-02	4.09617D-02	1.21952D-01	2.02390D-01	
0.0						0.0

********** Q /DE **********
-2.11870D-02 -1.48430D-02 -1.14143D-03 0.0 0.0

REAL	IMAG	-2*Z*W	O**2	ZETA	OMEGA	TAU
-6.12631D-01						1.63230D+00
-8.79386D-02						1.13716D+01
0.0						0.0
0.0						0.0

********** THET/DE **********
-2.11870D-02 -1.48430D-02 -1.14143D-03 0.0

REAL	IMAG	-2*Z*W	O**2	ZETA	OMEGA	TAU
-6.12631D-01						1.63230D+00
-8.79386D-02						1.13716D+01
0.0						0.0

NUMERATORS OF TRANSFER FUNCTIONS /DE

********** H /DE **********
1.61?35D-01 9.06967D-02 -2.94290D+00 -6.04443D-02

REAL	IMAG	-2*Z*W	O**2	ZETA	OMEGA	TAU
-2.?5266D-02						4.87174D+01
-4.?4411D+00						2.20065D-01
4.?0421D+00						-2.49737D-01

********** GAMA/DE **********
7.57?47D-04 4.34914D-04 -1.37465D-02 -2.57288D-04 0.0

REAL	IMAG	-2*Z*W	O**2	ZETA	OMEGA	TAU
-4.?4842D+00						2.19857D-01
3.?9286D+00						-2.50447D-01
-1.?7060D-02						5.34588D+01
0.0						0.0

Control System 1

Performance index is defined to minimize the deviations in the inertial speed and altitude.

$$V = \frac{1}{2}\int_0^\infty (10\Delta u_{PG}^2 + 100\Delta h^2 + .1\delta_t^2 + \delta_e^2)\,dt$$

Total control law

$$\begin{bmatrix} \delta_t \\ \delta_e \end{bmatrix} = \begin{bmatrix} .97 & -.124 & .04 & .693 & .223 \\ -1.35 & 8.59 & -5.11 & -45.18 & -9.99 \end{bmatrix} \begin{bmatrix} \Delta u_{PG} \\ \Delta w_{PG} \\ q \\ \Delta\theta \\ \Delta h \end{bmatrix}$$

$$+ \begin{bmatrix} 99.4 & -280.8 \\ 0 & 0 \end{bmatrix} \begin{bmatrix} u_w \\ w_w \end{bmatrix}$$

Units

Δu_{PG}, Δw_{PG} - ft/sec

q, $\Delta\theta$, δ_e - deg/sec, deg, deg

Δh - ft

δ_t - lbs

********** CH. EQ. **********

1.00000D+00 6.07076D+00 1.94059D+01 3.55045D+01 3.02140D+01 6.15287D-01

REAL	IMAG	-2*Z*W	O**2	ZETA	OMEGA	TAU
-1.04066D+00	2.31596D+00	-2.08132D+00	6.44663D+00	4.09866D-01	2.53902D+00	4.79150D+01
-2.08703D-02						
-1.98429D+00	7.97343D-01	-3.96858D+00	4.57316D+00	9.27891D-01	2.13849D+00	

NUMERATORS OF TRANSFER FUNCTIONS /DT

********** U /DT **********

3.78530D-04 2.24484D-03 7.32829D-03 1.34357D-02 1.14904D-02

REAL	IMAG	-2*Z*W	O**2	ZETA	OMEGA	TAU
-1.06014D+00	2.39284D+00	-2.12028D+00	6.84959D+00	4.05072D-01	2.61717D+00	
-1.90507D+00	8.95772D-01	-3.81014D+00	4.43169D+00	9.04952D-01	2.10516D+00	

********** W /DT **********

-2.99670D-07 8.52138D-04 -5.66419D-03 -7.75330D-03 -4.85746D-03

REAL	IMAG	-2*Z*W	O**2	ZETA	OMEGA	TAU
-6.22244D-01	5.78896D-01	-1.24449D+00	7.22308D-01	7.32149D-01	8.49887D-01	
7.91036D+00						-1.26417D-01
2.83692D+03						-3.52495D-04

********** Q /DT **********

6.26270D-06 -1.50549D-05 -3.48631D-05 -2.20703D-05 0.0

REAL	IMAG	-2*Z*W	O**2	ZETA	OMEGA	TAU
4.01089D+00						-2.49321D-01
-8.03490D-01	4.82736D-01	-1.60698D+00	8.78631D-01	8.57190D-01	9.37353D-01	
0.0						0.0

********** THET/DT **********

6.26270D-06 -1.50549D-05 -3.48631D-05 -2.20703D-05

REAL	IMAG	-2*Z*W	O**2	ZETA	OMEGA	TAU
-8.03490D-01	4.82736D-01	-1.60698D+00	8.78631D-01	8.57190D-01	9.37353D-01	
4.01089D+00						-2.49321D-01

NUMERATORS OF TRANSFER FUNCTIONS /DT

********** H /DT **********

-4.25786D-06 4.59884D-04 2.35665D-03 1.37028D-04

REAL	IMAG	-2*Z*W	O**2	ZETA	OMEGA	TAU
-5.88207D-02						1.70008D+01
-4.84556D+00						2.06374D-01
1.12913D+02						-8.85641D-03

********** GAMA/DT **********

1.40156D-09 2.27725D-06 1.14365D-05 1.39908D-06 6.48041D-07

REAL	IMAG	-2*Z*W	O**2	ZETA	OMEGA	TAU
-5.66755D-02	2.34011D-01	-1.13351D-01	5.79732D-02	2.35387D-01	2.40776D-01	
-4.92395D+00						2.03089D-01
-1.61976D+03						6.17375D-04

NUMERATORS OF TRANSFER FUNCTIONS /DE

********** U /DE **********

6.53460D-03 1.73685D-01 3.23512D-01 4.51043D-01 2.55888D-04

REAL	IMAG	-2*Z*W	O**2	ZETA	OMEGA	TAU
						1.76194D+03
-5.67557D-04						
-9.45788D-01	1.37851D+00	-1.89158D+00	2.79480D+00	5.65742D-01	1.67177D+00	
-2.46871D+01						4.05069D-02

********** W /DE **********

-1.61930D-01 -4.62309D+00 -2.36182D-01 -1.89145D-01 -1.08175D-04

REAL	IMAG	-2*Z*W	O**2	ZETA	OMEGA	TAU
-2.45831D-02	2.00876D-01	-4.91662D-02	4.09556D-02	1.21473D-01	2.02375D-01	
-5.72317D-04						1.74728D+03
-2.85002D+01						3.50875D-02

********** Q /DE **********

-2.11870D-02 -1.48509D-02 -1.14697D-03 -4.91501D-07 0.0

REAL	IMAG	-2*Z*W	O**2	ZETA	OMEGA	TAU
						1.63228D+00
-6.12640D-01						1.13802D+01
-8.78719D-02						2.32060D+03
-4.30922D-04						0.0
0.0						

********** THET/DE **********

-2.11870D-02 -1.48509D-02 -1.14697D-03 -4.91501D-07

REAL	IMAG	-2*Z*W	O**2	ZETA	OMEGA	TAU
						2.32060D+03
-4.30922D-04						1.13802D+01
-8.78719D-02						1.63228D+00
-6.12640D-01						

NUMERATORS OF TRANSFER FUNCTIONS /DE

********** H /DE **********
1.61835D-01 9.07581D-02 -2.94286D+00 -6.15271D-02

REAL	IMAG	-2*Z*W	O**2	ZETA	OMEGA	TAU
-2.08943D-02						4.78599D+01
-4.54412D+00						2.20065D-01
4.00420D+00						-2.49738D-01

********** GAMA/DE **********
7.57347D-04 4.35202D-04 -1.37463D-02 -2.62341D-04 1.44317D-08

REAL	IMAG	-2*Z*W	O**2	ZETA	OMEGA	TAU
5.48536D-05						-1.82303D+04
-1.91282D-02						5.22787D+01
-4.54842D+00						2.19857D-01
3.99285D+00						-2.50448D-01

Control system 2

Performance index is defined to minimize the deviations in inertial speed, altitude and altitude rate.

$$V = \frac{1}{2}\int_0^\infty (10\Delta u_{PG}^2 + 100\Delta h^2 + 100\Delta\dot{h}^2 + .1\delta_t^2 + \delta_e^2)dt$$

Total control law

$$\begin{bmatrix} \delta_t \\ \delta_e \end{bmatrix} = \begin{bmatrix} .77 & -18.14 & .057 & 67.97 & .24 & -17.95 \\ -2.07 & 12.24 & -6.91 & -65.8 & -9.99 & -.04 \end{bmatrix} \begin{bmatrix} \Delta u_{PG} \\ \Delta w_{PG} \\ q \\ \Delta\theta \\ \Delta h \\ \Delta\dot{h} \end{bmatrix}$$

$$+ \begin{bmatrix} 99.4 & -280.8 \\ 0 & 0 \end{bmatrix} \begin{bmatrix} u_w \\ w_w \end{bmatrix}$$

Units

Δu_{PG}, Δw_{PG}, $\Delta\dot{h}$ - ft/sec

q, $\Delta\theta$, δ_e - deg/sec, deg, deg

δ_t - lbs

Δh - ft

********** CH. EQ. **********
1.00000D+00 7.65773D+00 2.89896D+01 5.22011D+01 3.05579D+01 6.15374D-01 2.42330D-06

REAL	IMAG	-2*Z*W	O**2	ZETA	OMEGA	TAU
-2.08316D+00	2.74812D+00	-4.16632D+00	1.18917D+01	6.04088D-01	3.44843D+00	
-2.46468D+00						4.05732D-01
-1.00585D+00						9.94181D-01
-2.08697D-02						4.79164D+01
-3.93870D-06						2.53891D+05

NUMERATORS OF TRANSFER FUNCTIONS /DT

********** U /DT **********

3.78530D-04 2.85156D-03 1.10234D-02 1.97791D-02 1.14903D-02 0.0

REAL	IMAG	-2*Z*W	O**2	ZETA	OMEGA	TAU
-2.11440D+00	2.88102D+00	-4.22880D+00	1.27710D+01	5.91663D-01	3.57365D+00	
-2.24634D+00						4.45169D-01
-1.05811D+00						9.45078D-01
0.0						0.0

********** W /DT **********

-2.99670D-07 7.02736D-04 -8.36703D-03 -1.04352D-02 -4.85744D-03 0.0

REAL	IMAG	-2*Z*W	O**2	ZETA	OMEGA	TAU
2.33306D+03						
1.31493D+01						-4.28622D-04
-5.87747D-01	4.27689D-01	-1.17549D+00	5.28365D-01	8.08581D-01	7.26887D-01	-7.60494D-02
0.0						0.0

********** Q /DT **********

6.26270D-06 -2.46019D-05 -4.69939D-05 -2.20702D-05 0.0 0.0

REAL	IMAG	-2*Z*W	O**2	ZETA	OMEGA	TAU
5.42982D+00						
-7.50743D-01	2.92244D-01	-1.50149D+00	6.49022D-01	9.31884D-01	8.05619D-01	-1.84168D-01
0.0						0.0
0.0						0.0

********** THET/DT **********

6.26270D-06 -2.46019D-05 -4.69939D-05 -2.20702D-05 0.0

REAL	IMAG	-2*Z*W	O**2	ZETA	OMEGA	TAU
5.42982D+00						
-7.50743D-01	2.92244D-01	-1.50149D+00	6.49022D-01	9.31884D-01	8.05619D-01	-1.84168D-01
0.0						0.0

NUMERATORS OF TRANSFER FUNCTIONS /DT

********** H /DT **********

-4.25786D-06 6.01966D-04 2.97357D-03 1.48756D-04 5.97824D-10

REAL	IMAG	-2*Z*W	O**2	ZETA	OMEGA	TAU
-4.01915D-06						2.48809D+05
-5.05393D-02						1.97866D+01
-4.72931D+00						2.11447D-01
1.46157D+02						-6.84194D-03

********** HDT /DT **********

-4.25800D-06 6.01983D-04 2.97366D-03 1.48558D-04 -2.72745D-07 -1.34977D-07

REAL	IMAG	-2*Z*W	O**2	ZETA	OMEGA	TAU
2.51752D-02						-3.97216D+01
-3.78330D-02	1.97557D-02	-7.56661D-02	1.82162D-03	8.86424D-01	4.26805D-02	
-4.72937D+00						2.11444D-01
1.46157D+02						-6.84197D-03

********** GAMA/DT **********

1.40156D-09 2.97600D-06 1.45306D-05 1.81170D-06 6.48041D-07 0.0

REAL	IMAG	-2*Z*W	O**2	ZETA	OMEGA	TAU
-2.11846D+03						4.72041D-04
-4.77541D+00						2.09406D-01
-5.90910D-02	2.05458D-01	-1.18182D-01	4.57046D-02	2.76402D-01	2.13786D-01	
0.0						0.0

NUMERATORS OF TRANSFER FUNCTIONS /DE

********** U /DE **********
6.53460D-03 1.73688D-01 3.23557D-01 4.51135D-01 2.79840D-05 0.0

REAL	IMAG	-2*Z*W	O**2	ZETA	OMEGA	TAU
-2.46874D+01						4.05064D-02
-9.46159D-01	1.37882D+00	-1.89232D+00	2.79635D+00	5.65807D-01	1.67223D+00	
-6.20331D-05						1.61204D+04
0.0						0.0

********** W /DE **********
-1.61930D-01 -4.62309D+00 -2.36229D-01 -1.89143D-01 -1.18238D-05 0.0

REAL	IMAG	-2*Z*W	O**2	ZETA	OMEGA	TAU
-2.85002D+01						3.50875D-02
-2.48432D-02	2.00907D-01	-4.96863D-02	4.09809D-02	1.22720D-01	2.02437D-01	
-6.25174D-05						1.59956D+04
0.0						0.0

********** Q /DE **********
-2.11870D-02 -1.48511D-02 -1.14701D-03 -5.48552D-08 0.0 0.0

REAL	IMAG	-2*Z*W	O**2	ZETA	OMEGA	TAU
-6.12583D-01						1.63243D+00
-8.83210D-02						1.13223D+01
-4.78541D-05						2.08968D+04
0.0						0.0
0.0						0.0

********** THET/DE **********
-2.11870D-02 -1.48511D-02 -1.14701D-03 -5.48552D-08 0.0

REAL	IMAG	-2*Z*W	O**2	ZETA	OMEGA	TAU
-6.12583D-01						1.63243D+00
-8.83210D-02						1.13223D+01
-4.78541D-05						2.08969D+04
0.0						0.0

NUMERATORS OF TRANSFER FUNCTIONS /DE

********** H /DE **********

1.61835D-01 9.07600D-02 -2.94285D+00 -6.15385D-02 -2.42336D-07

REAL	IMAG	-2*Z*W	O**2	ZETA	OMEGA	TAU
						2.53891D+05
-3.93870D-06						4.78600D+01
-2.08943D-02						2.20065D-01
-4.54412D+00						-2.49738D-01
4.00420D+00						

********** HDT /DE **********

1.61840D-01 9.07591D-02 -2.94303D+00 -6.15462D-02 -5.51353D-06 -3.28617D-10

REAL	IMAG	-2*Z*W	O**2	ZETA	OMEGA	TAU
-4.48560D-05	5.78818D-05	-8.97120D-05	5.36236D-09	6.12552D-01	7.32282D-05	
-2.08099D-02						4.80540D+01
-4.54417D+00						2.20062D-01
4.00427D+00						-2.49733D-01

********** GAMA/DE **********

7.57347D-04 4.35211D-04 -1.37462D-02 -2.62389D-04 4.44786D-10 0.0

REAL	IMAG	-2*Z*W	O**2	ZETA	OMEGA	TAU
						2.19857D-01
-4.54842D+00						-2.50448D-01
3.99284D+00						5.24147D+01
-1.90786D-02						-5.89974D+05
1.69499D-06						0.0
0.0						

Control system 3

Performance indices are the same as for control systems 1 and 2. The gain on the velocity is changed to

$$K_{11} = \frac{aX_u}{X_{\delta_t}} = -5.03\ (99.4) = -500$$

Total control law to minimize airspeed and altitude deviation:

$$\begin{bmatrix} \delta_t \\ \delta_e \end{bmatrix} = \begin{bmatrix} -500 & -.124 & .04 & .693 & .223 \\ -1.35 & 8.59 & -5.11 & -45.18 & -9.99 \end{bmatrix} \begin{bmatrix} \Delta u_{PG} \\ \Delta w_{PG} \\ q \\ \Delta\theta \\ \Delta h \end{bmatrix}$$

$$+ \begin{bmatrix} -500 & -280.8 \\ 0 & 0 \end{bmatrix} \begin{bmatrix} u_w \\ w_w \end{bmatrix}$$

Total control law to minimize airspeed, altitude, and altitude rate deviation:

$$\begin{bmatrix} \delta_t \\ \delta_e \end{bmatrix} = \begin{bmatrix} -500 & -18.14 & .057 & 67.97 & .24 & -17.95 \\ -2.07 & 12.24 & -6.91 & -65.8 & -9.99 & -.04 \end{bmatrix} \begin{bmatrix} \Delta u_{PG} \\ \Delta w_{PG} \\ q \\ \Delta\theta \\ \Delta h \\ \Delta \dot{h} \end{bmatrix}$$

$$+ \begin{bmatrix} -500 & -280.8 \\ 0 & 0 \end{bmatrix} \begin{bmatrix} u_w \\ w_w \end{bmatrix}$$

Units

Δu_{PG}, Δw_{PG}, $\Delta \dot{h}$ - ft/sec

q, $\Delta\theta$, δ_e - deg/sec, deg, deg

δ_t - lbs

Δh - ft

********** CH. EQ. **********
1.00000D+00 6.25966D+00 2.05262D+01 3.91616D+01 3.69189D+01 6.34938D+00

REAL	IMAG	-2*Z*W	O**2	ZETA	OMEGA	TAU
-1.03480D+00	2.31561D+00	-2.06959D+00	6.43286D+00	4.07994D-01	2.53631D+00	
-2.16368D-01						4.62176D+00
-1.98685D+00	7.83719D-01	-3.97370D+00	4.56179D+00	9.30245D-01	2.13583D+00	

NUMERATORS OF TRANSFER FUNCTIONS /DT

********** U /DT **********
3.78530D-04 2.24484D-03 7.32829D-03 1.34357D-02 1.14904D-02

REAL	IMAG	-2*Z*W	O**2	ZETA	OMEGA	TAU
-1.06014D+00	2.39284D+00	-2.12028D+00	6.84959D+00	4.05072D-01	2.61717D+00	
-1.90507D+00	8.95772D-01	-3.81014D+00	4.43169D+00	9.04952D-01	2.10516D+00	

********** W /DT **********
-2.99670D-07 8.52138D-04 -5.66419D-03 -7.75330D-03 -4.85746D-03

REAL	IMAG	-2*Z*W	O**2	ZETA	OMEGA	TAU
-6.22244D-01	5.78896D-01	-1.24449D+00	7.22308D-01	7.32149D-01	8.49887D-01	
7.91036D+00						-1.26417D-01
2.83692D+03						-3.52495D-04

********** Q /DT **********
6.26270D-06 -1.50549D-05 -3.48631D-05 -2.20703D-05 0.0

REAL	IMAG	-2*Z*W	O**2	ZETA	OMEGA	TAU
4.01089D+00						-2.49321D-01
-8.03490D-01	4.82736D-01	-1.60698D+00	8.78631D-01	8.57190D-01	9.37353D-01	
0.0						0.0

********** THET/DT **********
6.26270D-06 -1.50549D-05 -3.48631D-05 -2.20703D-05

REAL	IMAG	-2*Z*W	O**2	ZETA	OMEGA	TAU
-8.03490D-01	4.82736D-01	-1.60698D+00	8.78631D-01	8.57190D-01	9.37353D-01	
4.01089D+00						-2.49321D-01

NUMERATORS OF TRANSFER FUNCTIONS /DT

********** H /DT **********
-4.25786D-06 4.59884D-04 2.35665D-03 1.37028D-04

REAL	IMAG	-2*Z*W	O**2	ZETA	OMEGA	TAU
-5.88207D-02						1.70008D+01
-4.84556D+00						2.06374D-01
1.12913D+02						-8.85641D-03

********** GAMA/DT **********
1.40156D-09 2.27725D-06 1.14365D-05 1.39908D-06 6.48041D-07

REAL	IMAG	-2*Z*W	O**2	ZETA	OMEGA	TAU
-5.66755D-02	2.34011D-01	-1.13351D-01	5.79732D-02	2.35387D-01	2.40776D-01	
-4.92395D+00						2.03089D-01
-1.61976D+03						6.17375D-04

NUMERATORS OF TRANSFER FUNCTIONS /DE

********** U /DE **********
6.53460D-03 1.73685D-01 3.23512D-01 4.51043D-01 2.55888D-04

REAL	IMAG	-2*Z*W	O**2	ZETA	OMEGA	TAU
						1.76194D+03
-5.67557D-04						
-9.45788D-01	1.37851D+00	-1.89158D+00	2.79480D+00	5.65742D-01	1.67177D+00	
-2.46871D+01						4.05069D-02

********** W /DE **********
-1.61930D-01 -4.65368D+00 -1.10795D+00 -1.74464D-01 -1.08175D-04

REAL	IMAG	-2*Z*W	O**2	ZETA	OMEGA	TAU
-1.19063D-01	1.53227D-01	-2.38125D-01	3.76544D-02	6.13575D-01	1.94047D-01	
						1.60644D+03
-6.22495D-04						
-2.85001D+01						3.50876D-02

********** Q /DE **********
-2.11870D-02 -1.88735D-02 -3.76037D-03 -4.91501D-07 0.0

REAL	IMAG	-2*Z*W	O**2	ZETA	OMEGA	TAU
						1.69461D+00
-5.90105D-01						3.32701D+00
-3.00570D-01						7.64577D+03
-1.30791D-04						0.0
0.0						

********** THET/DE **********
-2.11870D-02 -1.88735D-02 -3.76037D-03 -4.91501D-07

REAL	IMAG	-2*Z*W	O**2	ZETA	OMEGA	TAU
						7.64577D+03
-1.30791D-04						3.32701D+00
-3.00570D-01						1.69461D+00
-5.90105D-01						

NUMERATORS OF TRANSFER FUNCTIONS /DE

********** H /DE **********
1.61835D-01 1.21343D-01 -2.93122D+00 -6.34951D-01

REAL	IMAG	-2*Z*W	O**2	ZETA	OMEGA	TAU
-2.15249D-01						4.64577D+00
4.01045D+00						-2.49349D-01
-4.54499D+00						2.20023D-01

********** GAMA/DE **********
7.57347D-04 5.78260D-04 -1.36916D-02 -2.94440D-03 1.44317D-08

REAL	IMAG	-2*Z*W	O**2	ZETA	OMEGA	TAU
4.90130D-06						-2.04028D+05
-2.13667D-01						4.68018D+00
3.99958D+00						-2.50026D-01
-4.54946D+00						2.19807D-01

********** CH. EQ. **********

1.00000D+00 7.84670D+00 3.04131D+01 5.77044D+01 4.04323D+01 6.35174D+00 2.42330D-06

REAL	IMAG	-2*Z*W	O**2	ZETA	OMEGA	TAU
-2.07570D+00	2.74575D+00	-4.15139D+00	1.18476D+01	6.03042D-01	3.44204D+00	
-2.48392D+00						4.02590D-01
-9.94322D-01						1.00571D+00
-2.17068D-01						4.60686D+00
-3.81519D-07						2.62110D+06

NUMERATORS OF TRANSFER FUNCTIONS /DT

********** U /DT **********

3.78530D-04 2.85156D-03 1.10234D-02 1.97791D-02 1.14903D-02 0.0

REAL	IMAG	-2*Z*W	O**2	ZETA	OMEGA	TAU
-2.11440D+00	2.88102D+00	-4.22880D+00	1.27710D+01	5.91663D-01	3.57365D+00	
-2.24634D+00						4.45169D-01
-1.05811D+00						9.45078D-01
0.0						0.0

********** W /DT **********

-2.99670D-07 7.02736D-04 -8.36703D-03 -1.04352D-02 -4.85744D-03 0.0

REAL	IMAG	-2*Z*W	O**2	ZETA	OMEGA	TAU
2.33306D+03						-4.28622D-04
1.31493D+01						-7.60494D-02
-5.87747D-01	4.27689D-01	-1.17549D+00	5.28365D-01	8.08581D-01	7.26887D-01	
0.0						0.0

********** Q /DT **********

6.26270D-06 -2.46019D-05 -4.69939D-05 -2.20702D-05 0.0 0.0

REAL	IMAG	-2*Z*W	O**2	ZETA	OMEGA	TAU
5.42982D+00						-1.84168D-01
-7.50743D-01	2.92244D-01	-1.50149D+00	6.49022D-01	9.31884D-01	8.05619D-01	
0.0						0.0
0.0						0.0

********** THET/DT **********

6.26270D-06 -2.46019D-05 -4.69939D-05 -2.20702D-05 0.0

REAL	IMAG	-2*Z*W	O**2	ZETA	OMEGA	TAU
5.42982D+00						-1.84168D-01
-7.50743D-01	2.92244D-01	-1.50149D+00	6.49022D-01	9.31884D-01	8.05619D-01	
0.0						0.0

NUMERATORS OF TRANSFER FUNCTIONS /DT

********** H /DT **********

-4.25786D-06 6.01966D-04 2.97357D-03 1.48756D-04 5.97824D-10

REAL	IMAG	-2*Z*W	O**2	ZETA	OMEGA	TAU
-4.01915D-06						2.48809D+05
-5.05393D-02						1.97866D+01
-4.72931D+00						2.11447D-01
1.46157D+02						-6.84194D-03

********** HDT /DT **********

-4.25800D-06 6.01983D-04 2.97366D-03 1.48558D-04 -2.72745D-07 -1.34977D-07

REAL	IMAG	-2*Z*W	O**2	ZETA	OMEGA	TAU
2.51752D-02						-3.97216D+01
-3.78330D-02	1.97557D-02	-7.56661D-02	1.82162D-03	8.86424D-01	4.26805D-02	
-4.72937D+00						2.11444D-01
1.46157D+02						-6.84197D-03

********** GAMA/DT **********

1.40156D-09 2.97600D-06 1.45306D-05 1.81170D-06 6.48041D-07 0.0

REAL	IMAG	-2*Z*W	O**2	ZETA	OMEGA	TAU
-2.11846D+03						4.72041D-04
-4.77541D+00						2.09406D-01
-5.90910D-02	2.05458D-01	-1.18182D-01	4.57046D-02	2.76402D-01	2.13786D-01	
0.0						0.0

NUMERATORS OF TRANSFER FUNCTIONS /DE

********** U /DE **********

6.53460D-03 1.73688D-01 3.23557D-01 4.51135D-01 2.79840D-05 0.0

REAL	IMAG	-2*Z*W	O**2	ZETA	OMEGA	TAU
-2.46874D+01						4.05064D-02
-9.46159D-01	1.37882D+00	-1.89232D+00	2.79635D+00	5.65807D-01	1.67223D+00	
-6.20331D-05						1.61204D+04
0.0						0.0

********** W /DE **********

-1.61930D-01 -4.65369D+00 -1.10834D+00 -1.74455D-01 -1.18238D-05 0.0

REAL	IMAG	-2*Z*W	O**2	ZETA	OMEGA	TAU
-2.85001D+01						3.50876D-02
-1.19383D-01	1.53405D-01	-2.38766D-01	3.77854D-02	6.14158D-01	1.94385D-01	
-6.78047D-05						1.47482D+04
0.0						0.0

********** Q /DE **********

-2.11870D-02 -1.88753D-02 -3.76145D-03 -5.48553D-08 0.0 0.0

REAL	IMAG	-2*Z*W	O**2	ZETA	OMEGA	TAU
-5.89981D-01						1.69497D+00
-3.00896D-01						3.32341D+00
-1.45846D-05						6.85654D+04
0.0						0.0
0.0						0.0

********** THET/DE **********

-2.11870D-02 -1.88753D-02 -3.76145D-03 -5.48552D-08 0.0

REAL	IMAG	-2*Z*W	O**2	ZETA	OMEGA	TAU
-5.89981D-01						1.69497D+00
-3.00896D-01						3.32341D+00
-1.45846D-05						6.85656D+04
0.0						0.0

NUMERATORS OF TRANSFER FUNCTIONS /DE

********** H /DE **********

1.61835D-01 1.21357D-01 -2.93121D+00 -6.35192D-01 -2.42336D-07

REAL	IMAG	-2*Z*W	O**2	ZETA	OMEGA	TAU
-3.81517D-07						2.62112D+06
-2.15331D-01						4.64401D+00
4.01044D+00						-2.49349D-01
-4.54499D+00						2.20023D-01

********** HDT /DE **********

1.61840D-01 1.21357D-01 -2.93139D+00 -6.35234D-01 -5.24871D-06 -3.28617D-10

REAL	IMAG	-2*Z*W	O**2	ZETA	OMEGA	TAU
-4.13029D-06	2.23669D-05	-8.26057D-06	5.17337D-10	1.81591D-01	2.27450D-05	
-2.15324D-01						4.64416D+00
4.01052D+00						-2.49344D-01
-4.54504D+00						2.20020D-01

********** GAMA/DE **********

7.57347D-04 5.78326D-04 -1.36916D-02 -2.94552D-03 4.44771D-10 0.0

REAL	IMAG	-2*Z*W	O**2	ZETA	OMEGA	TAU
-4.54946D+00						2.19806D-01
3.99958D+00						-2.50026D-01
-2.13744D-01						4.67849D+00
1.50999D-07						-6.62257D+06
0.0						0.0

Control system 4

Performance index to minimize deviation in energy using the throttle:

$$V = \frac{1}{2}\int_0^\infty (100\Delta E^2 + \delta_t^2)dt$$

Performance index to regulate altitude and airspeed:

$$V = \frac{1}{2}\int_0^\infty (1000\Delta u_{PA}^2 + 100\Delta h^2 + \delta_e^2)dt$$

The gain on ΔE obtained from the first performance is replaced by a higher gain obtained from a higher weighting. The final control law is given by

$$\begin{bmatrix} \delta_t \\ \delta_e \end{bmatrix} = \begin{bmatrix} -1.23 & -10.83 & 13.22 & 57.2 & 316.23 & 0 \\ 5.72 & 8.61 & -5.31 & -45.6 & 0 & -10 \end{bmatrix} \begin{bmatrix} \Delta u_{PA} \\ \Delta w_{PA} \\ q \\ \Delta\theta \\ \Delta E \\ \Delta h \end{bmatrix}$$

Units

Δu_{PG}, Δw_{PG} - ft/sec

q, $\Delta\theta$, δ_e - deg/sec, deg, deg

δ_t - lbs

Δh - ft

ΔE - ft

********** CH. EQ. **********

1.00000D+00 7.16572D+00 2.61622D+01 5.42422D+01 6.30485D+01 2.78155D+01 5.65247D-02

REAL	IMAG	-2*Z*W	O**2	ZETA	OMEGA	TAU
-1.22816D+00	2.15719D+00	-2.45632D+00	6.16187D+00	4.94765D-01	2.48231D+00	
-1.90439D+00	1.17206D+00	-3.80878D+00	5.00044D+00	8.51632D-01	2.23617D+00	
-2.04156D-03						4.89821D+02
-8.98577D-01						1.11287D+00

NUMERATORS OF TRANSFER FUNCTIONS /DT

********** U /DT **********
3.78530D-04 2.33978D-03 7.54777D-03 1.35567D-02 1.14907D-02 0.0

REAL	IMAG	-2*Z*W	O**2	ZETA	OMEGA	TAU
-1.11264D+00	2.26638D+00	-2.22529D+00	6.37445D+00	4.40691D-01	2.52477D+00	
-1.97797D+00	9.21837D-01	-3.95594D+00	4.76214D+00	9.06396D-01	2.18223D+00	
0.0						0.0

********** W /DT **********
-2.99670D-07 1.27361D-03 6.64365D-03 -8.01375D-03 -4.85759D-03 0.0

REAL	IMAG	-2*Z*W	O**2	ZETA	OMEGA	TAU
4.25525D+03						-2.35004D-04
-6.13221D+00						1.63073D-01
1.37534D+00						-7.27091D-01
-4.51673D-01						2.21399D+00
0.0						0.0

********** Q /DT **********
6.26270D-06 4.19543D-05 2.14788D-06 -2.20709D-05 0.0 0.0

REAL	IMAG	-2*Z*W	O**2	ZETA	OMEGA	TAU
-6.56507D+00						1.52321D-01
-8.02733D-01						1.24574D+00
6.68725D-01						-1.49538D+00
0.0						0.0
0.0						0.0

********** THET/DT **********
6.26270D-06 4.19543D-05 2.14788D-06 -2.20709D-05 0.0

REAL	IMAG	-2*Z*W	O**2	ZETA	OMEGA	TAU
-6.56507D+00						1.52321D-01
-8.02733D-01						1.24574D+00
6.68725D-01						-1.49538D+00
0.0						0.0

NUMERATORS OF TRANSFER FUNCTIONS /DT

********** H /DT **********

-4.25786D-06 3.73119D-05 2.23597D-03 8.30894D-03 0.0

REAL	IMAG	-2*Z*W	O**2	ZETA	OMEGA	TAU
2.91076D+01						-3.43553D-02
-1.62082D+01						6.16970D-02
-4.13630D+00						2.41762D-01
0.0						0.0

********** E /DT **********

2.51500D-03 1.55112D-02 5.07471D-02 9.35201D-02 8.61557D-02 1.78747D-04

REAL	IMAG	-2*Z*W	O**2	ZETA	OMEGA	TAU
-2.07938D-03						4.80913D+02
-1.02437D+00	2.30000D+00	-2.04874D+00	6.33933D+00	4.06852D-01	2.51780D+00	
-2.05833D+00	1.07468D+00	-4.11666D+00	5.39166D+00	8.86449D-01	2.32200D+00	

********** GAMA/DT **********

1.40156D-09 3.06027D-07 1.08819D-05 3.96282D-05 6.48057D-07 0.0

REAL	IMAG	-2*Z*W	O**2	ZETA	OMEGA	TAU
-1.74874D+02						5.71841D-03
-3.93696D+01						2.54003D-02
-4.08833D+00						2.44599D-01
-1.64275D-02						6.08735D+01
0.0						0.0

NUMERATORS OF TRANSFER FUNCTIONS /DE

********** U /DE **********
6.53460D-03 1.64942D-01 3.00042D-01 4.40356D-01 3.68750D-01 0.0

REAL	IMAG	-2*Z*W	O**2	ZETA	OMEGA	TAU
-2.33975D+01						4.27395D-02
-3.20690D-01	1.37951D+00	-6.41379D-01	2.00590D+00	2.26428D-01	1.41630D+00	
-1.20236D+00						8.31700D-01
0.0						0.0

********** W /DE **********
-1.61930D-01 -4.75250D+00 -3.95368D+00 -1.96960D-01 -1.55741D-01 0.0

REAL	IMAG	-2*Z*W	O**2	ZETA	OMEGA	TAU
-2.84937D+01						3.50955D-02
-8.53163D-01						1.17211D+00
-1.13660D-03	1.98903D-01	-2.27320D-03	3.95636D-02	5.71425D-03	1.98906D-01	
0.0						0.0

********** Q /DE **********
-2.11870D-02 -3.20149D-02 -1.26275D-02 -7.34042D-04 0.0 0.0

REAL	IMAG	-2*Z*W	O**2	ZETA	OMEGA	TAU
-8.75528D-01						1.14217D+00
-5.65570D-01						1.76813D+00
-6.99673D-02						1.42924D+01
0.0						0.0
0.0						0.0

********** THET/DE **********
-2.11870D-02 -3.20149D-02 -1.26275D-02 -7.34042D-04 0.0

REAL	IMAG	-2*Z*W	O**2	ZETA	OMEGA	TAU
-8.75528D-01						1.14217D+00
-5.65570D-01						1.76813D+00
-6.99673D-02						1.42924D+01
0.0						0.0

NUMERATORS OF TRANSFER FUNCTIONS /DE

********** H /DE **********

1.61835D-01 2.20257D-01 -2.89512D+00 -2.50812D+00 -5.65247D-03

REAL	IMAG	-2*Z*W	O**2	ZETA	OMEGA	TAU
-2.25956D-03						4.42564D+02
-8.43431D-01						1.18563D+00
-4.54640D+00						2.19954D-01
4.03110D+00						-2.48071D-01

********** E /DE **********

1.61840D-01 1.50280D+00 2.52870D+00 1.83629D-01 -5.06234D-02 0.0

REAL	IMAG	-2*Z*W	O**2	ZETA	OMEGA	TAU
-7.11207D+00						1.40606D-01
-2.08398D+00						4.79851D-01
-1.96856D-01						5.07985D+00
1.07208D-01						-9.32766D+00
0.0						0.0

********** GAMA/DE **********

7.57347D-04 1.04043D-03 -1.35236D-02 -1.17063D-02 -5.64119D-06 0.0

REAL	IMAG	-2*Z*W	O**2	ZETA	OMEGA	TAU
-4.55114D+00						2.19725D-01
4.02183D+00						-2.48643D-01
-8.43995D-01						1.18484D+00
-4.82161D-04						2.07399D+03
0.0						0.0

Appendix C

OBSERVER DESIGN

This appendix describes the application of the observer system design methods described in Section 3 of this report. The control law resulting from the regulation of Δu and Δh using both throttle and elevator is described mechanized as an observer system. Three sensors were assumed to be available for feedback control purposes, one for each degree of freedom of motion of the aircraft. In general, this is the maximum that would normally be required to insure system realizability for most physical plants such as aircraft. The three sensors chosen were $\Delta u(t)$, $\Delta h(t)$ and $q(t)$. Only the $\Delta h(t)$ measurement is absolutely required, others could have been substituted for the $\Delta u(t)$ and $q(t)$ states. The altitude error, however, is unobservable in the control sense through any other single sensor, so it is a required measurement for the observer system. All three sensors represent inertial measurement and are obtainable with relatively low inherent sensor noise content. A deterministic observer system is considered a realistic way to define a control system for this application to preserve the robustness of the state feedback shear alleviation control law.

Among the groups of measurements Δh and u, Δh and q, and Δu and q, there are three minimum phase transmission zeros located at s = -4.525, s = -2.39 and s = -0.6497. The zeros at s = -4.525 and s = -2.39 were chosen for the observer design to replace two state measurements because they would represent more stabel observer poles and because this selection resulted in observer parameters that could easily be mechanized. Applying Equations of Section 3 yielded the observer

$$\begin{bmatrix} \dot{z}_1(t) \\ \dot{z}_2(t) \end{bmatrix} = \begin{bmatrix} -4.525 & 0 \\ 0 & -2.39 \end{bmatrix} \begin{bmatrix} z_1(t) \\ z_2(t) \end{bmatrix} + \begin{bmatrix} -.0875 & -95.3 & 4.52 \\ -.0011 & 25.49 & 2.39 \end{bmatrix} \begin{bmatrix} \Delta u(t) \\ \Delta h(t) \\ q(t) \end{bmatrix} \tag{C-1}$$

When this observer was substituted into the control law of Control System 1 to replace the state measurements $\Delta\omega$ and $\Delta\theta$, the resulting control law is given by

$$\begin{bmatrix} \delta_t(t) \\ \delta_e(t) \end{bmatrix} = \begin{bmatrix} .981 & .779 & .025 & -.241 & -.319 \\ -2.43 & -.801 & -3.966 & 14.38 & 21.52 \end{bmatrix} \begin{bmatrix} \Delta u(t) \\ \Delta h(t) \\ q(t) \\ z_1(t) \\ z_2(t) \end{bmatrix} \quad \text{(C-2)}$$

The observer control law produced somewhat lower overall feedback gains, indicating that the observers had not reduced the observability of the system and,in fact, had improved it somewhat. It is felt, therefore, that the observer system should be easily mechanizable.

1. Report No.	2. Government Accession No.	3. Recipient's Catalog No.
NASA CR-166022		

4 Title and Subtitle	5. Report Date
CONTROL CONCEPTS FOR THE ALLEVIATION OF WINDSHEARS AND GUSTS	July 1982
	6. Performing Organization Code

7. Author(s)	8. Performing Organization Report No
E.G. Rynaski and K.S. Govindaraj	6896-F-1

9 Performing Organization Name and Address	10. Work Unit No.
Calspan Advanced Technology Center PO Box 400 Buffalo, NY 14225	11. Contract or Grant No NAS1-16691
	13. Type of Report and Period Covered
12. Sponsoring Agency Name and Address National Aeronautics and Space Administration Langley Research Center Hampton, Virginia 23665	14. Sponsoring Agency Code

15. Supplementary Notes

Langley Technical Monitor - Mr. Aaron Ostroff

16. Abstract

This report describes a study of automatic control system design methods for gust and shear alleviation. It is shown that automatic gust/shear alleviation systems can be quite effective if both throttle and elevator are used in harmony to produce the forces and moments required to counter the effects of the windshear. It is shown that regulation with respect to ground speed or airspeed results in very similar system designs. Consideration was given to the application of the NASA total energy probe in the detection of windshear and criteria for alleviation. Finally, the theory and application of robust output observers was extended with design examples showing how implementation of the control laws can be accomplished using observers, and thereby resulting in less complex control system configurations.

17. Key Words (Selected by Author(s))	18. Distribution Statement
Windshear Alleviation Energy Rate Probe Observer Design Methods	Unclassified - Unlimited

19. Security Classif. (of this report)	20. Security Classif. (of this page)	21. No. of Pages	22. Price*
Unclassified	Unclassified	175	

*For sale by the Clearinghouse for Federal Scientific and Technical Information, Springfield, Virginia 22151.